(12)

HDL-SR-82-8
November 1982

' ectures on Crystal Field Theory

by Clyde A. Morrison

U.S. Army Electronics Research
and Development Command
Harry Diamond Laboratories
Adelphi, MD 20783

The findings in this report are not to be construed as an official Department of the Army position unless so designated by other authorized documents.

Citation of manufacturers' or trade names does not constitute an official indorsement or approval of the use thereof.

Destroy this report when it is no longer needed. Do not return it to the originator.

UNCLASSIFIED

SECURITY CLASSIFICATION OF THIS PAGE (When Data Entered)

REPORT DOCUMENTATION PAGE		READ INSTRUCTIONS BEFORE COMPLETING FORM
1. REPORT NUMBER HDL-SR-82-8	2. GOVT ACCESSION NO. AD-A122 791	3. RECIPIENT'S CATALOG NUMBER
4. TITLE (and Subtitle) Lectures on Crystal Field Theory		5. TYPE OF REPORT & PERIOD COVERED Special Report 6. PERFORMING ORG. REPORT NUMBER
7. AUTHOR(s) Clyde A. Morrison		8. CONTRACT OR GRANT NUMBER(s)
9. PERFORMING ORGANIZATION NAME AND ADDRESS Harry Diamond Laboratories 2800 Powder Mill Road Adelphi, MD 20783		10. PROGRAM ELEMENT, PROJECT, TASK AREA & WORK UNIT NUMBERS
11. CONTROLLING OFFICE NAME AND ADDRESS U. S. Army Materiel Development and Readiness Command Alexandria, VA 22333		12. REPORT DATE November 1982 13. NUMBER OF PAGES 123
14. MONITORING AGENCY NAME & ADDRESS(if different from Controlling Office)		15. SECURITY CLASS. (of this report) UNCLASSIFIED 15a. DECLASSIFICATION/DOWNGRADING SCHEDULE

16. DISTRIBUTION STATEMENT (of this Report)

Approved for public release; distribution unlimited.

17. DISTRIBUTION STATEMENT (of the abstract entered in Block 20, if different from Report)

18. SUPPLEMENTARY NOTES

HDL Project: 399B30

19. KEY WORDS (Continue on reverse side if necessary and identify by block number)

Crystal fields
Spherical tensors
Racah algebra

20. ABSTRACT (Continue on reverse side if necessary and identify by block number)

This report covers a series of lectures given from November 2 through December 2, 1981. The early work done at the Harry Diamond Laboratories (HDL) and the motivation for that work is given in the first lecture. Later lectures cover work done at HDL in the recent past as well as ongoing research. These latter lec-

DD FORM 1 JAN 73 1473 EDITION OF 1 NOV 65 IS OBSOLETE

UNCLASSIFIED

SECURITY CLASSIFICATION OF THIS PAGE (When Data Entered)

20. ABSTRACT (cont'd)

tures are interspersed with lectures which are intended to familiarize the audience with the notation employed at HDL. The last few lectures contain matter under investigation presently at HDL and other laboratories in the U.S. and Europe.

Preface

This is a collection of lectures delivered at the Universidade Federal de Pernambuco, Recife, Brazil, between 2 November 1981 and 2 December 1981. The visit to Recife was a response to an invitation of Professor Gilberto F. de Sâ of the Physics Department. In the preparation of these notes I made many requests of the research workers still at HDL for earlier results and recollections of our early work. Among those most frequently consulted were Donald Wortman and Nick Karayianis and I wish to thank them for their prompt responses and their valuable suggestions. The later work and a critical reading of the entire rough notes of the lectures were done by my coworker Richard P. Leavitt. To him I owe a special thanks for numerous helpful suggestions. A number of suggestions from my Brazilian colleagues helped make the lectures more clear. Particular among these were Professor Oscar Malta and Professor Alfredo A. da Gama both of whom I wish to thank for their help. I would also like to thank Evandro J. T. de Araujo Gouveia for his suggestions and finding errors in the notes. In all of the efforts to make the lectures more complete I owe special thanks to Professor Gilberto F. de Sâ. Lastly I would like to thank the entire physics department at the University of Recife for making our stay in Recife a warm and pleasant experience. Both my wife and myself have never before experienced such a pleasant display of hospitality. To all the members of the physics department my wife and I say "muinto obrigado."

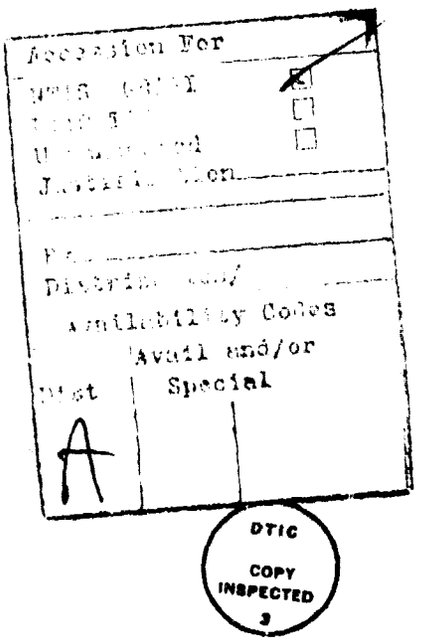

CONTENTS

	Page
PREFACE	3
1. INTRODUCTION	9
2. ANGULAR MOMENTUM ALGEBRA	11
2.1 Angular Momentum Operators	11
2.2 Clebsch-Gordan Coefficients	13
2.3 Wigner-Echart Theorem	16
2.4 Racah Coefficients	18
2.5 Racah Algebra	22
3. FREE-ION HAMILTONIAN	27
3.1 Background for Free Rare-Earth Ions	27
3.2 Significant Free Rare-Earth Ion Interactions	30
3.2.1 Coulomb Interaction	30
3.2.2 Spin-Orbit Interaction	31
3.2.3 Interconfigurational Interaction	36
3.2.4 Other Interactions	36
3.3 Summary	37
4. CRYSTAL-FIELD INTERACTIONS	37
4.1 Phenomenological Theory of Crystal Fields	37
4.1.1 Matrix Elements of H_3 in J States	39
4.1.2 Numerical Example: ^4F_J states of Nd^{+3}	42
4.2 Classical Point-Charge Model	48
4.3 Point-Charge Model Developed at HDL	54
4.3.1 Introduction	54
4.3.2 Screening and Wave Function Spread	55
4.3.3 Effective Charge and Position	56
5. CRYSTAL-FIELD EFFECTS NOT YET FULLY INCORPORATED	60
5.1 Self-Consistent Point Dipole and Point Multipole	60
5.2 Self-Consistent Results for Scheelite Structure	64
5.3 Self-Induced Effects	68

CONTENTS (Cont'd)

Page

6. MISCELLANEOUS CRYSTAL-FIELD EFFECTS 74

6.1 Judd's Interaction for Two Electrons 74
6.2 Slater Integral Shifts 79
6.3 Shifts of Energy Gap $4f^N$-$4f^{N-1}n\ell$ 80

LITERATURE CITED 87

ANNOTATED BIBLIOGRAPHY 91

DISTRIBUTION 121

APPENDIX

APPENDIX A.--RELATIONS THAT ARE USEFUL IN ANALYSIS OF RARE-EARTH ION SPECTRA..... 99

APPENDIX B.--ELECTROSTATICS 107

TABLES

1. Electronic Structure of Triply Ionized Rare-Earth Ions 28

2. Relativistic Hartree-Fock Integrals for Triply Ionized Rare-Earth Ions 32

3. Nonrelativistic Hartree-Fock Integrals for Triply Ionized Rare-Earth Ions 32

4. Free Ion Energy Levels of Triply Ionized Praseodymium and Corresponding Centroids in Two Crystals 34

5. Free-Ion Parameters for Triply Ionized Rare-Earth Ions in $LaCl_3$ Obtained from Fitting Experimental Data 35

6. Free-Ion Parameters for Triply Ionized Rare-Earth Ions in LaF_3 Obtained from Fitting Experimental Data 35

7. Eigenvalues of Casimir's Operators for States of f^2 36

TABLES (Cont'd)

Page

8. Nonrelativistic Hartree-Fock Expectation Values of $\langle r^k \rangle$, Nuclear Spin, and Magnetic Moments of Triply Ionized Rare-Earth Ions 37

9. Values of $\langle J \| U^k \| J \rangle \sqrt{2\ell+1} \langle \ell \| C_k \| \ell \rangle$ 42

10. Crystallographic Axial and Angular Relationships and Characteristic Symmetry of Crystal Systems 51

11. Crystallographic Data for $LiYF_4$ Tetragonal Space Group 88 Z = 4 52

12. Lattice Sums for the Y site at (0, 0, 1/2) for $LiYF_4$ with $Z_Y = 3$, $Z_{Li} = 1$, $Z_F = -1$, $\alpha_f = 0.104$ Å^3 52

13. Crystallographic Data for YCl_3 Monoclinic Space Group 12 Z = 4 53

14. Lattice Sums for Y site at (0, 0.166, 0) for YCl_3, Even-n A_{nm} only, All A_{nm} Real 54

15. Phenomenological B_{nm} for Six Rare-Earth Ions in $CaWO_4$ 57

16. Derived Crystal-Field Parameters, $B_{nm}(\tau; q_o \eta)$, for $4f^N$ Configurations of Triply Ionized Rare-Earth Ions 58

17. Values for $\tau \langle r^n \rangle_{HF}$, σ_n, and ρ_n for $4f^n$ Configuration of Triply Ionized Rare-Earth Ions 59

18. Space Group 88: Coordinates of All Ions in a Unit Cell of $YLiF_4$ and Dipole Moments of Each Ion 64

19. Values of $\vec{R} \cdot \vec{P}$ for Different Sites in Scheelite 67

20. $\underset{\sim}{G}$ Tensor and X-Ray Data for Several Compounds 69

21. Axial Components of Crystal Field for Two Values of Polarizability of Oxygen and Oxygen Charge Units 69

TABLES (Cont'd)

Page

22. Experimental Energy of Lowest Energy Level of $4f^{N-1}5d$ for Free Ion 83

23. Ligand Distance, R, and Multiplicity, Z, for Compounds Listed in Table 22 84

24. Sum S of Equation (313) for Values in Table 23, $\Delta^{0}_{fd} - \Delta_{fd}$ from Table 22, and σ_2 Computed from Equation (311) 84

1. INTRODUCTION

The work at the U.S. Army Harry Diamond Laboratories (HDL) on the experiment and theory of rare-earth ions in transparent host materials was begun in the early 1960's. This was after workers at Bell Telephone Laboratories (Johnson et al, 1962)* demonstrated the first continuous operating laser using neodymium (Nd) in calcium tungstate ($CaWO_4$). It was decided at that time that the HDL group would concentrate on Nd:$CaWO_4$. The group was limited in number at any given time, but over the span of years many research workers were participants. A list of publications pertinent to the theoretical analysis and experimental work on triply ionized rare-earth ions in solids is given in the annotated bibliography.

The plan that the group was to follow during the first two years and still follows is the following: (1) As many as possible of the rare-earth ions were to be doped into the host material $CaWO_4$, and the optical data were to be carefully recorded. (2) These data were to be analyzed by any techniques existing in the literature or developed at HDL to obtain phenomenological crystal-field parameters. (3) A theoretical derivation of the crystal-field parameters was to be developed which gave not only the parameters which were obtained from the experimental data, but also a set of odd-k crystal-field components. (4) The odd-k crystal-field components were to be used to calculate the electric dipole transition probabilities using the theory of Judd (1962) and Ofelt (1962).

As of 1970, all these objectives had been met for $CaWO_4$ (and consequently to a lesser extent for any solid where the rare-earth ion occupies a site of S_4 symmetry). During this time, a number of new theories as well as significant modifications of existing theories were developed. The most important theory thus developed was the HDL three-parameter theory of crystal fields. This theory was a blending of the much older point-charge model, including the effects of covalency and wave-function expansion and screening of the field of the point charge. These effects were encompassed in the three parameters, and a consistent set of these parameters was found for the triply ionized rare-earth series in the host $CaWO_4$. The phenomenological crystal-field parameters used in the development of the theory were those obtained by using an effective spin-orbit Hamiltonian developed by Nick Karayianis at HDL. The optical data were taken by Donald E. Wortman and Ruben T. Farrar of HDL.

Because of the large number of literature citations, these are given in abbreviated form only, not footnoted on each page. Complete literature references are given alphabetically by author in the Literature Cited section.

Since 1970, a number of new additions have been made in the theory, and the ability to analyze the optical data has been achieved. These include:

(1) The development of lattice sums (point-charge model) for any crystalline solid (230 different space groups).
(2) The self-consistent inclusion of the dipole fields for any crystalline solid.
(3) The calculation of the phenomenological crystal-field parameters from experimental data for any solid having point symmetry higher than C_1 or C_i.
(4) The calculation of transition probabilities, Zeeman splitting factors, Judd-Ofelt intensity parameters, branching ratios, and lifetimes for any point symmetry higher than C_1 or C_i.

Of the recent work at HDL done on rare earths, the most significant is the work done on rare-earth ions in lanthanum trifluoride (Ln:LaF_3, Ln=rare-earth ion) (C_2 symmetry) and reported in two papers. Morrison and Leavitt (1979) reported an analysis of the low-temperature optical data which had been previously reported by workers in other laboratories (very much by W. T. Carnall of Argonne National Laboratory). In our analysis, the point-charge lattice sums were used to obtain starting crystal-field parameters in a least-squares fitting. Consequently, sets of crystal-field parameters for almost all the rare-earth ions were obtained which were consistent through the entire series. In the second paper (Leavitt and Morrison, 1980), the results of the lattice sum for the odd-k crystal-field components were used to calculate the Judd-Ofelt intensity parameters and lifetimes for the entire rare-earth series. Wherever possible, these were compared to experimental data, and the agreement was found to be very good.

At present, with J. B. Gruber and N. C. Chang, we are analyzing data on triply ionized rare-earth ions in yttrium oxide (Y_2O_3). This material has two types of sites that the rare-earth ion can occupy, C_2 and C_{3i}. A paper on "The Analysis of the Spectra of Kramers Ions in the C_2 Sites" has been published (Chang, Gruber, Leavitt, and Morrison, 1982). A second paper, "Optical Spectra, Energy Levels, and Crystal-Field Analysis of Tripositive Rare-Earth Ions in Y_2O_3. II. Non-Kramers Ions in C_2 Sites" has been published (Leavitt, Gruber, Chang, and Morrison, 1982). We are now writing a third paper on the rare-earth ions in Y_2O_3 for the rare-earth ions in the C_{3i} sites. This latter paper also will summarize all the work on C_2 sites.

If we find time and money, we intend to extend our computation ability to incorporate more of the free-ion interactions. Also, we would like to incorporate in our programs many of the theories that we have developed at HDL over the last few years. The inclusion of the self-consistent dipole contributions to our theory of crystal fields should improve both the energy-level calculations and the transition probabilities.

2. ANGULAR MOMENTUM ALGEBRA

2.1 Angular Momentum Operators

In classical mechanics, the angular momentum of a particle is defined by

$$\vec{\ell} = \vec{r} \times p \ . \tag{1}$$

Actually, we should specify that the angular momentum so defined is about a particular origin, and $\vec{r}$ is the vector distance from the reference point to the particle with momentum $\vec{p}$.

If we use the commutation relations

$$[x_i, p_j] = i\hbar\delta_{ij} \tag{2}$$

with $x_i = x$, y, or z, then we can obtain the commutation rules for angular momentum,

$$[\ell_x, \ell_y] = i\hbar\ell_z, \ [\ell_y, \ell_z] = i\hbar\ell_x, \text{ and } [\ell_z, \ell_x] = i\hbar\ell_y \ , \tag{3}$$

which are the basic commutation rules for the Cartesian components of the angular momentum. For convenience here we shall drop the $\hbar$ in the commutation relations. This does not mean that we drop $\hbar$ throughout; we restore $\hbar$ simply by writing the interactions involving the angular momentum so that the $\hbar$ is contained in the constants. As an example of this, we consider the spin-orbit Hamiltonian

$$H_2 = \frac{1}{2m^2c^2} \frac{1}{r} \frac{\partial U}{\partial r} \vec{\ell}\cdot\vec{s} \ , \tag{4}$$

with $\vec{\ell}$ and $\vec{s}$ (the spin angular momentum, $\vec{s}$, we will discuss later) containing $\hbar$ as in equation (3). When written in terms of unitless $\vec{\ell}$ and $\vec{s}$, we have

$$H_2 = \frac{\hbar^2}{2m^2c^2} \frac{1}{r} \frac{\partial U}{\partial r} \vec{\ell}\cdot\vec{s} \tag{5}$$

where $\vec{\ell}$ and $\vec{s}$ obey the commutation rules in equation (3) but $\hbar = 1$.

For our purposes here, we want to use the spherical representation of $\vec{\ell}$, which is given by

$$\begin{aligned} \ell_{+1} &= -\frac{1}{\sqrt{2}} (\ell_x + i\ell_y) \ , \\ \ell_0 &= \ell_z \ , \\ \ell_{-1} &= \frac{1}{\sqrt{2}} (\ell_x - i\ell_y) \ , \end{aligned} \tag{6}$$

and the commutation rules are

$$[\ell_0, \ell_{+1}] = \ell_{+1} ,$$
$$[\ell_{-1}, \ell_0] = \ell_{-1} , \tag{7}$$
$$[\ell_{+1}, \ell_{-1}] = -\ell_0 .$$

The eigenfunctions of the angular momentum are the spherical harmonics, $Y_{\ell m}(\theta, \phi)$ and

$$\ell_z |\ell m\rangle = m|\ell m\rangle ,$$
$$\ell_{\pm 1}|\ell m\rangle = \mp \frac{1}{\sqrt{2}} [(\ell \mp m)(\ell \pm m+1)]^{1/2} |\ell; m\pm 1\rangle , \tag{8}$$

where

$$|\ell m\rangle = Y_{\ell m}(\theta, \phi) .$$

Frequently, we shall use the unit vector $\hat{r}$ to indicate the argument of $Y_{\ell m}$, thus:

$$Y_{\ell m}(\theta, \phi) = Y_{\ell m}(\hat{r}) .$$

When the $Y_{\ell m}$ are wave functions such as in equation (8), we have

$$Y_{\ell m}(\hat{r}) = |\ell m\rangle .$$

The wave functions have the property that

$$\langle \ell' m' | \ell m\rangle = \delta_{\ell \ell'} \delta_{mm'} .$$

Further, we shall assume that the spin angular momentum, $\vec{s}$, obeys the same commutation relations as equation (7); the two-component spinor wave functions are represented by the wave function $|sm_s\rangle$, so that the single electron wave function for orbital and spin angular momentum is

$$|\ell m_\ell\rangle |sm_s\rangle . \tag{9}$$

The wave functions given by equation (9) then obey the following:

$$\ell_o |\ell m_\ell\rangle |sm_s\rangle = m_\ell |\ell m_\ell\rangle |sm_s\rangle ,$$
$$(\vec{\ell})^2 |\ell m_\ell\rangle |sm_s\rangle = \ell(\ell+1) |\ell m_\ell\rangle |sm_s\rangle , \tag{10}$$

$$s_o|\ell m_\ell\rangle|sm_s\rangle = m_s|\ell m_\ell\rangle|sm_s\rangle \ ,$$

$$(\vec{s})^2|\ell m_\ell\rangle|sm_s\rangle = s(s+1)|\ell m_\ell\rangle|sm_s\rangle \ ,$$

where, of course, s = 1/2. A further property of the spherical harmonics is

$$IY_{\ell m}(\hat{r}) = (-1)^\ell Y_{\ell m}(\hat{r}) \quad , \tag{11}$$

where the inversion operator is $I\hat{r} = -\hat{r}$, a property that will be used frequently in our analysis. While many of the interaction terms of the Hamiltonian were derived by using spherical harmonics, it is convenient to introduce the tensor operators

$$C_{\ell m}(\hat{r}) = \sqrt{\frac{4\pi}{2\ell+1}}\ Y_{\ell m}(\hat{r}) \tag{12}$$

Since $Y^*_{\ell m}(\hat{r}) = (-1)^m Y_{\ell,-m}(\hat{r})$, we have

$$C^*_{\ell m}(\hat{r}) = (-1)^m C_{\ell,-m}(\hat{r}) \quad . \tag{13}$$

The use of $C_{\ell m}$ rather than $Y_{\ell m}$ in the interaction terms eliminates almost all the factors of 4π. An example of this is the coupling rule for spherical harmonics (Rose, 1957: 61):

$$Y_{kq}Y_{nm} = \sum_\ell \left[\frac{(2k+1)(2n+1)}{4\pi(2\ell+1)}\right]^{1/2} \langle k(0)n(0)|\ell(0)\rangle\langle k(q)n(m)|\ell(q+m)\rangle Y_{\ell,q+m} \ , \tag{14}$$

but

$$C_{kq}C_{nm} = \sum_\ell \langle k(0)n(0)|\ell(0)\rangle\langle k(q)n(m)|\ell(q+m)\rangle C_{\ell,q+m} \quad . \tag{15}$$

In equations (14) and (15) all the tensor operators have the same argument.

2.2 Clebsch-Gordan Coefficients

For our purpose, it is convenient to define the Clebsch-Gordan (C-G) coefficients as the coefficients in the transformation from two

angular momentum spaces, say, $\vec{\ell}$ and $\vec{s}$, to form the composite space $\vec{j}$. That is,

$$|jm\rangle = \sum_{\mu} \langle \ell(\mu)s(m-\mu)|j(m)\rangle |\ell\mu\rangle |s,m-\mu\rangle \ , \tag{16}$$

where the quantity $\langle \ell(\mu)s(m-\mu)|j(m)\rangle$ is a C-G coefficient. Since we wish to have orthonormal basis, we have

$$\begin{aligned} \langle j'm'|jm\rangle &= \delta_{jj'}\delta_{mm'} \\ &= \sum_{\mu\mu'} \langle \ell(\mu)s(m-\mu)|j(m)\rangle\langle \ell(\mu')s(m'-\mu')|j'(m')\rangle \end{aligned} \tag{17}$$

since

$$\langle \ell\mu'|\ell\mu\rangle = \delta_{\mu\mu'} \quad \text{and} \quad \langle s,m'-\mu'|s,m-\mu\rangle = \delta_{m-\mu,m'-\mu'} \ . \tag{18}$$

Thus, we have

$$\delta_{jj'} = \sum_{\mu} \langle \ell(\mu)s(m-\mu)|j(m)\rangle\langle \ell(\mu)s(m-\mu)|j'(m)\rangle \ , \tag{19}$$

an important and very useful result. If we assume (correctly) that the same coefficients connect the $\vec{j}$ space to the $\vec{\ell}$ and $\vec{s}$ spaces, we can obtain another condition on the C-G coefficients, namely,

$$\delta_{\ell\ell'}\delta_{ss'} = \sum_{j} \langle \ell(m_\ell)s(m_s)|j(m_\ell+m_s)\rangle\langle \ell'(m_\ell)s'(m_s)|j(m_\ell+m_s)\rangle \ . \tag{20}$$

Some other relations among C-G coefficients are

$$\langle a(\alpha)b(\beta)|c(\gamma)\rangle = 0 \text{ if } |\alpha| > a, \text{ or } |\beta| > b, \text{ or } |\gamma| > c$$

$$\text{and if } \gamma \neq \alpha + \beta \ .$$

The C-G coefficients vanish unless the three angular momenta obey the triangle condition, or $|a - b| \leq c \leq a + b$ and any permutation of a, b, or c. Further properties of the C-G coefficients are given in appendix A.

The commutation relations for the spherical components of the angular momentum of a single electron given in equations (7) and (8) can be written compactly in terms of C-G coefficients as

$$[\ell_\mu, \ell_\nu] = \sqrt{2}\ \langle 1(\nu)1(\mu)|1(\mu+\nu)\rangle \ell_{\mu+\nu} \tag{7a}$$

and

$$[s_\mu, s_\nu] = \sqrt{2}\ \langle 1(\nu)1(\mu)|1(\mu+\nu)\rangle s_{\mu+\nu} \quad . \tag{8a}$$

The total angular orbital momentum operator for a system of N electrons is

$$\vec{L} = \sum_i^N \vec{\ell}(i) \quad , \tag{21}$$

and the total spin angular momentum operator is

$$\vec{S} = \sum_i^N \vec{s}(i) \quad . \tag{22}$$

The spherical components of these operators obey the same commutation relations as equations (7a) and (8a), or

$$[L_\mu, L_\nu] = \sqrt{2}\ \langle 1(\nu)1(\mu)|1(\mu+\nu)\rangle L_{\mu+\nu} \tag{23}$$

and

$$[S_\mu, S_\nu] = \sqrt{2}\ \langle 1(\nu)1(\mu)|1(\mu+\nu)\rangle S_{\mu+\nu} \quad . \tag{24}$$

Also, it should be noted that

$$[L_\mu, \ell_\nu(i)] = \sqrt{2}\ \langle 1(\nu)1(\mu)|1(\mu+\nu)\rangle \ell_{\mu+\nu}(i) \tag{25}$$

and

$$[S_\mu, s_\nu(i)] = \sqrt{2}\ \langle 1(\nu)1(\mu)|1(\mu+\nu)\rangle s_{\mu+\nu}(i) \quad . \tag{26}$$

Consequently, from using equations (23) through (26), we have

$$[L_\mu, C_{kq}(i)] = \sqrt{k(k+1)}\ \langle k(q)1(\mu)|k(q+\mu)\rangle C_{k,q+\mu}(i) \quad , \tag{27}$$

$$[J_\mu, C_{kq}(i)] = [L_\mu, C_{kq}(i)] \tag{28}$$

with

$$\vec{J} = \vec{L} + \vec{S} \quad . \tag{29}$$

2.3 Wigner-Echart Theorem

The Wigner-Echart theorem states that if we have a spherical tensor T_{kq} in the space spanned by the wave functions $|JM\rangle$, then the matrix elements are

$$\langle J'M'|T_{kq}|JM\rangle = \langle J(M)k(q)|J'(M')\rangle\langle J'\|T_k\|J\rangle \quad . \tag{30}$$

The projection (q) dependence is contained in the C-G coefficients, and the factors $\langle J'\|T_k\|J\rangle$ are called the reduced matrix elements.

If we have a mixed spherical tensor, rank κ, projection λ, in spin space and rank k, projection q, in orbital space, the Wigner-Echart theorem then is

$$\begin{aligned}&\langle L'M_L'S'M_S'|T^{\kappa k}_{\lambda q}|LM_LSM_S\rangle \\ &= \langle L(M_L)k(q)|L'(M_L')\rangle\langle S(M_S)\kappa(\lambda)|S'(M_S')\rangle \\ &\quad \times \langle L'S'\|T^{\kappa k}\|LS\rangle \quad .\end{aligned} \tag{31}$$

Since the C-G coefficient is purely a geometrical factor, all the physics is contained in the reduced matrix element. The Wigner-Echart theorem allows the extraction of the geometrical factors from many complicated matrix elements; it also serves as perhaps the main motivation for the development of Racah algebra in dealing with angular momentum states.

Because of the power of the Wigner-Echart theorem, it occurred to Racah to cast the various operators representing the interactions in terms of universal quantities that could be tabulated for a frequently used many-particle system. Toward this end, Racah introduced the unit spherical tensors for the electronic configuration $n\ell^N$ which we define as

$$\langle \ell'm'|u_{kq}|\ell m\rangle = \langle \ell(\mu)k(q)|\ell(m')\rangle\delta_{\ell\ell'}$$

for the orbital space and

$$\begin{aligned}&\langle \ell'm's'mi|v^{\kappa k}_{\lambda q}|\ell msms\rangle \\ &= \langle \ell(m)k(q)|\ell(m')\rangle\langle s(m_s)\kappa(\lambda)|s(m_s')\rangle \\ &\quad \times \delta_{\ell\ell'}\delta_{ss'} \quad ,\end{aligned} \tag{32}$$

for orbital and spin space.

The generalization to an N-electron system is simply

$$U_{kq} = \sum_i^N u_{kq}(i)$$

and

$$V^{\kappa k}_{\lambda q} = \sum_i^N v^{\kappa k}_{\lambda q}(i) \quad . \tag{33}$$

A simple and often used example of these tensors in orbital space is (we shall omit the upper limit on the i sum in the remainder of the discussion)

$$\begin{aligned} \sum_i C_{kq}(i) &= \sum_i \langle \ell \| C_k \| \ell \rangle u_{kq}(i) \\ &= \langle \ell \| C_k \| \ell \rangle U_{kq} \end{aligned} \quad , \tag{34}$$

where

$$\begin{aligned} \langle \ell \| C_k \| \ell \rangle &= \langle \ell(0) k(0) | \ell(0) \rangle \\ L_\mu &= \sum_i \ell_\mu(i) \\ &= \sum_i \langle \ell \| \ell \| \ell \rangle u_{1\mu}(i) \\ &= \langle \ell \| \ell \| \ell \rangle U_{1\mu} \quad , \text{ and} \\ \langle \ell \| \ell \| \ell \rangle &= \sqrt{\ell(\ell+1)} \quad . \end{aligned} \tag{35}$$

An example of a tensor in a mixed spin and orbital space occurs in the hyperfine interaction H_5, given by

$$H_5 = \left(2\beta\beta_N \mu_N / I\right) \sum_i \vec{N}_i \cdot \vec{I} / r_i^3 \quad , \tag{36}$$

where β is the Bohr magneton, β_N is the nuclear magneton, μ_N is the nuclear moment, and I is the nuclear spin. Now

$$\vec{N}_i = \vec{\ell}_i - \vec{s}_i + 3\vec{r}_i \left(\vec{r}_i \cdot \vec{s}_i\right)/r_i^2 \tag{37}$$

or

$$N_q(i) = \ell_q(i) - \sqrt{10} \sum_{\nu} \langle 1(\nu)2(q-\nu)|1(q)\rangle s_\nu(i) C_{2,q-\nu}(i) \qquad (38)$$

(we shall show later how eq (38) is obtained from eq (37)).

The part of $N_q(i)$ containing $\ell_q(i)$ can be written in terms of U_{1q}, as in the second part of equation (35):

$$\sum_i s_\nu(i) C_{2,q-\nu}(i) = \langle s\|s\|s\rangle \langle \ell\|C_2\|\ell\rangle V^1_{\nu,q-\nu}{}^2 \, . \qquad (39)$$

A component of $\vec{N} = \sum_i \vec{N}_i$ can be written

$$N_q = \sqrt{\ell(\ell+1)}\, V_{1q} - \sqrt{10}\, \sqrt{s(s+1)} \langle \ell(0)2(0)|\ell(0)\rangle \times \sum_\nu \langle 1(\nu)2(q-\nu)|1(q)\rangle V^1_{\nu,q-\nu}{}^2 \, . \qquad (40)$$

Thus, equation (36) can be written

$$H_5 = \left(2\beta\beta_N \mu_N / I\right) \langle 1/r^3 \rangle \sum_q N_q I^*_q \, , \qquad (41)$$

with N_q given by equation (40).

2.4 Racah Coefficients

The Racah coefficients arise in the coupling of three angular momenta (Rose, 1957: 107) to form a final resultant. In the coupling of the angular momenta, we consider two coupling schemes:

$$\text{scheme A:} \quad \vec{j}_1 + \vec{j}_2 = \vec{j}_{12}, \quad \vec{j}_{12} + \vec{j}_3 = \vec{j} \, , \qquad (42)$$

$$\text{scheme B:} \quad \vec{j}_1 + \vec{j}_3 = \vec{j}_{13}, \quad \vec{j}_{13} + \vec{j}_2 = \vec{j} \, . \qquad (43)$$

Coupling scheme A is represented by the wave function

$$|A\rangle = \sum_{m_1 m_2 m_3} \langle j_1(m_1) j_2(m_2)|j_{12}(m_1+m_2)\rangle \langle j_{12}(m_1+m_2) j_3(m_3)|j(m)\rangle \times |j_1 m_1 j_2 m_2 j_3 m_3\rangle \, ; \qquad (44)$$

scheme B is represented by the wave function

$$|B\rangle = \sum_{m_1 m_2 m_3} \langle j_1(m_1) j_3(m_3) | j_{13}(m_1+m_3)\rangle \langle j_{13}(m_1+m_3) j_2(m_2) | j(m)\rangle \times |j_1 m_1 j_2 m_2 j_3 m_3\rangle \quad . \tag{45}$$

The coupling schemes A and B are connected by a unitary transformation

$$|B\rangle = \sum_A \langle A|B\rangle |A\rangle \quad ; \tag{46}$$

the coefficients of the unitary transformation are determined by taking the inner product of equation (44) with equation (45).

We define the Racah coefficients as follows:

$$W(j_1 j_{12} j_{13} j_3; j_1 j) = \frac{1}{[(2j_{12}+1)(2j_{13}+1)]^{1/2}} \langle A|B\rangle \quad . \tag{47}$$

Thus,

$$[(2j_{12}+1)(2j_{13}+1)]^{1/2} W(j_2 j_{12} j_{13} j_3; j_1 j)$$

$$= \sum_{m_1 m_2} \langle j_1(m_1) j_2(m_2) | j_{12}(m_1+m_2)\rangle \langle j_{12}(m_1+m_2) j_3(m-m_1-m_2) | j(m)\rangle \tag{48}$$

$$\times \langle j_1(m_1) j_3(m-m_1-m_2) | j_{13}(m-m_2)\rangle \langle j_{13}(m-m_2) j_2(m_2) | j(m)\rangle \quad .$$

The following equation can be obtained from equation (48):

$$\langle j_2(m_2) j_1(m_1) | j_{12}(m_1+m_2)\rangle \langle j_{12}(m_1+m_2) j_3(m-m_1-m_2) | j(m)\rangle$$

$$= \sum_{j_{13}} [(2j_{12}+1)(2j_{13}+1)]^{1/2} W(j_2 j_1 j j_3; j_{12} j_{13}) \tag{49}$$

$$\times \langle j_1(m_1) j_3(m-m_1-m_2) | j_{13}(m-m_2)\rangle \langle j_2(m_2) j_{13}(m-m_2) | j(m)\rangle \quad ,$$

which is a relationship used often in our analysis.

The Racah coefficient is related to the symmetrized "6j" symbol by the following equation:

$$W(abcd;ef) = (-)^{a+b+c+d} \begin{Bmatrix} a & b & e \\ d & c & f \end{Bmatrix} \quad . \tag{50}$$

Certain symmetry relations exist for the "6j" symbols:

$$\begin{Bmatrix} j_1 & j_2 & j_3 \\ \ell_1 & \ell_2 & \ell_3 \end{Bmatrix} = \begin{Bmatrix} j_2 & j_1 & j_3 \\ \ell_2 & \ell_1 & \ell_3 \end{Bmatrix} = \begin{Bmatrix} j_1 & j_3 & j_2 \\ \ell_1 & \ell_3 & \ell_2 \end{Bmatrix} = \begin{Bmatrix} j_1 & \ell_2 & \ell_3 \\ \ell_1 & j_2 & j_3 \end{Bmatrix} \tag{51}$$

and all combinations of the relations in equation (47). The four triads $(j_1\ j_2\ j_3)$, $(j_1\ \ell_2\ \ell_3)$, $(\ell_1\ j_2\ \ell_3)$, and $(\ell_1\ \ell_2\ j_3)$ must be able to form a triangle. That is,

$$|j_1-j_2| \le j_3 \le j_1+j_2, \tag{52}$$

with similar relations for the other triads.

An example of the use of Racah coefficients is in the calculation of single-electron matrix elements of the operator

$$E_{k'q} = \sum_{\lambda} \langle k(q-\lambda)1(\lambda)|k'(q)\rangle C_{k,q-\lambda}{}^{\ell}{}_{\lambda} \quad , \tag{53}$$

which arises in numerous applications. We consider the matrix element

$$\langle \ell'm'|E_{k'q}|\ell m\rangle = \langle \ell(m)k'(q)|\ell'(m')\rangle \langle \ell'\|E_{k'}\|\ell\rangle \tag{54}$$

by application of the Wigner-Echart theorem, equation (30). Also, by taking the same matrix element of equation (53) we have

$$\langle \ell'm'|E_{k'q}|\ell m\rangle = \sum_{\lambda} \langle k(q-\lambda)1(\lambda)|k'(q)\rangle \langle \ell'm'|C_{k,q-\lambda}{}^{\ell}{}_{\lambda}|\ell m\rangle \quad . \tag{55}$$

Now we further consider the matrix element in equation (55) to obtain

$$\langle \ell'm'|C_{k,q-\lambda}{}^{\ell}{}_{\lambda}|\ell m\rangle = \sum_{\ell''m''} \langle \ell'm'|C_{k,q-\lambda}|\ell''m''\rangle \langle \ell''m''|\ell_{\lambda}|\ell m\rangle \quad , \tag{56}$$

where we have used matrix algebra on the product of two operators. If we apply the Wigner-Echart theorem to the last matrix element in equation (56), we obtain

$$\langle \ell''m''|\ell_{\lambda}|\ell m\rangle = \langle \ell(m)1(\lambda)|\ell''(m'')\rangle \delta_{\ell\ell''} \langle \ell\|\ell\|\ell\rangle \quad ; \tag{57}$$

also, $m'' = m + \lambda$ as required by the C-G coefficient. It can be shown that

$$\langle \ell\|\ell\|\ell\rangle = \sqrt{\ell(\ell+1)} \quad . \tag{58}$$

Then,

$$\langle \ell''m''|\ell_\lambda|\ell m\rangle = \langle \ell(m)1(\lambda)|\ell''(m+\lambda)\rangle \delta_{\ell\ell''}\sqrt{\ell(\ell+1)} \quad . \tag{59}$$

Using these results in the remaining C-G in equation (56), we have

$$\langle \ell'm'|C_{k,q-\lambda}|\ell(m+\lambda)\rangle = \langle \ell(m+\lambda)k(q-\lambda)|\ell'(m')\rangle\langle \ell'\|C_k\|\ell\rangle \quad . \tag{60}$$

Substituting the result of equations (60) and (59) into equation (56), we have

$$\begin{aligned}\langle \ell'm'|C_{k,q-\lambda}\ell_\lambda|\ell m\rangle &= \sqrt{\ell(\ell+1)}\langle \ell'\|C_k\|\ell\rangle\langle \ell(m)1(\lambda)|\ell(m+\lambda)\rangle \\ &\quad \times \langle \ell(m+\lambda)k(q-\lambda)|\ell'(m')\rangle \quad ,\end{aligned} \tag{61}$$

giving the matrix element in equation (55). If we substitute the result of equation (61) into equation (55), then we have

$$\langle \ell'm'|E_{k'q}|\ell m\rangle = \sqrt{\ell(\ell+1)}\,\langle \ell'\|C_k\|\ell\rangle S \quad , \tag{62}$$

where

$$S = \sum_\lambda \langle k(q-\lambda)1(\lambda)|k'(q)\rangle\langle \ell(m)1(\lambda)|\ell(m+\lambda)\rangle\langle \ell(m+\lambda)k(q-\lambda)|\ell'(m')\rangle \quad . \tag{63}$$

The last two C-G coefficients in equation (63) can be recoupled by using equation (49) or

$$\begin{aligned}&\langle \ell(m)1(\lambda)|\ell(m+\lambda)\rangle\langle \ell(m+\lambda)k(q-\lambda)|\ell'(m')\rangle \\ &\quad = \sum_f \sqrt{(2f+1)(2\ell+1)}\; W(\ell 1\ell' k;\ell f)\langle \ell(\lambda)k(q-\lambda)|f(q)\rangle \\ &\quad\quad \times \langle \ell(m)f(q)|\ell'(m')\rangle \quad .\end{aligned} \tag{64}$$

The C-G coefficients in equation (64) can be rearranged by using the symmetry rules to give

$$\langle 1(\lambda)k(q-\lambda)|f(q)\rangle = (-1)^{1+k-f}\langle k(q-\lambda)1(\lambda)|f(q)\rangle \quad . \tag{65}$$

This C-G coefficient and the first C-G coefficient in equation (63) are the only two C-G coefficients containing λ, so that

$$\sum_\lambda \langle k(q-\lambda)1(\lambda)|k'(q)\rangle\langle k(q-\lambda)1(\lambda)|f(q)\rangle = \delta_{fk'} \tag{66}$$

because of the orthogonality, as shown in equation (19), of the C-G coefficients. Thus, we get

$$S = (-1)^{1+k-k'}\sqrt{(2k'+1)(2\ell+1)}\; W(\ell 1\ell' k;\ell k')\langle \ell(m)k'(q)|\ell'(m')\rangle \quad , \tag{67}$$

which when substituted into equation (62) gives

$$\langle \ell'm'|E_{k'q}|\ell m\rangle = (-1)^{1+k-k'}\sqrt{\ell(\ell+1)(2\ell+1)(2k'+1)}\; W(\ell 1\ell' k;\ell k')\langle \ell'\|C_k\|\ell\rangle \times \langle \ell(m)k'(q)|\ell'(m')\rangle \quad . \tag{68}$$

Upon comparing the result given in equation (54) with equation (68), we have

$$\langle \ell'\|E_{k'}\|\ell\rangle = (-1)^{1+k-k'}[\ell(\ell+1)(2\ell+1)(2k'+1)]^{1/2}\langle \ell'\|C_k\|\ell\rangle \times W(\ell 1\ell' k;\ell k') \quad , \tag{69}$$

which is a useful relation if we wished to express the tensor $E_{k'q}$ in terms of unit spherical tensors; in that case we would specialize equation (69) to $\ell' = \ell$ and simply replace C_{kq} in equation (34) by E_{kq} with the reduced matrix element given by equation (69). We shall have frequent occasion to express our results in terms of Racah coefficients by using equation (49).

2.5 Racah Algebra

It is convenient in many vector problems to express the vectors in terms of spherical bases given by

$$\hat{e}_{\pm 1} = \mp(\hat{e}_x \pm i\hat{e}_y)/\sqrt{2} \quad , \qquad \hat{e}_0 = \hat{e}_z \quad . \tag{70}$$

Then $\hat{e}^*_\mu = (-1)^\mu \hat{e}_{-\mu}$,

$$\hat{e}_\mu \times \hat{e}_\nu = -i\sqrt{2}\langle 1(\nu)1(\mu)|1(\mu+\nu)\rangle \quad , \qquad \hat{e}^*_\mu \cdot \hat{e}_\nu = \delta_{\mu\nu} \quad . \tag{71}$$

The vector $\vec{A}$ can be written

$$\vec{A} = \sum_{\mu} \hat{e}^{*}_{\mu} A_{\mu} \qquad (72)$$

$$= \sum_{\mu} \hat{e}_{\mu} A^{*}_{\mu}$$

and

$$\vec{A} \cdot \vec{B} = \sum_{\mu} A^{*}_{\mu} B_{\mu}$$

$$= \sum_{\mu} A_{\mu} B^{*}_{\mu} \qquad (73)$$

$$= \sum_{\mu} (-1)^{\mu} A_{-\mu} B_{\mu} \ .$$

Thus, $\vec{\ell} \cdot \vec{s}$ in equation (5) can be written

$$\vec{\ell} \cdot \vec{s} = \sum \ell^{*}_{\mu} s_{\mu} \qquad (74)$$

so that the spin-orbit interaction given in equation (5) is immediately in spherical tensors, since ℓ_{μ} and s_{μ} are spherical tensors.

As an application of Racah algebra and some of the other material discussed above, we shall derive the gradient formula (Rose, 1957: 120). A convenient form for the gradient operator is

$$\nabla = \hat{r} \frac{\partial}{\partial r} - i \frac{\hat{r} \times \vec{\ell}}{r} \ , \qquad (75)$$

and we would like

$$\text{grad } \phi(r) C_{kq}(\hat{r}) \equiv \left[\nabla, \phi(r) C_{kq}\right] \ . \qquad (76)$$

First we observe that

$$\hat{r} C_{kq} = \sum_{\lambda} (-1)^{\lambda} \hat{e}_{-\lambda} C_{1\lambda} C_{kq}$$

$$= \sum_{\lambda, k'} (-1)^{\lambda} \hat{e}_{-\lambda} \langle 1(0) k(0) | k'(0) \rangle \langle 1(\lambda) k(q) | k'(q+\lambda) \rangle C_{k', q+\lambda} \ , \qquad (77)$$

where we have used the coupling rule for spherical harmonics, equation (15) (Rose, 1957: 61). Now we write

$$\hat{r} \times \vec{\ell} = \sum_{\alpha\beta} (-1)^{\alpha+\beta} \hat{e}_\alpha \times \hat{e}_\beta C_{1-\alpha} \ell_{-\beta} \quad ; \tag{78}$$

we use equation (71) to eliminate the cross product to produce

$$\hat{r} \times \vec{\ell} = -i\sqrt{2} \sum_{\lambda,\alpha} (-1)^\lambda \langle 1(\lambda-\alpha)1(\alpha)|1(\lambda)\rangle \hat{e}_\lambda C_{1-\alpha} \ell_{\alpha-\lambda} \quad , \tag{79}$$

where we have replaced the sum on β by letting $\beta = \lambda - \alpha$. Now in calculating the commutation we need only consider the operators in equation (79); thus, we need

$$[C_{1-\alpha} \ell_{\alpha-\lambda}, C_{kq}] \quad . \tag{80}$$

Since $\phi(r)$ commutes with $C_{1-\alpha} \ell_{\lambda-\alpha}$, we need not consider it at present. First we expand the commutator to obtain

$$[C_{1-\alpha} \ell_{\alpha-\lambda}, C_{kq}] = C_{1-\alpha} \ell_{\alpha-\lambda} C_{kq} - C_{kq} C_{1-\alpha} \ell_{\alpha-\lambda} \quad ; \tag{81}$$

we then use

$$\ell_{\alpha-\lambda} C_{kq} = [\ell_{\alpha-\lambda}, C_{kq}] + C_{kq} \ell_{\alpha-\lambda} \tag{82}$$

in equation (81) to obtain

$$[C_{1-\alpha} \ell_{\alpha-\lambda}, C_{kq}] = C_{1-\alpha} [\ell_{\alpha-\lambda}, C_{kq}] + C_{1-\alpha} C_{kq} \ell_{\alpha-\lambda} - C_{kq} C_{1-\alpha} \ell_{\alpha-\lambda} \quad . \tag{83}$$

The last two terms cancel since $C_{1-\alpha}$ and C_{kq} commute. Thus, we obtain

$$[C_{1-\alpha} \ell_{\alpha-\lambda}, C_{kq}] = C_{1-\alpha} [\ell_{\alpha-\lambda}, C_{kq}] \tag{84}$$

$$= C_{1-\alpha} \sqrt{k(k+1)} \langle k(q)1(\alpha-\lambda)|k(q+\alpha-\lambda)\rangle C_{k,q+\alpha-\lambda} \quad , \tag{85}$$

where we have used equation (27) with $L_{\alpha-\lambda} = \ell_{\alpha-\lambda}$ (which are identical in the commutation brackets). The result in equation (85) is not quite in the form we want, but by using the coupling rule for spherical harmonics given in equation (15), we finally obtain

$$[C_{1-\alpha} \ell_{\alpha-\lambda}, C_{kq}] = \sqrt{k(k+1)} \langle k(q)1(\alpha-\lambda)|k(q+\alpha-\lambda)\rangle \tag{86}$$

$$\times \sum_{k''} \langle k(0)1(0)|k''(0)\rangle \langle k(q-\alpha-\lambda)1(-\alpha)|k''(q-\lambda) C_{k'',q-\lambda} \quad .$$

In equations (75), (76), and (79), we need

$$\left[\vec{r}\times\vec{\ell}, C_{kq}\right] \quad ; \tag{87}$$

we can see from equations (86) and (79) that, when this is formed, the terms dependent on α are

$$S = \sum_{\alpha} \langle 1(\alpha-\lambda)1(-\alpha)|1(\lambda)\rangle\langle k(q)1(\alpha-\lambda)|k(q+\alpha-\lambda)\rangle \times \langle k(q+\lambda-\alpha)1(-\alpha)|k''(q-\lambda)\rangle \quad ; \tag{88}$$

that is,

$$\left[\vec{r}\times\vec{\ell}, C_{kq}\right] = i\sqrt{2} \sum_{\lambda,\alpha,k''} (-1)^{\lambda}\hat{e}_{\lambda}\langle k(0)1(0)|k''(0)\rangle\sqrt{k(k+1)} \times S C_{k'',q-\lambda} \tag{89}$$

with S given by equation (88). The sum, S, given by equation (88) can be reduced. First we write

$$\langle k(q)1(\alpha-\lambda)|k(q+\alpha-\lambda)\rangle\langle k(q+\alpha-\lambda)1(-\alpha)|k''(q-\lambda)\rangle = \sum_{f} \sqrt{(2f+1)(2k+1)}\, W(k1k''1;kf)\langle 1(\alpha-\lambda)1(-\alpha)|f(-\lambda)\rangle\langle k(q)f(-\lambda)|k''(q-\lambda)\rangle \quad , \tag{90}$$

where we have used equation (49). Thus, the sum over α contains the terms

$$\sum_{\alpha} \langle 1(\alpha-\lambda)1(-\alpha)|1(-\lambda)\rangle\langle 1(\alpha-\lambda)1(-\alpha)|f(-\lambda)\rangle = \delta_{f1} \tag{91}$$

by the orthogonality of the C-G coefficients. We can use equations (91) and (90) in equation (88) to obtain

$$S = \sqrt{3(2k+1)}\, W(k1k''1;k1)\langle k(q)1(-\lambda)|k''(q-\lambda)\rangle \quad . \tag{92}$$

Using the results of equation (92) in equation (89) gives

$$\left[\vec{r}\times\vec{\ell}, C_{kq}\right] = i\sqrt{6k(k+1)(2k+1)} \sum_{\lambda} (-1)^{\lambda}\hat{e}_{-\lambda} \sum_{k''} \langle k(0)1(0)|k(0)\rangle W\langle k1k''1;k1\rangle \times \langle k(q)1(\lambda)|k''(q+\lambda)\rangle C_{k'',q+\lambda} \quad , \tag{93}$$

where we have changed the sign of λ in the sum. Multiplying the results given in equation (93) by $-i\phi(r)/r$ and combining them with equation (33), we have (changing k" to k')

$$\left[\nabla, \phi(r)C_{kq}\right] = \sum_{\lambda} (-1)^{\lambda} \hat{e}_{-\lambda} \sum_{k'} \left[\frac{\partial \phi}{\partial r} + \frac{\phi}{r}\sqrt{6k(k+1)(2k+1)}\; W(k1k'1;k1)\right] \times \langle k(0)1(0)|k'(0)\rangle\langle k(q)1(\lambda)|k'(q+\lambda)\rangle C_{k',q+\lambda} \quad . \tag{94}$$

The Racah coefficients in equation (94) are of simple form and are given by Rose (1957: 227). These are

$$W(k1k'1;k1) = -\left[\frac{k}{6(k+1)(2k+1)}\right]^{1/2} \quad , \qquad k' = k + 1$$
$$= \left[\frac{k+1}{6k(2k+1)}\right]^{1/2} \quad , \qquad k' = k - 1 \tag{95}$$

which are the only values of k' allowed. These results used in equation (94) can be written as

$$\left[\nabla, \phi(r)C_{kq}\right] = \sum_{\lambda} (-1)^{\lambda} \hat{e}_{-\lambda} \sum_{k'} \langle k(q)1(\lambda)|k'(q+\lambda)\rangle C_{k',q+\lambda} D^{k'} \phi(r) \quad , \tag{96}$$

where

$$D^{k'} = \sqrt{\frac{k+1}{2k+1}}\left(\frac{\partial}{\partial r} - \frac{k}{r}\right) \quad , \qquad k' = k + 1 \quad , \tag{96a}$$

$$D^{k'} = -\sqrt{\frac{k}{2k+1}}\left(\frac{\partial}{\partial r} + \frac{k+1}{r}\right) \quad , \qquad k' = k - 1 \quad , \tag{96b}$$

and we have used the result

$$\langle k(0)1(0)|k+1(0)\rangle = \sqrt{\frac{k+1}{2k+1}} \text{ and}$$

$$\langle k(0)1(0)|k-1(0)\rangle = -\sqrt{\frac{k}{2k+1}}$$

(from Rose, 1957: 225). The two most common forms of $\phi(r)$ that we will encounter are r^k and $1/r^{k+1}$. For $\phi(r) = r^k$, we obtain

$$\left[\nabla_{\mu}, r^k C_{kq}\right] = -\sqrt{k(2k+1)}\; \langle k(q)1(\mu)|k-1(q+\mu)\rangle r^{k-1} C_{k-1,q+\mu} \quad , \tag{97}$$

and for $\phi = 1/r^{k+1}$,

$$\left[\nabla_\mu, 1/r^{k+1}C_{kq}\right] = -\sqrt{(k+1)(2k+1)}\ \langle k(q)1(\mu)|k+1(q+\mu)\rangle 1/r^{k+2}C_{k+1,q+\mu} \quad . \tag{98}$$

The results given in equation (98) are easily checked for k = 0, since for k = 0 we have

$$\left[\nabla_\mu, 1/r\right] = -\langle 0(q)1(\mu)|1(q+\mu)\rangle 1/r^2 C_{1,q+\mu} \quad , \tag{98a}$$

and from the properties of the C-G coefficients, we know that q = o and $\langle 0(\mu)1(\mu)|1(\mu)\rangle = 1$. Then

$$\left[\nabla_\mu, 1/r, C_{1q}\right] = -C_{1\mu}/r^2 \quad . \tag{98b}$$

Also, we know from vector analysis that

$$\text{grad } 1/r = -\vec{r}/r^3 \tag{98c}$$

and

$$\vec{r} = r \sum (-1)^\mu \hat{e}_{-\mu} C_{1\mu} \quad . \tag{98d}$$

Then we substitute equation (98d) in (98c) to obtain

$$(\text{grad } 1/r)_\mu = -C_{1\mu}/r^2 \quad , \tag{98e}$$

which is identical with the result of equation (98b). We shall use the result given in equation (94) frequently later on, particularly in the form given in equations (97) and (98).

3. FREE-ION HAMILTONIAN

3.1 Background for Free Rare-Earth Ions

The approximations made in the analysis of rare-earth ions are not new. In fact, they go back to the old Bohr orbit theory. Since many of you may not be familiar with these assumptions and may not remember many of the concepts and much of the technical jargon used in the field of atomic spectra, I will review some of these briefly. Although generalities may exist, I will stick strictly to those concepts which apply to rare-earth ions or, more strictly, triply ionized rare-earth ions. The triply ionized rare-earth ions are characterized by the electronic structure shown in table 1.

TABLE 1. ELECTRONIC STRUCTURE OF TRIPLY IONIZED RARE-EARTH IONS

Number	Element	Symbol	Outermost electron shell
57	Lanthanum	La	$4d^{10}4f^{0}5s^{2}5p^{6}$
58	Cerium	Ce	$4d^{10}4f^{1}5s^{2}5p^{6}$
59	Praseodymium	Pr	$4d^{10}4f^{2}5s^{2}5p^{6}$
60	Neodymium	Nd	$4d^{10}4f^{3}5s^{2}5p^{6}$
61	Promethium	Pm	$4d^{10}4f^{4}5s^{2}5p^{6}$
62	Samarium	Sm	$4d^{10}4f^{5}5s^{2}5p^{6}$
63	Europium	Eu	$4d^{10}4f^{6}5s^{2}5p^{6}$
64	Gadolinium	Gd	$4d^{10}4f^{7}5s^{2}5p^{6}$
65	Terbium	Tb	$4d^{10}4f^{8}5s^{2}5p^{6}$
66	Dysprosium	Dy	$4d^{10}4f^{9}5s^{2}5p^{6}$
67	Holmium	Ho	$4d^{10}4f^{10}5s^{2}5p^{6}$
68	Erbium	Er	$4d^{10}4f^{11}5s^{2}5p^{6}$
69	Thulium	Tm	$4d^{10}4f^{12}5s^{2}5p^{6}$
70	Ytterbium	Yb	$4d^{10}4f^{13}5s^{2}5p^{6}$
71	Lutetium	Lu	$4d^{10}4f^{14}5s^{2}5p^{6}$

In the rare-earth series, it is assumed that the atomic interactions are very strong; thus, when an ion is placed in a crystal, the crystalline electric field acts as a perturbation on the ion. This assumption allows the notation developed for the free ion to be used with the reservation that many of the "good" quantum numbers of the free ion are not quite good when the ion is present in the crystal. It is assumed that the free rare-earth ions have the zeroth-order Hamiltonian

$$H_o = \sum_{i=1}^{N}\left[\frac{p_i^2}{2m} + U(r_i)\right], \tag{99}$$

where $\vec{p}_i$ is the momentum of the ith electron and $U(r_i)$ is an appropriate spherical average potential of the remaining (other than the N, 4f) electrons in the ion. The single-electron solutions to equation (99) are taken in the form (Schiff, 1968)

$$\psi = R_{n\ell}(r)Y_{\ell m}(\hat{r}) \quad , \tag{100}$$

where the $Y_{\ell m}(\hat{r})$ are the spherical harmonics with $\ell = 3$ for f electrons. (Remember that $\ell = 0$ for s, $\ell = 1$ for p, and $\ell = 2$ for d electrons.) The radial functions in equation (100) are taken to be the same for all the f electrons in the ion, while the angular functions, along with the spin of each electron, must form a determinantal function so as to obey the exclusion principle. Depending on whatever determinantal function

is chosen, the radial functions can be found by some self-consistent method. These radial functions (Freeman and Watson, 1962; Fraga et al, 1976; Cowan and Griffin, 1976) have been found for the Hund ground states of all the rare earths from cerium (Ce^{3+}) through ytterbium (Yb^{3+}).

The Hund ground state for the rare-earth ions with $N \leq 7$ is given by assuming that all N spins are parallel and that each angular momentum projection is the maximum allowed by the exclusion principle. (In eq (100), ℓ is the angular momentum and m is its projection.) Thus, the Hund ground state for two electrons is the determinantal function

$$\alpha(1)Y_{\ell,\ell}(1)\alpha(2)Y_{\ell,\ell-1}(2) - \alpha(1)Y_{\ell,\ell-1}(1)\alpha(2)Y_{\ell,\ell}(2) \quad ,$$

where α is the spin "up" wave function (β = spin "down"). A convenient notation for such a determinant is

$$\{\overset{+}{\ell},\overset{+}{\ell-1}\} \quad , \tag{101}$$

where the upper sign is the spin projection (+ = up, - = down) and ℓ and $\ell-1$ are the z projection of the angular momentum (m in eq (100)). Thus, the Hund ground state equation (101) for $4f^2$ praseodymium (Pr^{3+}) has total spin, S, and total angular momentum, L, given by

$$S = 1/2 + 1/2 = 1,$$

$$L = \ell + \ell - 1 = 2\ell - 1 = 5 \text{ (for f, } \ell = 3) \quad .$$

Hence, the ground state is L = 5, with multiplicity of 2S + 1 = 3. In the so-called Russell-Saunders notation, this state is referred to as ^3H, as given by the table:

Total angular momentum, L, of ion	0 1 2 3 4 5 6 7 . . . .
Russell-Saunders label for the state	S P D F G H I K . . . . (continues alphabetically).

In this notation, the technical reference to such a state is a *term*; other terms for Pr^{3+} are ^1I, ^3P, and ^1S (Condon and Shortly, 1959). For the ion Ce^{3+}, which has one f electron, the atom notation becomes identical to that of the ion, that is, $\ell = L = 3$ and $s = S = 1/2$ with the single term ^2F. Those ions in the series for $N > 7$ have the same terms as for $N < 7$, and their Hund state can be constructed simply as

$$\{\overset{+}{\ell},\overset{+}{\ell-1},\overset{+}{\ell-2}, \ldots,\overset{+}{\ell-(2\ell+1)};\overset{-}{\ell},\overset{-}{\ell-1}, \ldots,\overset{-}{\ell-p+1}\} \quad , \tag{102}$$

where the number of f electrons is $N = 7 + p$. The ℓ^N shell is completely filled when $N = 2(2\ell+1)$, which for f electrons is triply ionized

lutetium (Lu^{3+}). As an example, consider triply ionized terbium (Tb^{3+}), which has the $4f^8$ configuration. The determinantal wave function is

$$\begin{matrix} + & + & + & + & + & + & + & - \\ \{3 & 2 & 1 & 0 & -1 & -2 & -3 & 3\} \end{matrix} \quad , \tag{103}$$

where total angular momentum L = 3 and total spin angular momentum S = 6/2 = 3. Thus, the Hund ground state is ^7F. In all cases, the Hund term has been found to have the lowest energy in atomic systems. In general, the wave functions for the higher terms are very difficult to construct, but sophisticated techniques have been devised for the orderly development of a set of wave functions for each ion in the entire rare-earth series (Nielson and Koster, 1964). The Hamiltonian given in equation (99) has the same value for all terms of the configuration $4f^N$; consequently, we ignore H_o in the future discussion.

3.2 Significant Free Rare-Earth Ion Interactions

3.2.1 Coulomb Interaction

The largest contribution to the Hamiltonian for a rare-earth ion is the electrostatic interaction of the 4f electrons, which may be written

$$H_1 = \sum_{i>j} \frac{e^2}{|\vec{r}_i - \vec{r}_j|} \quad , \tag{104}$$

where

$$\vec{r}_{ij} = \vec{r}_i - \vec{r}_j \quad .$$

The matrix elements of this interaction for the state $\{3\ \frac{1}{2}\}$ (the ^3H term) of Pr^{3+} are

$$\langle {}^3H|H_1|{}^3H\rangle = F_0 - 25F_2 - 51F_4 - 13F_6 \quad , \tag{105}$$

where the F_k are frequently referred to as the Slater parameters. These F_k are related to the parameters $F^{(k)}$ (also frequently referred to as "Slater integrals") by the following:

$$F_0 = F^{(0)},\ F_2 = F^{(2)}/225,\ F_4 = F^{(4)}/1089,\ \text{and}\ F_6 = 25F^{(6)}/184{,}041 \quad .$$

(This relation is strictly for f electrons; a different relation exists for d electrons.) The $F^{(k)}$ are radial expectation values given by

$$F^{(k)} = e^2 \int_0^\infty \int_0^\infty \frac{r_<^k}{r_>^{k+1}} [R_{n\ell}(r_1) R_{n\ell}(r_2)]^2 \, dr_1 \, dr_2 \quad , \tag{106}$$

where

$$\int_0^\infty R_{n\ell}^2(r)\, dr = 1 \quad ,$$

$$\frac{r<}{r>} = \frac{r_i}{r_j} \quad \text{if } r_i < r_j \text{ and}$$

$$= \frac{r_j}{r_i} \quad \text{if } r_i > r_j \quad .$$

The confusion created by the two sets of F's does not end at this point; there is still one further set of parameters, E^k, called the Racah parameters, which are used to express the matrix elements of equation (104). The relation of E^k to $F^{(k)}$ and F_k is given in a number of places (for example, Judd, 1963: 206).

3.2.2 Spin-Orbit Interaction

The second interaction of reasonable magnitude in the free ion is the spin-orbit coupling, which is

$$H_2 = \sum_{i=1}^{N} \xi(r_i) \vec{l}_i \cdot \vec{s}_i \quad , \tag{107}$$

where

$$\xi(r_i) = \frac{h^2}{2m^2c^2} \frac{1}{r_i} \frac{dU(r_i)}{dr_i} \quad .$$

This interaction was derived from relativity theory in the Bohr orbit quantum mechanics, but is a natural consequence of a nonrelativistic approximation to the Dirac equation. Values of $F^{(k)}$ and ζ (where $\zeta = \langle 4f|\xi(r)|4f\rangle$) from Hartree-Fock wave functions are given in tables 2 and 3. In the rare-earth series, the interaction, H_2, is quite strong and is in general much larger than the interaction of the rare-earth electrons with the crystal fields.

Consequently, it is convenient to perform all the calculations in a set of basis functions in which H_1 and H_2 are diagonal. The set of functions that achieves this is the total angular momentum function $|JM_J\rangle$, where the total angular momentum operator $\vec{J} = \vec{L} + \vec{S}$.

TABLE 2. RELATIVISTIC HARTREE-FOCK INTEGRALS FOR TRIPLY IONIZED RARE-EARTH IONS[a] (all in cm^{-1})

N	R^{3+}	F^2	F^4	F^6	ζ	M^0	M^2	M^4
1	Ce	-	-	-	696.41	-	-	-
2	Pr	98723	61937	44564	820.22	1.991	1.110	0.752
3	Nd	102720	64462	46386	950.51	2.237	1.248	0.846
4	Pm	106520	66856	48111	1091.46	2.492	1.391	0.943
5	Sm	110157	69143	49758	1243.60	2.756	1.540	1.044
6	Eu	113663	71373	51342	1407.71	3.031	1.694	1.149
7	Gd	117058	73470	52873	1584.45	3.318	1.855	1.258
8	Tb	120366	75541	54361	1774.46	3.615	2.022	1.372
9	Dy	123592	77558	55810	1998.44	3.924	2.195	1.490
10	Ho	126751	79530	57227	2197.06	4.246	2.376	1.612
11	Er	129850	81462	58615	2431.00	4.580	2.563	1.739
12	Tm	132897	83361	59978	2680.97	4.928	2.758	1.872
13	Yb	-	-	-	2947.69	-	-	-

[a] *R. D. Cowan and D. C. Griffin, 1976, J. Opt. Soc. Am. 66, 1010.*

TABLE 3. NONRELATIVISTIC HARTREE-FOCK INTEGRALS FOR TRIPLY IONIZED RARE-EARTH IONS[a] (all in cm^{-1})

N	R^{3+}	F^2	F^4	F^6	ζ	M^0	M^2	M^4
1	Ce	-	-	-	778.14	-	-	-
2	Pr	105120	66213	47718	919.16	2.2610	1.2669	0.8601
3	Nd	109731	69165	49860	1069.87	2.5478	1.4294	0.9709
4	Pm	113640	71641	51647	1228.24	2.8261	1.5865	1.0779
5	Sm	117222	73893	53269	1397.79	3.1079	1.7453	1.1859
6	Eu	120885	76204	54937	1583.54	3.4093	1.9153	1.3016
7	Gd	124644	78585	56655	1786.68	3.7320	2.0976	1.4258
8	Tb	127137	80091	57722	1990.51	4.0130	2.2544	1.5320
9	Dy	129960	81829	58962	2214.87	4.3231	2.4281	1.6500
10	Ho	132929	83670	60281	2458.58	4.6552	2.6144	1.7766
11	Er	135859	85486	61580	2719.76	5.0004	2.8081	1.9081
12	Tm	138754	87276	62864	2999.22	5.3590	3.0092	2.0448
13	Yb	-	-	-	3299.82	-	-	-

[a] *S. Fraga, K. M. S. Saxena, and J. Karwowski, 1976, Physical Sciences Data 5, Handbook of Atomic Data (Elsevier, New York).*

The spin-orbit interaction H_2 given in equation (107) commutes with the total angular momentum and, consequently, since H_1 also commutes with $\vec{J}^2$, the wave functions can be characterized by the eigenvalues of $\vec{J}^2$ and J_z. That is, we can write ψ_{JM} or $|JM\rangle$ for the wave functions with

$$J^2|JM\rangle = J(J+1)|JM\rangle \tag{108}$$

and

$$J_z|JM\rangle = M|JM\rangle \quad .$$

For any term of given L and S (eigenvalues of $\vec{L}^2$ and $\vec{S}^2$), the values of J are restricted to

$$|L - S| \leq J \leq |L + S| \quad .$$

Then the wave functions are customarily written ψ_{JMLS} or $|JMLS\rangle$, and we have

$$\begin{aligned} L^2|JMLS\rangle &= L(L+1)|JMLS\rangle \quad , \\ S^2|JMLS\rangle &= S(S+1)|JMLS\rangle \quad , \\ J^2|JMLS\rangle &= J(J+1)|JMLS\rangle \quad , \\ J_z|JMLS\rangle &= M|JMLS\rangle \quad , \end{aligned} \tag{109}$$

and

$$\langle J'M'L'S'|H_1 + H_2|JMLS\rangle \propto \delta_{JJ'}\delta_{MM'} \quad . \tag{110}$$

As implied in equation (110), the energy H_1 and H_2 is independent of M, or each J level of the free ion is 2J+1-fold degenerate. The matrix elements in equation (110) do not vanish generally for $L' = L \pm 1$ and $S' = S \pm 1$; thus, L and S are *not* strictly good quantum numbers. Nevertheless, the energy levels are labeled as though they were, as in the Russell-Saunders notation, $^{2S+1}L_J$. An example of the energy levels for the $4f^2$ configuration of the free ion (Pr^{3+}) is given in table 4. Also included is the same ion, Pr^{3+}, in the host materials lanthanum trichloride ($LaCl_3$) and lanthanum trifluoride (LaF_3).

The results in table 4 are interesting in that they show that most of the energy levels observed in the free ion are lowered when the ion is embedded in a solid. This shift in the energy levels is a general effect and is not restricted to Pr^{3+}, but exists in all the rare-earth ions where a comparison with energy levels of the free ion can be made. In fact, this shift has been observed by Low (1958a,b) in ions with an unfilled d shell. The first explanation of this shift in energies was by Morrison et al (1967), where it was shown that if the

ion under investigation was assumed to be embedded in a solid of homogeneous dielectric constant, ε, then a decrease in the Slater integrals is given by

$$\Delta F^{(k)} = -e^2(\varepsilon-1)(k+1)(\langle r^k\rangle)^2/\{b^{2k+1}[\varepsilon+k(\varepsilon+1)]\} \quad , \qquad (111)$$

where b is the radius of a fictitious cavity surrounding the rare-earth ion. The result given in equation (111) was first successfully applied to Co^{++} in $MgAl_2O_4$. Later, Newman (1973) showed that the shift in $F^{(k)}$ given in equation (111) was sufficiently large to predict the shifts in the energy levels for rare-earth ions. More recently, Morrison (1980) derived the result

$$\Delta F^{(k)} = -\sum_i \frac{\alpha_i Z_i e^2}{R_i^{2k+4}} \left(\langle r^k\rangle\right)^2 \quad , \qquad (112)$$

where α_i is the polarizability of the Z_i ligands at R_i and $\langle r^k\rangle$ is the radial expectation value of r^k. The result given in equation (112) is believed to be more fundamental than that of equation (111) because the latter explicitly accounts for the local coordination of the rare-earth ion. Morrison (1980) gives a predicted shift in the spin-orbit parameter, ζ, but because of the smallness of the predicted shift and the errors in the fitting of the experimental data, no comparisons were made.

TABLE 4. FREE ION ENERGY LEVELS OF TRIPLY IONIZED PRASEODYMIUM AND CORRESPONDING CENTROIDS IN TWO CRYSTALS[a] (all in cm^{-1})

[LS]J	Free	$LaCl_3$	LaF_3
$^3H_4$	0	0	0
$^3H_5$	2152	2119	2163
$^3H_6$	4389	4307	4287
$^3F_2$	4997	4848	5015
$^3F_3$	6415	6248	6368
$^3F_4$	6855	6684	6831
$^1G_4$	9921	9704	9801
$^1D_2$	17334	16640	16847
$^3P_0$	21390	20385	20727
$^3P_1$	22007	21987	21314
$^1I_6$	22212	21327	-
$^3P_2$	23160	22142	22546
$^1S_0$	50090	48710	46786

[a] *G. H. Dieke, 1968, Spectra and Energy Levels of Rare Earth Ions in Crystals (Interscience, New York), p. 200.*

Because of the lack of experimental data on the free-ion spectra of rare-earth ions, measurement of the shift in the Slater integrals is possible only for Pr^{3+}. The experimental $F^{(k)}$ for triply ionized rare earths in LaF_3 and $LaCl_3$ have been obtained by Carnall et al (1978), and these results are given in tables 5 and 6. These data can be used in conjunction with equation (112) to obtain results that can perhaps be applied to an arbitrary host material to predict a priori the energy level shift of that host.

TABLE 5. FREE-ION PARAMETERS FOR TRIPLY IONIZED RARE-EARTH IONS IN $LaCl_3$ OBTAINED FROM FITTING EXPERIMENTAL DATA[a] (all in cm^{-1})

Ion[b]	F^2	F^4	F^6	α	β	γ	ζ
Pr	68368	50008	32743	22.9	-674	(1520)	744
Nd	71866	52132	35473	22.1	-650	1586	880
Pm	75808	54348	38824	21.0	-645	1425	1022
Sm	78125	56809	40091	21.6	-724	(1700)	1168
Eu	84399	60343	41600	16.8	(-640)	(1750)	1331
Gd	85200	60399	44847	(19)	(-643)	1644	(1513)
Tb	90012	64327	42951	17.5	(-630)	(1880)	1707
Dy	92750	65699	45549	17.2	-622	1881	1920
Ho	95466	67238	46724	17.2	-621	2092	2137
Er	98203	69647	49087	15.9	-632	(2017)	2370

[a] *W. T. Carnall, H. Crosswhite, and H. M. Crosswhite, 1978, Argonne National Laboratory, ANL-78-XX-95.*

[b] *Values in parentheses were not varied in the fitting.*

TABLE 6. FREE-ION PARAMETERS FOR TRIPLY IONIZED RARE-EARTH IONS IN LaF_3 OBTAINED FROM FITTING EXPERIMENTAL DATA[a] (all in cm^{-1})

Ion[b]	F^2	F^4	F^6	α	β	γ	ζ
Pr	69305	50675	32813	(21)	-842	1625	750.8
Nd	73036	52624	35793	21.28	-583	1443	884.9
Pm	(77000)	(55000)	(37500)	(21.00)	(-560)	(1400)	(1022.)
Sm	79914	57256	40424	20.07	-563	1436	1177.2
Eu	(84000)	(60000)	(42500)	(20.0)	(-570)	(1450)	(1327)
Gd	85587	61361	45055	(20.0)	(-590)	(1450)	1503.5
Tb	91220	65798	43661	19.81	(-600)	(1400)	1702
Dy	94877	67470	45745	17.64	-608	1498	1912
Ho	97025	68885	47744	18.98	-579	1570	2144
Er	100274	70555	49900	17.88	-599	1719	2381
Tm	102459	72424	51380	(17.0)	-737	(1700)	2640

[a] *W. T. Carnall, H. Crosswhite, and H. M. Crosswhite, 1978, Argonne National Laboratory, ANL-78-XX-95.*

[b] *Values in parentheses were not varied in the fitting.*

3.2.3 Interconfigurational Interaction

An interaction that has been frequently used in fitting the "free" ion levels of rare-earth ions in a crystal is the so-called interconfigurational mixing or the Trees interaction. This interaction has been parametrized by Wybourne and Rajnak (Wybourne, 1965) and is

$$H_{10} = \alpha L(L+1) + \beta G(G_2) + \gamma G(R_7) \quad , \tag{113}$$

where α, β, and γ are parameters adjusted to fit the experimental data. The operator $G(G_2)$ is the Casimir operator for the group G_2, and $G(G_7)$ is the similar operator for R_7 (note that $L^2 = L(L+1)$ is the Casimir's operator for the group R_3). The values for these operators for all the states are tabulated by Wybourne (1965: 73). The values for the state of f^2 are given in table 7. The values of α, β, and γ obtained by fitting experimental data for the rare-earth ions are given in tables 5 and 6. To my knowledge, no successful attempts to derive theoretical values of α, β, and γ have been published.

3.2.4 Other Interactions

Many other interactions are considered in the free ion, such as spin-other-orbit, orbit-orbit, and configuration interaction. All of these to a greater or lesser extent improve the fit of theoretical energy levels to the experimental data. We will omit these interactions from further discussion since H_1, H_2, and H_{10} give a sufficient representation of the free ion for our purposes here. However, we shall list a number of interactions including the above which have been considered by various research workers (Wortman et al, 1973a,b):

H_1 = the Coulomb interaction
H_2 = the spin-orbit interaction
H_3 = the crystal-field interaction
H_4 = the interaction with a magnetic field (Zeeman effect)
H_5 = the hyperfine interaction
H_6 = the spin-spin interaction
H_7 = the nuclear quadrupole interaction
H_8 = the spin-other-orbit interaction
H_9 = the orbit-orbit interaction
H_{10} = the interconfigurational interaction
H_{11} = the spin-crystal-field interaction

The notation listed above is that of Judd (1963), with a few obvious additions.

TABLE 7. EIGENVALUES OF CASIMIR'S OPERATORS FOR STATES OF f^2

State	α	12b	5γ
^3P	2	12	5
^3F	12	6	5
^3H	30	12	5
^1S	0	0	0
^1D	6	14	7
^1G	20	14	7
^1I	42	14	7

3.3 Summary

We have considered the Coulomb interaction, H_1, and the spin-orbit interaction, H_2, for the configuration $4f^N$ in the free ion. The wave functions that are chosen as a basis for diagonalization of these interactions is $|JMLS\rangle$, and the resulting energy levels are labeled according to the Russell-Saunders notation as given in section 3.1. This same notation (plus additional quantum numbers) will be used for describing an ion in a crystal. The values of $\langle r^k \rangle$ that are needed in equations (111) and (112) are given in table 8. The wave functions used for the calculation of the energy levels of a rare-earth ion in a solid will be the combination that simultaneously diagonalizes H_1 and H_2.

TABLE 8. NONRELATIVISTIC HARTREE-FOCK EXPECTATION VALUES OF $\langle r^k \rangle$, NUCLEAR SPIN, AND MAGNETIC MOMENTS OF TRIPLY IONIZED RARE-EARTH IONS[a] (atomic units)

N	R^{3+}	$\langle r^2 \rangle$	$\langle r^4 \rangle$	$\langle r^6 \rangle$	$\langle r^{-3} \rangle$	I	μ_N
1	Ce	1.1722	3.0818	15.549	4.88571	7/2	0.9
2	Pr	1.0632	2.5217	11.492	5.52708	5/2	4.3
3	Nd	0.97822	2.1317	8.9525	6.17823	7/2	-1.08
4	Pm	0.91401	1.8701	7.4224	6.82779	7/2	2.7
5	Sm	0.86059	1.6700	6.3365	7.49427	7/2	-0.67
6	Eu	0.81064	1.4898	5.3886	8.20108	5/2	3.464
7	Gd	0.76368	1.3267	4.5589	8.95054	3/2	-0.254
8	Tb	0.73523	1.2508	4.2673	9.66059	3/2	1.99
9	Dy	0.70484	1.1644	3.9002	10.42528	5/2	-0.46
10	Ho	0.67481	1.0788	3.5296	11.23504	7/2	4.12
11	Er	0.64714	1.0028	3.2111	12.07835	7/2	-0.564
12	Tm	0.62154	0.93514	2.9355	12.95607	2	0.047
13	Yb	0.59678	0.87030	2.6713	13.87743	5/2	-0.6776

[a] *S. Fraga, K. M. S. Saxena, and J. Karwowski, 1976, Physical Sciences Data 5, Handbook of Atomic Data (Elsevier, New York).*

4. CRYSTAL-FIELD INTERACTIONS

4.1 Phenomenological Theory of Crystal Fields

In the presence of a crystal field, we take the interaction of the rare-earth ion whose configuration is $4f^N$ as

$$H_3 = \sum_{kq} B_{kq}^{+} \sum_{i=1}^{N} C_{kq}(\hat{r}_i) \quad , \tag{114}$$

where the C_{kq} are unnormalized spherical harmonics given by

$$C_{kq}(\hat{r}) = \sqrt{\frac{4\pi}{2k+1}}\, Y_{kq}(\hat{r}) \quad .$$

The use of C_{kq} in place of Y_{kq} seems trivial, but it saves writing a tremendous number of factors of 4π and $2k+1$ in the interactions. The use of the C_{kq} in expressions for electronic interactions (along with other shorthand notation that we will not use) is practically universal. The number of terms in equation (114) that needs to be considered is limited by the symmetry of the site occupied by the rare-earth ion. Also, since we will be discussing only the $4f^N$ configuration, k is limited to values of 6 or less. This limitation arises because, independent of the basis chosen, individual matrix elements of C_{kq} will have to be considered, and these are such that $\langle f|C_{kq}|f\rangle = 0$ if $k > 2f = 6$.

The highest possible symmetry that an ion can experience in a crystal is full cubic (for example, $Cs_2NaLnCl_6$, where Ln = any rare-earth ion); in that case, two B_{kq} are necessary, B_{40} and B_{60}, since $B_{44} = (5/\sqrt{70})B_{40}$ and $B_{64} = -\sqrt{(7/2)}B_{60}$ and $B_{kq} = 0$ for k odd. Because of the simplicity of the calculations, the ion is often assumed to occupy a point of cubic symmetry with perturbations. In general, this assumption is not very productive. On the other hand, in many solids the rare-earth ions occupy a site with no symmetry (such as LnP_5O_{14}, where Ln = a rare-earth ion; these are the pentaphosphates, one of the best known laser host materials for Nd). In this case, all the B_{kq} are allowed, which for the $4f^N$ configuration are B_{20}, B_{21}, B_{22}, B_{40}, B_{41}, . . . B_{66}. Since each B_{kq}, $q \neq 0$, is complex, there are 27 parameters. Unfortunately, the technical importance of the rare earths in these low-symmetry solids complicates the problem of calculating energy levels for practical application. At present, we assume that the ion is in a slightly more symmetric position in the pentaphosphates for simplicity in the calculation (Morrison, Wortman, Karayianis, 1977) but have no idea how good these approximations are.

We have been assuming in equation (114) that the B_{kq} are the same for each electron, which is a universal assumption made when dealing with rare-earth ions. We will continue with this assumption here. The B_{kq} are referred to as the crystal-field parameters and, as the name implies, are used as parameters when fitting the experimental data.

In the early days of the experimental investigations of rare-earth ions in solids, relatively few materials could be grown as single crystals with a small amount of rare earth contained substitutionally. An exception was lanthanum trichloride ($LaCl_3$), which was the crystal used by the Johns Hopkins Laboratory under the direction of Gerhardt Dieke, who in the span of 10 to 15 years, along with his graduate students, had reported the absorption and emission spectra of nearly every rare-earth ion. In one of Dieke's publications (Dieke and Crosswhite,

1963), he gave an energy level diagram of the results of this research. This diagram became so popular that it is generally referred to as a "Dieke chart" and is found in practically every laboratory where the spectra of rare-earth ions are being investigated or rare-earth ion lasers are being designed. These Dieke charts are invaluable for the investigation of a new crystalline material (commonly referred to as a "host") that has been grown to contain a low atomic percentage of a particular rare-earth ion. A common method for referring to a substitutional doping is $Y_{3(1-x)}Nd_{3x}Al_5O_{12}$, for $x \times 100$ percent neodymium-doped yttrium aluminum garnet. When a solid contains a rare-earth ion as one of its constituents, such as the excellent laser material NdP_5O_{14}, it is referred to as a stoichiometric laser material. A primary requirement of a host material, besides being transparent in the region of interest, is that one of the atomic constituents be trivalent and have nearly the same ionic radius as the ion in the rare-earth series. Also, the solid should have no absorption bands in the region of interest. The most common ion meeting these requirements is yttrium, and most of the rare-earth doped laser crystals have this element as a constitutent, although several of the rare-earth ions themselves meet these requirements, such as La^{3+}, Lu^{3+}, and for particular purposes gadolinium Gd^{3+}.

4.1.1 Matrix Elements of H_3 in J States

In order to make full use of tabulated data in our calculations, it is necessary to make some modifications in equation (114). Neilson and Koster (1964) have calculated the reduced matrix elements of the unit spherical tensors introduced by Racah. The $C_{kq}(i)$ can be written in terms of those tensors as

$$C_{kq}(i) = \sqrt{2\ell+1}\ \langle \ell \| C_k \| \ell \rangle u_q^k(i) \tag{115}$$

and

$$\sum_i C_{kq}(i) = \sqrt{2\ell+1}\ \langle \ell \| C_k \| \ell \rangle U_q^{(k)} \quad , \tag{116}$$

where

$$\langle \ell \| C_k \| \ell \rangle = \langle \ell(0) k(0) | \ell(0) \rangle \quad .$$

Thus equation (114) may be written

$$H_3 = \sum_{kq} B_{kq}^{+} \sqrt{2\ell+1}\ \langle \ell \| C_k \| \ell \rangle U_q^{(k)} \quad . \tag{117}$$

The reduced matrix elements tabulated by Neilson and Koster are for L-S states, so we must relate the matrix elements in the J basis to L-S basis. To do this we construct the state

$$|JMLS\rangle = \sum_{\mu} \langle L(\mu)S(M-\mu)|J(M)\rangle |L\mu SM-\mu\rangle \quad . \tag{118}$$

Then

$$\langle J'M'L'S'|U_q^{(k)}|JMLS\rangle = \langle J(M)k(q)|J'(M')\rangle \langle J'L'S'\|U^{(k)}\|JLS\rangle \quad , \tag{119}$$

by application of the Wigner-Echart theorem. If now we calculate the matrix element in equation (119) by using the wavefunctions of equation (118), we have

$$\begin{aligned} &\langle J'M'L'S'|U_q^{(k)}|JMLS\rangle \\ &\quad = \sum_{\mu\mu'} \langle L(\mu)S(M-\mu)|J(M)\rangle \langle L'(\mu')S'(M'-\mu')|J'(M')\rangle \\ &\quad \times \langle L'\mu'S'M'-\mu'|U_q^{(k)}|L\mu SM-\mu\rangle \quad . \end{aligned} \tag{120}$$

The matrix elements,

$$\begin{aligned} &\langle L'\mu'S'M'-\mu'|U_q^{(k)}|L\mu SM-\mu\rangle \\ &\quad = \delta_{SS'}\delta_{M'-\mu',M-\mu}\langle L(\mu)k(q)|L'(\mu')\rangle \langle L'S'\|U^{(k)}\|LS\rangle \quad , \end{aligned} \tag{121}$$

are obtained using the Wigner-Echart theorem, with the knowledge that $U^{(k)}$ is a spherical tensor in orbital space only. In equation (120) the last C-G coefficient and the C-G in equation (121) can be rearranged to give

$$\begin{aligned} &\langle L(\mu)k(q)|L'(\mu')\rangle \langle L'(\mu')S(M-\mu)|J'(M')\rangle \\ &= (-1)^{L+k-L'}\langle k(q)L(\mu)|L'(\mu')\rangle \langle L'(\mu')S(M-\mu)|J'(M')\rangle \quad , \end{aligned} \tag{122}$$

where we have used the results $S' = S$ and $M' - \mu' = M - \mu$ given in equation (121). The two C-G coefficients given in equation (122) can be written

$$(-1)^{L+k-L'}\langle k(q)L(\mu)|L'(\mu')\rangle\langle L'(\mu')S(M-\mu)|J'(M')\rangle$$

$$= (-1)^{L+k-L'}\sum_f \sqrt{(2L'+1)(2f+1)}\ W(kLJ'S;L'f)\langle L(\mu)S(M-\mu)|f(M)\rangle \qquad (123)$$

$$\times \langle k(q)f(M)|J'(M')\rangle \quad .$$

Since all the dependance on μ is contained in the first C-G in equation (120) (the only one remaining) and the first of equation (123), this sum can be performed to give

$$\sum_\mu \langle L(\mu)S(M-\mu)|J(M)\rangle\langle L(\mu)S(M-\mu)|f(\mu)\rangle = \delta_{Jf} \qquad (124)$$

from the orthogonality of the C-G coefficients. Substituting these results back into equation (120) we have

$$\langle J'M'L'S'|U_q^{(k)}|JMLS\rangle = (-1)^{L+k-L'}\sqrt{(2L'+1)(2J+1)}\ W(kLJ'S;L'J)$$
$$\times \langle k(q)J(M)|J'(\mu')\rangle\langle L'S\|U^{(k)}\|LS\rangle\delta_{SS'} \quad . \qquad (125)$$

We have used the condition $f = J$ in equation (124) and the result in equation (121). To compare the result in equation (125) with equation (118), we need to rearrange the C-G in equation (125):

$$\langle J'L'S\|U^{(k)}\|JLS\rangle = (-1)^{L+J'-L'-J}\sqrt{(2L'+1)(2J+1)}\ W(kLJ'S;L'J)$$
$$\times \langle L'S\|U^{(k)}\|LS\rangle \quad . \qquad (126)$$

The matrix elements tabulated by Neilson and Koster (1964) are related to ours by

$$\left(L'S\|U^{(k)}\|LS\right) = \sqrt{2L'+1}\ \langle L'S\|U^{(k)}\|LS\rangle \quad . \qquad (127)$$

Finally the complete matrix elements of H_3 given in equation (117) are

$$\langle J'M'L'S|H_3|JMLS\rangle$$
$$= \sum_{kq} B_{kq}^{+}\langle J(M)k(q)|J'(M')\rangle\sqrt{2\ell+1}\ \langle \ell\|C_k\|\ell\rangle \qquad (128)$$
$$\times \langle J'L'S\|U^{(k)}\|JLS\rangle \quad ,$$

with

$$\langle J'L'S\|U^{(k)}\|JLS\rangle = (-1)^{L-L'+J'-J}\sqrt{2J+1}\; W(kLJ'S;L'J) \times (L'S\|U^{(k)}\|LS) \qquad (129)$$

and

$$\langle \ell\|C_k\|\ell\rangle = \langle \ell(0)k(0)|\ell(0)\rangle \quad .$$

For $\ell = 3$, $\langle \ell\|C_k\|\ell\rangle = -2/\sqrt{15}$, $2/\sqrt{22}$, and $-10/\sqrt{429}$ for $k = 2$, 4, and 6, respectively.

4.1.2 Numerical Example: ^4F_J States of Nd^{3+}

As a numerical example of the calculation of the crystal-field splitting, we will calculate the splitting for Nd^{3+} ($4f^3$) in a field of S_4 point symmetry. We shall assume that the levels are pure ^4F_J. We assume that L, S, and J are all good quantum numbers; then we consider matrix elements of H_3 in equation (128) with J' = J and L' = L. Thus,

$$\langle JM'LS|H_3|JMLS\rangle = \sum_{kq} B^*_{kq}\langle J(M)k(q)|(M')\rangle \times \langle J\|U^k\|J\rangle\sqrt{2\ell+1}\,\langle \ell(0)k(0)|\ell(0)\rangle \quad . \qquad (130)$$

The values of the reduced matrix elements $\langle J\|U^k\|J\rangle\sqrt{2\ell+1}\langle \ell\|C_k\|\ell\rangle$ for the ^4F state of Nd^{3+} are as in table 9. In obtaining these values we have used Neilson and Koster's results (1964) for the reduced matrix elements, $(LS\|U^k\|LS)$, for L = 3 and S = 3/2; the Racah coefficients (6 symbols) are found in Rotenberg et al (1969).

TABLE 9. VALUES OF $\langle J\|U^k\|J\rangle\sqrt{2\ell+1}\langle \ell\|C_k\|\ell\rangle$

J	k = 2	k = 4	k = 6
$\frac{3}{2}$	$\frac{2}{5}\left[\frac{1}{5}\right]^{1/2}$	0	0
$\frac{5}{2}$	$\frac{11}{2\cdot5}\left[\frac{1}{2\cdot5\cdot7}\right]^{1/2}$	$\frac{1}{2}\left[\frac{1}{2\cdot3\cdot7}\right]^{1/2}$	0
$\frac{7}{2}$	$\frac{1}{3}\left[\frac{5}{3\cdot7}\right]^{1/2}$	$\frac{1}{2\cdot3}\left[\frac{1}{7\cdot11}\right]^{1/2}$	$-\frac{2\cdot5}{3}\left[\frac{1}{3\cdot11\cdot13}\right]^{1/2}$
$\frac{9}{2}$	$\frac{1}{2\cdot3}\left[\frac{11}{2\cdot3}\right]^{1/2}$	$-\frac{1}{2\cdot3}\left[\frac{13}{2\cdot11}\right]^{1/2}$	$\frac{5}{3}\left[\frac{1}{2\cdot3\cdot11\cdot13}\right]^{1/2}$

The calculation of the energy levels is made somewhat simpler by using wave functions that transform according to some irreducible representation of the S_4 group (Koster et al, 1963). The irreducible representations of the S_4 group are all one-dimensional, but, since the ion under investigation has an odd number of electrons, the energy levels will be at least doubly degenerate. Thus, of the four irreducible representations--Γ_5, Γ_6, Γ_7, and Γ_8--only two need be chosen; we chose Γ_5 and Γ_7. The energy corresponding to Γ_6 is degenerate with Γ_5 and that corresponding to Γ_8 is degenerate with Γ_7. The wave functions belonging to Γ_7 with a particular J value are

$$|J\ \tfrac{8k+1}{2}\rangle \quad , \qquad -\tfrac{2J+1}{8} \leq k \leq \tfrac{2J-1}{8}$$

and those for Γ_5 are

$$|J\ \tfrac{8k-3}{2}\rangle \quad , \qquad -\tfrac{2J-3}{8} \leq k \leq \tfrac{2J+3}{8} \quad ,$$

where k is an integer, and the number of k values occurring for a given J is the number of times a representation will occur. The number of B_{kq} for the calcium site in calcium tungstate is five: i.e., B_{20}, B_{40}, B_{60}, B_{44}, and B_{64}. Of these parameters only the B_{64} is complex. The matrix elements of the crystal field given in the above equation are presented explicitly under particular states in the following paragraphs.

$^4F_{3/2}$

This level of the free ion is split into two doublets by the crystalline field. The wave functions corresponding to Γ_7 and to Γ_5 are $|\frac{3}{2}\ \frac{1}{2}\rangle$ and $|\frac{3}{2}\ -\frac{3}{2}\rangle$ respectively. From equation (130) we have

$$\langle \tfrac{3}{2}\ \tfrac{1}{2}\ |H_3|\ \tfrac{3}{2}\ \tfrac{1}{2}\rangle = -\tfrac{2}{25}\ B_{20} = E\left(\Gamma_7\ \tfrac{3}{2}\right) \qquad (131)$$

and

$$\langle \tfrac{3}{2}\ -\tfrac{3}{2}\ |H_3|\ \tfrac{3}{2}\ -\tfrac{3}{2}\rangle = \tfrac{2}{25}\ B_{20} = E\left(\Gamma_5\ \tfrac{3}{2}\right) \quad , \qquad (132)$$

where the appropriate values of the reduced matrix elements in equations (131) and (132) were taken from table 9. The total splitting of the $^4F_{3/2}$ state is then

$$\tfrac{4}{25}\ B_{20} \quad . \qquad (133)$$

$^4F_{5/2}$

Unlike the previous case, this state contains two Γ_5's, and their wave functions are $|\frac{5}{2}\frac{5}{2}>$ and $|\frac{5}{2}-\frac{3}{2}>$. The wave function for the Γ_7 state is $|\frac{5}{2}\frac{1}{2}>$. The energy for Γ_7 is

$$<\frac{5}{2}\frac{1}{2}|H_3|\frac{5}{2}\frac{1}{2}> = \frac{11}{700}\left[-4B_{20} + \frac{50}{33}B_{40}\right] = E(\Gamma_7\ \tfrac{5}{2}) \quad . \tag{134}$$

The necessary matrix elements for the energy in Γ_5 are

$$<\frac{5}{2}\frac{5}{2}|H_3|\frac{5}{2}\frac{5}{2}> = \frac{11}{700}\left[5B_{20} + \frac{25}{38}B_{40}\right] = b_{11} \quad , \tag{135}$$

$$<\frac{5}{2}-\frac{3}{2}|H_3|\frac{5}{2}-\frac{3}{2}> = \frac{11}{700}\left[-B_{20} - \frac{25}{11}B_{40}\right] = b_{22} \quad , \tag{136}$$

$$<\frac{5}{2}-\frac{3}{2}|H_3|\frac{5}{2}\frac{5}{2}> = \frac{1}{6\sqrt{14}}B_{44} = b_{12} \quad . \tag{137}$$

The two energy levels corresponding to Γ_5 are

$$E_1(\Gamma_5\ \tfrac{5}{2}) = \frac{b_{11} + b_{22} + \left[(b_{11} - b_{22})^2 + 4b_{12}b_{12}^*\right]^{1/2}}{2} \quad , \tag{138}$$

$$E_2(\Gamma_5\ \tfrac{5}{2}) = \frac{b_{11} + b_{22} - \left[(b_{11} - b_{22})^2 + 4b_{12}b_{12}^*\right]^{1/2}}{2} \quad . \tag{139}$$

$^4F_{7/2}$

This state contains two Γ_5's and two Γ_7's . The matrix elements for Γ_7 are

$$<\frac{7}{2}\frac{1}{2}|H_3|\frac{7}{2}\frac{1}{2}> = \frac{1}{99}\left[-\frac{55}{7}B_{20} + \frac{9}{14}B_{40} + \frac{50}{13}B_{60}\right] = a_{11} \quad , \tag{140}$$

$$<\frac{7}{2}-\frac{7}{2}|H_3|\frac{7}{2}-\frac{7}{2}> = \frac{1}{99}\left[11B_{20} + \frac{1}{2}B_{40} - \frac{10}{13}B_{60}\right] = a_{22} \quad , \tag{141}$$

$$<\frac{7}{2}-\frac{7}{2}|H_3|\frac{7}{2}\frac{1}{2}> = \frac{1}{99}\left[\frac{1}{\sqrt{2}}B_{44} - \frac{30}{13}\sqrt{10}\,B_{64}\right] = a_{12} \quad . \tag{142}$$

The two energy levels are

$$E_1(\Gamma_7\ \tfrac{7}{2}) = \frac{a_{11} + a_{22} + [(a_{11} - a_{22})^2 + 4a_{12}a_{12}^*]^{1/2}}{2} \quad , \qquad (143)$$

$$E_2(\Gamma_7\ \tfrac{7}{2}) = \frac{a_{11} + a_{22} - [(a_{11} - a_{22})^2 + 4a_{12}a_{12}^*]^{1/2}}{2} \quad . \qquad (144)$$

The matrix elements for Γ_5 are*

$$\langle \tfrac{7}{2}\ \tfrac{5}{2} |H_3| \tfrac{7}{2}\ \tfrac{5}{2} \rangle = \frac{1}{99}\left[\frac{11}{7} B_{20} - \frac{13}{14} B_{40} + \frac{50}{13} B_{60}\right] = b_{11} \quad , \qquad (145)$$

$$\langle \tfrac{7}{2}\ -\tfrac{3}{2} |H_3| \tfrac{7}{2}\ -\tfrac{3}{2} \rangle = \frac{1}{99}\left[-\frac{33}{7} B_{20} - \frac{3}{14} B_{40} - \frac{90}{13} B_{60}\right] = b_{22} \quad , \qquad (146)$$

$$\langle \tfrac{7}{2}\ -\tfrac{3}{2} |H_3| \tfrac{7}{2}\ \tfrac{5}{2} \rangle = \frac{1}{99}\left[\sqrt{\frac{15}{14}} B_{44} + \frac{20}{13}\sqrt{\frac{21}{2}} B_{64}\right] = b_{12} \quad . \qquad (147)$$

The corresponding energies are given by substituting the above values of b_{ij} into equations (138) and (139).

$^4F_{9/2}$

The number of Γ_7's in this state is three, with two Γ_5's. The matrix elements of the crystal field for Γ_7 are

$$\langle \tfrac{9}{2}\ \tfrac{9}{2} |H_3| \tfrac{9}{2}\ \tfrac{9}{2} \rangle = \frac{7}{396}\left[6B_{20} - \frac{18}{7} B_{40} + \frac{30}{91} B_{60}\right] = a_{11} \quad , \qquad (148)$$

$$\langle \tfrac{9}{2}\ \tfrac{1}{2} |H_3| \tfrac{9}{2}\ \tfrac{1}{2} \rangle = \frac{7}{396}\left[-4B_{20} - \frac{18}{7} B_{40} - \frac{80}{91} B_{60}\right] = a_{22} \quad , \qquad (149)$$

$$\langle \tfrac{9}{2}\ -\tfrac{7}{2} |H_3| \tfrac{9}{2}\ -\tfrac{7}{2} \rangle = \frac{7}{396}\left[2B_{20} + \frac{22}{7} B_{40} - \frac{110}{91} B_{60}\right] = a_{33} \quad , \qquad (150)$$

$$\langle \tfrac{9}{2}\ \tfrac{1}{2} |H_3| \tfrac{9}{2}\ \tfrac{9}{2} \rangle = \frac{7}{396}\left[-\frac{6}{7}\sqrt{5} B_{44} + \frac{150}{91} B_{64}\right] = a_{12} \quad , \qquad (151)$$

$$\langle \tfrac{9}{2}\ -\tfrac{7}{2} |H_3| \tfrac{9}{2}\ \tfrac{1}{2} \rangle = \frac{7}{396}\left[-\frac{10}{7}\sqrt{5} B_{44} + \frac{30}{91} B_{64}\right] = a_{23} \quad . \qquad (152)$$

*The symbol a_{ij} will be used for the matrix elements in Γ_7 and b_{ij} for those in Γ_5 to avoid introducing new symbols for each new value of J.

The three energies are given by the solutions of

$$E^3 - (a_{11}+a_{22}+a_{33})E^2 + (a_{11}a_{22}+a_{11}a_{33}+a_{22}a_{33}-a_{23}a_{23}^*-a_{12}a_{12}^*)E + a_{11}a_{23}a_{23}^* + a_{33}a_{12}a_{12}^* - a_{11}a_{22}a_{33} = 0 \quad . \tag{153}$$

The matrix elements for Γ_5 are

$$\left\langle \frac{9}{2}\ \frac{5}{2} \left| H_3 \right| \frac{9}{2}\ \frac{5}{2} \right\rangle = \frac{7}{396}\left[B_{20} + \frac{17}{7} B_{40} + \frac{100}{91} B_{60}\right] = b_{11} \quad , \tag{154}$$

$$\left\langle \frac{9}{2}\ -\frac{3}{2} \left| H_3 \right| \frac{9}{2}\ -\frac{3}{2} \right\rangle = \frac{7}{396}\left[-3B_{20} - \frac{3}{7} B_{40} + \frac{60}{91} B_{60}\right] = b_{22} \quad , \tag{155}$$

$$\left\langle \frac{9}{2}\ -\frac{3}{2} \left| H_3 \right| \frac{9}{2}\ \frac{5}{2} \right\rangle = \frac{7}{396}\left[-\frac{5}{7}\sqrt{30}\, B_{44} - \frac{40}{91}\sqrt{6}\, B_{64}\right] = b_{12} \quad . \tag{156}$$

The energies $E_i\left(\Gamma_5\ \frac{9}{2}\right)$ and $E_2\left(\Gamma_5\ \frac{9}{2}\right)$ are given by equations (138) and (139), respectively, using the b_{ij} given above.

Calculation

Three of the crystal-field parameters can be obtained quite simply from the experimental data. These are B_{20}, B_{40}, and B_{60}. If we express the sums, S_i, in terms of the E_i where the E_i are experimental data, then we obtain

$$S_{J-1/2} = \sum_i E_i\left(\Gamma_7 J\right) \quad ,$$

and

$$S_1 = -\frac{2}{25} B_{20} \quad , \tag{157}$$

$$S_2 = -\frac{11}{175} B_{20} + \frac{1}{42} B_{40} \quad , \tag{158}$$

$$S_3 = \frac{2}{63} B_{20} + \frac{8}{693} B_{40} + \frac{40}{1287} B_{60} \quad , \tag{159}$$

$$S_4 = \frac{1}{9} B_{20} - \frac{7}{198} B_{40} - \frac{40}{1287} B_{60} \quad , \tag{160}$$

where S_4 is for the $J = 9/2$ level. These equations can be inverted to give

$$B_{20} = -\frac{25}{2} S_1 \quad , \tag{161}$$

$$B_{40} = -33S_1 + 42S_2 \quad , \tag{162}$$

$$B_{60} = \frac{1001}{40} S_1 - \frac{78}{5} S_2 + \frac{1287}{40} S_3 \quad . \tag{163}$$

The other crystal-field parameters are slightly more involved. From equations (138) and (139) we have

$$B_{44} = 3\sqrt{14}\,[W_1^2 - N_1^2]^{1/2} \quad , \tag{164}$$

where

$$N_1 = -\frac{11}{4} S_1 + 2S_2 \quad \text{and} \quad W_1 = E_1\left(\Gamma_5\ \tfrac{5}{2}\right) - E_2\left(\Gamma_5\ \tfrac{5}{2}\right) \quad .$$

To determine B_{64}, we use equations (143) and (144) to give

$$a_{12}a_{12}^* = \frac{1}{4}\,[W_2^2 - N_2^2] \tag{165}$$

where

$$N_2 = \frac{7}{2} S_1 - \frac{2}{3} S_2 + \frac{3}{2} S_3 \quad \text{and} \quad W_2 = E_1\left(\Gamma_7\ \tfrac{7}{2}\right) - E_2\left(\Gamma_7\ \tfrac{7}{2}\right) \quad .$$

A similar expression can be obtained using equations (145) and (146) in equations (138) and (139), yielding

$$b_{12}b_{12}^* = \frac{1}{4}\,[W_3^2 - N_3^2] \quad , \tag{166}$$

where

$$N_3 = \frac{13}{6} S_1 - 2S_2 + \frac{7}{2} S_3 \quad \text{and} \quad W_3 = E_1\left(\Gamma_5\ \tfrac{7}{2}\right) - E_2\left(\Gamma_5\ \tfrac{7}{2}\right) \quad .$$

Substituting equations (142) and (143) into the left side of equations (165) and (166), we obtain two equations for B_{64}. These two equations can be solved simultaneously for both real and imaginary parts of B_{64} to give

$$R_6 = \frac{13}{20}\left[\frac{3\cdot99}{4}\left(W_2^2 + W_3^2 - N_2^2 - N_3^2\right) - 6\left(W_1^2 - N_1^2\right)\right]^{1/2} \quad , \tag{167}$$

$$\cos\,\theta = \frac{13}{20\sqrt{70}}\,\frac{\frac{15\cdot99}{8}\left(W_3^2 - N_3^2\right) - 8\left(W_1^2 - N_1^2\right) - \frac{7\cdot99}{8}\left(W_2^2 - N_2^2\right)}{R_6\left(W_1^2 - N_1^2\right]^{1/2}} \quad , \tag{168}$$

where

$$B_{64} = R_6 e^{i\theta} \quad .$$

All the crystal-field parameters can be determined once the experimental data are taken on the $^4F_{3/2}$, $^4F_{5/2}$, and $^4F_{7/2}$ levels.

As tedious as the above procedures may have seemed, the crystal-field parameters we obtain are only approximate since we have ignored L-S mixing by the spin-orbit coupling in the free ion and J mixing caused by the crystal field. Nevertheless, the crystal-field parameters obtained by the above procedure can serve as very good starting values in a fitting of a more sophisticated calculation to experimental crystal-field levels.

The crystal-field parameters B_{kq} obtained by the above procedure for Nd^{3+} in $CaWO_4$ are given below, along with crystal-field parameters for the same ion but with full diagonalization, that is, L-S mixing and J mixing (Wortman et al, 1977).

B_{kq}	B_{20}	B_{40}	B_{44}	B_{60}	RB_{64}	IB_{64}
above	403	-635	+711	-219	885	0
full diagonalization	509	-866	1042	-509	903	243

4.2 Classical Point-Charge Model

In the simplest model of the crystal field, the point-charge model introduced by Bethe (1929), the lattice is replaced by an array of point charges placed at the nuclei of the constituent ions. A multipole expansion is made of the point-charge potential energy at the rare-earth site. Thus, if $\vec{R}_{\ell mn}(j)$ is the vector position of constituent j at site j in the ℓ, m, nth cell, we have

$$H_3 = \sum_{\ell mn} \sum_j \frac{-e^2 Z_j}{|\vec{R}_{\ell mn}(j) - \vec{r}|} , \qquad (169)$$

where

$$\vec{R}_{\ell mn} = \ell\vec{a} + m\vec{b} + n\vec{c} + \vec{\rho}_j$$

and $\vec{a}$, $\vec{b}$, and $\vec{c}$ are lattice vectors. The charge at site j is eZ_j and $\vec{r}$ is the position of an electron on a rare-earth ion. The multipolar expansion of equation (169) is

$$H_3 = \sum_{\ell mn} \sum_j \frac{-e^2 Z_j r^k}{\left[R_{\ell m}(j)\right]^{k+1}} C_{kq}(\hat{r}) C^*_{kq}\left[\hat{R}_{\ell mn}(j)\right] \quad . \tag{170}$$

The multipolar crystal-field components A_{kq} are

$$A_{kq} = -e^2 \sum_{\ell mn} \sum_j \frac{Z_j C_{kq}\left[\hat{R}_{\ell mn}(j)\right]}{\left[R_{\ell mn}(j)\right]^{k+1}} \quad . \tag{171}$$

Thus the point-charge Hamiltonian is

$$H_3 = \sum_{kq} A^*_{kq} \sum_{i=1}^{N} r_i^k C_{kq}(\hat{r}_i) \quad , \tag{172}$$

where we have summed over all the N electrons in the $4f^N$ configuration. If all the lengths are measured in Å (10^{-8} cm), then

$$A_{kq} = -\frac{\alpha_o}{2\pi} \times 10^8 \sum_{\ell mn} \sum_j \frac{Z_j C_{kq}\left[\hat{R}_{\ell mn}(j)\right]}{\left[R_{\ell mn}(j)\right]^{k+1}} \quad , \tag{173}$$

where $\alpha_o = e^2/\hbar c$ ($\alpha_o/2\pi \times 10^8 = 116{,}140$)--that is, the fine-structure constant--and the units of $A_{kq} = \text{cm}^{-1}/\text{Å}^k$. If $\langle r^k \rangle$ is in Å units, then $A_{kq}\langle r^k \rangle = \text{cm}^{-1}$.

The sum in equation (173) always converges--even for the lowest k value (k = 0)--if taken in the order indicated. That is, the sum over j is performed with ℓ, m, and n fixed. The unit cell is neutral, that is,

$$\sum_j Z_j = 0 \quad . \tag{174}$$

In many cases (not all space groups) it is possible to choose an origin for the lattice coordinates such that the dipole moment of the unit cell vanishes; that is,

$$\sum_j \vec{\rho}_j Z_j = 0 \quad , \tag{175}$$

where $\vec{\rho}_j$ is the position of the jth charge in the unit cell. The result in equation (175) can be anticipated by observing the point symmetry of the ions in a specific solid. If the ions occupy C_1, C_2, C_s, C_{2v}, C_4, C_{4v}, C_3, C_{3v}, C_6, or C_{6v} point symmetry (Schoenflies notation), then it is impossible to satisfy equation (175) with these sites as the origin

in a unit cell. If it is possible to satisfy equation (175), then the sum given in equation (173) converges very rapidly. This can be shown from the expansion (Carlson and Rushbrooke, 1950)

$$\frac{C_{kq}(\widehat{\vec{R}-\vec{x}})}{|\vec{R}-\vec{x}|^{k+1}} = \sum_{a\alpha} \binom{2a+2k}{2a}^{1/2} \langle a(\alpha)k(q)|a+k(\alpha+q)\rangle x^a C_{a\alpha}(\hat{x}) \frac{C^*_{a+k,\alpha+q}(\hat{R})}{R^{a+k+1}} \quad . \tag{176}$$

With $\vec{\rho}_j = \vec{x}$ and $\vec{R}_{\ell mn}(0) = \vec{R}$ ($\vec{R}_{\ell mn}(j) = \vec{R}_{\ell mn}(0) + \vec{\rho}_j$), for the sum in equation (173) we have

$$\sum_{\ell mn} \sum_j \frac{Z_j C_{kq}\left[\hat{R}_{\ell mn}(j)\right]}{\left[R_{\ell mn}(j)\right]^{k+1}} = \sum_{\ell mn} \sum_{a\alpha} \binom{2a+2k}{2a}^{1/2} \langle a(\alpha)k(q)|a+k(\alpha+q)\rangle \tag{177}$$

$$\times \sum_j Z_j \rho_j^a C_{a\alpha}(\hat{\rho}_j) \frac{C^*_{a+k,\alpha+q}\left[\hat{R}_{\ell mn}(0)\right]}{\left[R_{\ell mn}(0)\right]^{a+k+1}} \quad .$$

Now if equation (175) is satisfied, then

$$\sum_j Z_j \rho_j C_{1\alpha}(\hat{\rho}_j) = 0 \quad . \tag{178}$$

Thus, the sum in equation (177) is for $a > 1$; we see that even for the lowest term, $k = 0$, we have the individual terms falling off as $1/R^2_{\ell mn}(0)$. While the expansions in equations (176) and (177) are good for demonstrating the rate of convergence, the computation of A_{kq} by equation (173) is more practical. However, in equation (173), the sum over j should be done for each cell first, with fixed values of ℓ, m, and n. In programming language, this is expressed by stating that the j loop is the innermost of the nested ℓ, m, n, and j loops. In some lattices, the condition in equation (175) may place some of the point charges on the cell faces. In these cases it is a simple matter to balance these charges by an adjustment to fractions of equal charges on opposite faces.

The convention we use for our lattice sums is that given in the International Tables for Crystallography (1952); table 10 is reproduced from volume I (the other two volumes give data strictly for x-ray crystallographers). The data used in the lattice sums are generally those reported in Acta Crystallographica, Section B. Care should be taken to make certain the correct setting is used.

Typical data used in the calculation of the lattice sums are given in table 11 ($LiYF_4$, calcium tungstate space group 88, Scheelite structure). All the data given in table 11 are given in the International Tables, except that the x, y, and z coordinates are determined by

TABLE 10. CRYSTALLOGRAPHIC AXIAL AND ANGULAR RELATIONSHIPS AND CHARACTERISTIC SYMMETRY OF CRYSTAL SYSTEMS

Space group	System	Axial and angular relationships	X-ray data needed for unit cell
1,2	Triclinic	$a \neq b \neq c$ $\alpha \neq \beta \neq \gamma \neq 90°$	a, b, c, α, β, γ
3 to 15	Monoclinic	First setting $a \neq b \neq c$ $\alpha = \beta = 90° \neq \gamma$	a, b, c, γ
		Second setting $a \neq b \neq c$ $\alpha = \gamma = 90° \neq \beta$	a, b, c, β
16 to 74	Orthorhombic	$a \neq b \neq c$ $\alpha = \beta = \gamma = 90°$	a, b, c
75 to 142	Tetragonal	$a = b \neq c$ $\alpha = \beta = \gamma = 90°$	a, c
143 to 167	Trigonal (may be taken as subdivision hexagonal)	(Rhombohedral axes) $a = b = c$ $\alpha = \beta = \gamma < 120° \neq 90°$ $a = b \neq c$ $\alpha = \beta = 90°$ $\gamma = 120°$	a, α
168 to 194	Hexagonal	$a = b \neq c$ $\alpha = \beta = 90°$ $\gamma = 120°$	a, c
195 to 230	Cubic	$a = b = c$ $\alpha = \beta = \gamma = 90°$	a

Source: International Tables, 1952, Vol. I, p. 11, table 2.3.1.

x-ray diffraction. The lattice constants a, b, and c are also determined by x-ray diffraction and, as customary, the true positions of the ions are xa, yb, and zc (these relations hold for all the ions in a unit cell). The polarizability (from Kittel, 1956: 165) of each ion is given at the bottom of table 11. For this particular solid, only the fluorine ions can have dipole moments that contribute to the crystal field (we shall discuss the role of the dipole moments later on). All the data for space group 88 are not contained in table 11 because the equivalent

positions given in the International Tables are generated inside the program. The centering position in the cell can be taken as either the Y or Li site, since these positions have S_4 symmetry, and their lowest crystal-field component is A_{20}. Equation (178) is therefore automatically satisfied. The resulting lattice sum for the Y site in $LiYF_4$ for the parameters in table 11 is given in table 12.

TABLE 11. CRYSTALLOGRAPHIC DATA FOR $LiYF_4$ (SCHEELITE, $CaWO_4$)
TETRAGONAL SPACE GROUP 88 (FIRST SETTING) Z = 4

Ion	Position	Symmetry	x	y	z
Y	4b	S_4	0	0	1/2
Li	4a	S_4	0	0	0
F	16f	C_1	0.2820	0.1642	0.0815

Notes: $a = 5.1668$, $b = a$, $c = 10.733$, $\alpha = 90°$, $\beta = 90°$, $\gamma = 90°$, $\alpha = 0.55$ Å^3, $\alpha_{Li} = 0.05$ Å^3, $\alpha_F = 1.04$ Å^3 *(reduced to 0.104 in the lattice sum)*, $Z_Y = +3$, $Z_{Li} = +1$, $Z_F = -1$.

TABLE 12. LATTICE SUMS FOR Y SITE AT (0, 0, 1/2) FOR $LiYF_4$ WITH $Z_Y = 3$, $Z_{Li} = 1$, $Z_F = -1$, $\alpha_F = 0.104$ Å^3

Lattice sum	Monopole A_{nm}		Dipole A_{nm}		Monopole and dipole	
	Real	Imaginary	Real	Imaginary	Real	Imaginary
A_{20}	1074	0	340	0	1414	0
A_{32}	373	859	-358	74.0	15	933
A_{40}	-1957	0	-98.1	0	-2055	0
A_{44}	-2469	-2362	-3.83	-80.3	-2473	-2442
A_{52}	1050	-2456	1.28	-74.7	1051	-2531
A_{60}	-17.2	0	7.96	0	-9.24	0
A_{64}	-615	-420	-29.03	-9.37	-644	-429
A_{72}	-15.7	0.90	1.55	-9.94	-14.2	-9.04
A_{76}	250	-63.8	17.8	7.96	268	-55.9

The sum covers all of the complete cells in a sphere of 30-Å radius and should be an accurate result. Also included in table 12 are the results for the dipole contributions due to the presence of dipoles at the fluorine sites (we shall discuss these terms later).

As a second example, we choose a very low symmetry solid, YCl_3, which is monoclinic space group 12. As can be seen in table 13, all the ions are in very low point-symmetry positions, and each position can have a dipole moment (another way of saying this is that each position has a onefold field, A_{1m}). We then have to consult the International Tables for a higher symmetry position in order to satisfy equation (175), which in this case is the site 4e with C_i symmetry. The C_i point group has only the inversion operation, and all the odd-n A_{nm} vanish in this symmetry. Thus if the position 4e is used, equation (175) will automatically be satisfied. The lattice sum for YCl_3 was also run over a lattice 30 × 30 × 30 and only the even-n A_{nm} are given in table 14. The dipole contributions were also calculated; these calculations were more complicated in this solid because of the three types of sites (Y, Cl_1, Cl_2). For many of the A_{nm}, the dipole contributions are much larger than the monopole terms. This frequently happens when the handbook values for the dipole polarizabilities are used. We have had more believable results when we reduce the polarizability to one tenth of the handbook value.

TABLE 13. CRYSTALLOGRAPHIC DATA FOR YCl_3 MONOCLINIC SPACE GROUP 12 (C2/m) (SECOND SETTING) Z = 4

Ion	Position	Symmetry	x	y	z
Y	4g	C_2	0	0.166	0
Cl_1	4i	C_s	0.211	0	0.247
Cl_2	8j	C_1	0.229	0.179	0.760
-	4e	C_i	1/4	1/4	0

Notes:
a = 6.92, b = 11.94, c = 6.44, α = 90, β = 111.0, γ = 90.
Charges: $q_Y = 3$, $q_{Cl} = -1$.
Polarizability: $\alpha_Y = 0.55$ Å^3, $\alpha_{Cl} = 3.66$ Å^3.

TABLE 14. LATTICE SUMS FOR Y SITE AT (0, 0.166, 0) FOR YCl_3, EVEN-n A_{nm} ONLY, ALL A_{nm} REAL

Lattice sum	Monopole	Dipole	Total
A_{20}	1738	3227	4965
A_{21}	-913	2916	2003
A_{22}	245	2574	2819
A_{40}	-73.9	246	172
A_{41}	85.8	-398	-312
A_{42}	-41.3	47.7	6.4
A_{43}	10.4	-791	-781
A_{44}	-3.64	516	512
A_{60}	-0.06	-80.2	-80.3
A_{61}	-3.76	21.3	17.5
A_{62}	3.35	-27.4	-24.0
A_{63}	-0.58	60.5	59.9
A_{64}	2.73	39.2	41.9
A_{65}	5.07	13.7	18.8
A_{66}	8.14	-65.9	-57.8

The lattice sums given in tables 12 and 14 are incomplete in that the results are not in a usable form for many of our computer programs. Before we can use these results, the A_{nm} should be rotated using the standard Euler angle-rotation matrix, so that the lattice sums, A'_{nm}, rotated from A_{nm} by the angles α, β, and γ are

$$A'_{nm} = \sum_{m'} D^{n}_{m',m}(\alpha,\beta,\gamma)A_{nm'} \quad .$$

Explicit forms for the $D^{n}_{m',m}(\alpha,\beta,\gamma)$ are given in Rose (1957, ch. IV).

4.3 Point-Charge Model Developed at HDL

4.3.1 Introduction

In the classical point-charge model, the crystal-field parameters, B_{nm}, for the crystal-field interaction of the form

$$H_3 = \sum_{nm} B^{*}_{nm} \sum_{i} C_{nm}(i) \qquad (179)$$

were calculated as

$$B_{nm} = \langle r^n \rangle A_{nm} \quad , \qquad (180)$$

where the $\langle r^n \rangle$ are the expectation values of r^n of the rare-earth ion, and the A_{nm} are the multipole components of the energy at the site occupied by the rare-earth ion. In the earlier models, the radial integrals used in the evaluation of r^n were taken from Hartree-Fock

calculations (Freeman and Watson, 1962), and the A_{nm} were calculated using the point charges at the valence values for the constituent ions. These calculations generally gave the twcfold field 10 times too large, the fourfold fields approximately in good agreement, and the sixfold fields 10 times too small.

4.3.2 Screening and Wave Function Spread

Several errors in the classical theory were immediately obvious. If the radial wave functions (Hartree-Fock) for the free ion were correct, then these wave functions should give the correct values for the Slater integrals F^2, F^4, and F^6. They did not for Pr^{3+}. A simple procedure was then applied. The radial wave functions were assumed to be of the form

$$\phi(r) = CR_{HF}(\tau r) \quad , \tag{181}$$

where τ is a parameter, C is a normalization factor, and $R_{HF}(r)$ are the Hartree-Fock radial wave functions. With the radial function given by equation (181), the Slater integrals become

$$F^k = \tau F^k_{HF} \quad , \tag{182}$$

and it was found that a value of τ of approximately 0.75 was needed to fit the F^k that are found by fitting the experimental spectra of Pr^{3+}. Thus, the Hartree-Fock radial wave functions had their maxima too near the origin and needed to be spread out even in the free ion, and perhaps more spreading was necessary for an ion in a solid.

From the radial wave functions given in equation (181), it is not difficult to show that

$$\begin{aligned} \langle f(r) \rangle &= \langle \phi | f(r) | \phi \rangle / \langle \phi | \phi \rangle \\ &= \langle f(r/\tau) \rangle_{HF} \quad , \end{aligned} \tag{183}$$

so that any quantity that has been calculated using Hartree-Fock functions is immediately obtained, particularly

$$\langle r^k \rangle = \langle r^k \rangle_{HF} / \tau^k \quad . \tag{184}$$

A second error of the classical method was the omission of the Sternheimer shielding factors (Sternheimer, 1951, 1966; Sternheimer et al, 1968). In 1951 Sternheimer showed that, in a multipolar expansion of the energy of a point charge embedded in a solid, the r^n should be replaced by $r^n(1 - \sigma_n)$, where the σ_n are the shielding factors. He further showed that these factors were independent of azimuthal angle;

that is, if the angular variation in the multipolar expansion was given by Y_{nm}, the σ_n were independent of m. The values of σ_n have been calculated for Pr^{3+} and Tm^{3+} and are

$$\begin{aligned} \sigma_2 &= 0.666,\ \sigma_4 = 0.09,\ \sigma_6 = 0.04 \text{ for } Pr^{3+} \ , \\ \sigma_2 &= 0.545,\ \sigma_4 = 0.09,\ \sigma_6 = 0.04 \text{ for } Tm^{3+} \ , \end{aligned} \tag{185}$$

where the replacement is

$$r^n \rightarrow r^n(1 - \sigma_n) \ . \tag{186}$$

More recent calculations of the shielding factors have been done (Sengupta and Artman, 1970, and perhaps others), which we shall need if further refinements of the theory are undertaken.

4.3.3 Effective Charge and Position

The crystal-field components, A_{nm}, are a function of the position of the ions in a solid; in solids such as $CaWO_4$ the $(WO_4)^{-2}$ complex is known to be covalent. That is, the charges on the tungsten and the oxygen ions are not necessarily at their valence values. If we let the charge on the tungsten ion be q_W, then we require that

$$q_W + 4q_O = -2 \tag{187}$$

with the charge on the oxygen being q_O. The result given in equation (187) then assumes that the Ca^{2+} site is purely ionic with charge 2. This assumption is consistent with many of the experimental results on compounds such as $CaWO_4$ or YVO_4. We introduced a second parameter, the effective position of the oxygen ion relative to the tungsten site that would reproduce the effective dipole moment seen from the Ca^{2+} site. This parameter, η, is introduced by

$$R_{O-W}(\text{effective}) = \eta R_{O-W}(\text{measured}) \ , \tag{188}$$

where R_{O-W} is the distance from the oxygen nucleus to the tungsten nucleus. Thus there are two parameters in the A_{nm}; q_O, the effective charge (t_W is eliminated by eq (187)), and η, the effective distance of the oxygen site from the tungsten site. The calculated crystal-field parameters B_{nm} then are

$$B_{nm}(\tau; q_O \eta) = \langle r^n \rangle_{HF}(1 - \sigma_n) A_{nm}(q_O, \eta)/\tau^n \ , \tag{189}$$

with the three parameters τ, q_O, and η.

The experimental data that were taken at HDL on the rare-earth ions in $CaWO_4$ were analyzed using the effective spin-orbit Hamiltonian (Karayianis, 1970), and a set of phenomenological B_{nm} was obtained. These, given in table 15, are the B_{nm} that the theory has to fit.

The fitting was done by minimizing the square quantity given by

$$Q = \sum_{nm} \left[B_{nm}(\tau; q_o \eta) - B_{nm} \right]^2 \quad , \tag{190}$$

where $B_{nm}(\tau; q_o \eta)$ is given by equation (189), and B_{nm} is from table 15, for each ion. The minimization was done with respect to τ, q_o, and η for each ion. Since the q_o and η are assumed to be ion independent and τ is assumed to be host independent, the average q_o and η were taken and fixed. The process was then repeated with minimization with respect to τ only. This process yielded the following:

$$q_o = -1.09, \ \eta = 0.977 \quad , \tag{191}$$

and the τ values were well fitted by

$$\tau = 0.767 - 0.00896N \quad , \tag{192}$$

where N is the number of f electrons in the configuration $4f^N$. The values of σ_n used in the above were not varied in the minimizing process but were interpolated from the values given in equation (185); that is,

$$\begin{aligned} \sigma_2 &= 0.6902 - 0.0121N \quad , \\ \sigma_4 &= 0.09 \text{ (all N)} \quad , \\ \sigma_6 &= -0.04 \text{ (all N)} \quad . \end{aligned} \tag{193}$$

TABLE 15. PHENOMENOLOGICAL B_{nm} FOR SIX RARE-EARTH IONS IN $CaWO_4$ (all in cm^{-1})

Ion	B_{20}	B_{40}	B_{44}	B_{60}	RB_{64}	IB_{64}
Nd	549	-942	1005	-17	947	1
Tb	468	-825	872	-290	595	160
Dy	428	-825	978	-7	448	2.5
Ho	436	-664	779	-33	558	196
Er	404	-685	728	12	452	164
Tm	417	-689	754	17	504	359

The predicted values of the $B_{nm}(\tau;q_o,\eta)$ for the entire rare-earth series are given in table 16. The results given in table 16 when compared to table 15 show that the difference between the derived $B_{nm}(\tau;q_o\eta)$ and the phenomenological B_{nm} is greater for the low-N ions in the $4f^N$ configuration. This may be a defect in the theory, but not enough data on the low-N ions are available for analysis. One of the significant results of the analysis was that it led to a reanalysis of the spectrum of Tb:$CaWO_4$ with a different interpretation of the experimental data (Leavitt et al, 1974).

TABLE 16. DERIVED CRYSTAL-FIELD PARAMETERS, $B_{nm}(\tau;q_o\eta)$, FOR $4f^N$ CONFIGURATION OF TRIPLY IONIZED RARE-EARTH IONS (all in cm^{-1})

N	Ion	B_{20}	B_{40}	B_{44}	B_{60}	RB_{64}	IB_{64}
1	Ce	441	-1429	1462	16	1251	52
2	Pr	424	-1224	1253	13	996	42
3	Nd	408	-1059	1083	11	805	34
4	Pm	411	-1017	1041	10	764	32
5	Sm	408	-938	960	9	676	28
6	Eu	408	-887	908	8	626	26
7	Gd	406	-824	843	7	559	23
8	Tb	424	-856	876	8	591	25
9	Dy	428	-831	851	7	563	24
10	Ho	418	-756	774	6	488	20
11	Er	415	-707	724	6	439	18
12	Tm	435	-729	746	6	454	19
13	Yb	434	-701	717	6	429	18

The values used are
$\sigma_2 = 0.6902 - 0.0121N$, $\sigma_4 = 0.09$ (all N),
$\sigma_6 = -0.04$ (all N), $\tau = 0.767 - 0.00896N$,
$q = -1.09$, and $\eta = 0.977$.

More recent work on $CaWO_4$ (Morrison et al, 1977) obtains the following values:

$$\sigma_2 = 0.6846 - 0.00895N,$$
$$\sigma_4 = 0.02356 + 0.00182N,$$
$$\tau = 0.75(1.0387 - 0.0129N),$$
$$\sigma_6 = -0.04238 + 0.00014N,$$
$$q_o = -1.150, \text{ and}$$
$$\eta = 0.962.$$

The σ_n values are interpolated from the calculations of Erdös and Kang (1972) for Pr^{3+} and Tm^{3+}. The factors in equation (189) were combined so that

$$\rho_n = \langle r^n \rangle (1 - \sigma_n)/\tau^n \quad , \tag{195}$$

and the ρ_n along with the τ are given in table 17. Thus we have

$$B_{nm}(\tau; q_0, \eta) = \rho_n A_{nm}(q_0, \eta) \quad . \tag{196}$$

TABLE 17. VALUES FOR τ, $\langle r^n \rangle_{HF}$, σ_n, AND ρ_n FOR $4f^n$ CONFIGURATION OF TRIPLY IONIZED RARE-EARTH IONS[a]

Ion	N	τ	$\langle r^2 \rangle_{HF}$	$\langle r^4 \rangle_{HF}$	$\langle r^6 \rangle_{HF}$	σ^2	σ_4	σ_6	ρ_2	ρ_4	ρ_6
Ce	1	0.7693	0.3360	0.2709	0.4659	0.6757	0.0254	-0.0422	0.1841	0.7536	2.3417
Pr	2	0.7597	0.3041	0.2213	0.3459	0.6667	0.0272	-0.0421	0.1756	0.6464	1.8754
Nd	3	0.7500	0.2803	0.1882	0.2715	0.6578	0.0290	-0.0420	0.1706	0.5776	1.5897
Pm	4	0.7403	0.2621	0.1655	0.2247	0.6488	0.0308	-0.0418	0.1679	0.5339	1.4213
Sm	5	0.7306	0.2472	0.1488	0.1929	0.6398	0.0327	-0.0417	0.1668	0.5049	1.3210
Eu	6	0.7210	0.2347	0.1353	0.1686	0.6309	0.0345	-0.0415	0.1666	0.4836	1.2503
Gd	7	0.7113	0.2232	0.1237	0.1477	0.6220	0.0363	-0.0414	0.1668	0.4656	1.1873
Tb	8	0.7016	0.2129	0.1131	0.1287	0.6130	0.0381	-0.0413	0.1673	0.4990	1.1232
Dy	9	0.6919	0.2033	0.1037	0.1119	0.6041	0.0399	-0.0411	0.1681	0.4341	1.0614
Ho	10	0.6823	0.1945	0.0954	0.0981	0.5951	0.0418	-0.0410	0.1692	0.4217	1.0119
Er	11	0.6726	0.1865	0.0883	0.0874	0.5861	0.0436	-0.0408	0.1706	0.4126	0.9826
Tm	12	0.6629	0.1790	0.0820	0.0787	0.5772	0.0454	-0.0407	0.1722	0.4053	0.9649
Yb	13	0.6532	0.1717	0.0753	0.0681	0.5683	0.0472	-0.0406	0.1737	0.3938	0.9120

[a] *The units of* $\langle r^n \rangle_{HF}$ *and* ρ_n *are in* A^n.

At present we use the results given in table 17 to calculate crystal-field parameters given by equation (196) and use these parameters as starting values to best fit experimental data. We generally use $A_{nm}(q,\eta)$ with $\eta = 1$ in the process (q here is the effective charge on the ligands, not necessarily oxygen). After obtaining the best-fit B_{nm}, we return to the calculation of $A_{nm}(q)$ and vary q to obtain the best fit by minimizing the quantity

$$Q = \sum_{nm} \left[B_{nm} - \rho_n A_{nm}(q) \right]^2 \quad . \tag{197}$$

Following this, we obtain the $A_{nm}(q)$ for odd n and use them to calculate the intensities using the Judd-Ofelt theory.

At present we have not included the dipole contribution to the $A_{nm}(q)$ but intend to do so as soon as possible. The old η in the three-parameter theory will be replaced by α, the polarizability of the constituent ions in low-symmetry sites. We believe that this latter proce-

dure (including finding new ρ_n values) will give much better results than obtained by the older theory. In our projected reanalysis we will have the good phenomenological B_{nm} for $R^{3+}:LaF_3$, $R^{3+}:LaCl_3$, and $R^{3+}:LiYF_4$ (these are reported by Morrison and Leavitt, 1981), and will soon have $R^{3+}:Y_2O_3$, in addition to the B_{nm} for $R^{3+}:CaWO_4$ used in the older theory. These data should be sufficient to form a very stringent test of a newer three-parameter theory.

5. CRYSTAL-FIELD EFFECTS NOT YET FULLY INCORPORATED

5.1 Self-Consistent Point Dipole and Point Multipole

In section 4 we discussed the point-charge contribution to the multipolar field components A_{nm}. It was early recognized by Hutchings and Ray (1963) that the multipolar components of the constituent ions contribute to the A_{nm} at the site occupied by the rare-earth ion. For a point charge eZ_i located at $\vec{R}_i$ from a rare-earth site, we have the electric potential

$$\phi(\vec{r}) = \frac{eZ_i}{|\vec{R}_i - \vec{r}|} \quad . \tag{198}$$

The potential energy of the rare-earth electron at r is

$$\begin{aligned} U(\vec{r}) &= -e\phi(r) \\ &= -e^2 Z_i \sum_{nm} \frac{r^n}{R_i^{n+1}} C_{nm}(\hat{r}) C^+_{nm}(\hat{R}_i) \quad , \end{aligned} \tag{199}$$

where we have expanded the denominator of equation (198) in the spherical tensors discussed in section 2. If we write equation (199) as

$$U(\vec{r}) = \sum_{nm} A^*_{nm} r^n C_{nm}(r) \quad , \tag{200}$$

then

$$A^{(0)}_{nm} = -e^2 \sum_i \frac{Z_i C_{nm}(\hat{R}_i)}{R_i^{n+1}} \quad , \tag{201}$$

where the sum on i covers all the ions of charge eZ_i in the solid. This result we derived in section 4, expressed in slightly different form. It seems natural to extend equation (200) to the form

$$U(\vec{r}) = \sum_{\substack{nm \\ k}} A_{nm}^{(k)*} r^n C_{nm}(\hat{r}) \quad , \tag{202}$$

and relate the $A_{nm}^{(k)}$ to the various k-pole moments of ligands at $\vec{R}_i$. To relate the $A_{nm}^{(k)}$ to the multipole moments, eQ_{kq}, we need first to express the electric potential at the rare-earth electron due to the multipole moment $eQ_{kq}(i)$ at $\vec{R}_i$.

The electric potential due to a multipole distribution at $\vec{R}_i$ is given by

$$\phi(\vec{r}) = e \sum_{\substack{kq \\ nm}} (-1)^k Q_{kq}(i) \binom{2k+2n}{2n}^{1/2} \langle n(m)k(q)|n+k(m+q)\rangle \times \frac{C^*_{n+k,m+q}(\hat{R}_i)}{R_i^{n+k+1}} r^n C_{nm}(\hat{r}) \tag{203}$$

where

$$\binom{2k+2n}{2n} = \frac{(2k+2n)!}{(2n)!\,(2k)!}$$

(the details of the derivation of this result will be given later). Thus, since $U(\vec{r}) = -e\phi(\vec{r})$ we find, using equation (202), that

$$A_{nm}^{(k)} = -e^2 \sum_{q,i} (-1)^k Q^*_{kq}(i) \binom{2n+2k}{2n}^{1/2} \langle n(m)k(q)|n+k(m+q)\rangle \times \frac{C_{n+k,m+q}(\hat{R}_i)}{R_i^{n+k+1}} \quad . \tag{204}$$

If we let k = 0 in equation (204), we obtain (if k = 0, q = 0)

$$A_{km}^{(0)} = -e^2 \sum_i Q^*_{00}(i) \frac{C_{nm}(\hat{R}_i)}{R_i^{n+1}} \quad , \tag{205}$$

which is identical to the result given in equation (201) if we identify $Q^*_{00}(i)$ with Z_i (the number of charges) given there. The result for k = 1 is

$$A_{nm}^{(1)} = e^2 \sum_{q,i} Q^*_{1q} \binom{2n+2}{2n}^{1/2} \langle n(m)1(q)|n+1(m+q)\rangle \times \frac{C_{n+1,m+q}(\hat{R}_i)}{R_i^{n+2}} \quad , \tag{206}$$

since

$$Q^{*}_{1q} = (-1)^{q} Q_{1-q} \quad ,$$

$$\langle n(m)1(q) | n+1(m+q)\rangle = (-1)^{1-q}\sqrt{\frac{2n+3}{2n+1}}\,\langle 1(-q)n+1(m+q) | n(m)\rangle \quad .$$

Then with these substitutions in equation (206), we have

$$A^{(1)}_{nm} = -e^{2} \sum_{q,i} \sqrt{(n+1)(2n+3)}\; Q^{(i)}_{1q} \langle 1(q)n+1(m-q) | n(m)\rangle \times \frac{C_{n+1,m-q}(\hat{R}_i)}{R_i^{n+2}} \quad , \tag{207}$$

which is indentical to the result previously published (Morrison, 1976), if we identify $eQ_{1q}(i) \equiv p_{1q}(i)$. Thus, if we knew the $Q_{kq}(i)$, we could easily calculate the $A^{(k)}_{nm}$ by using equation (204). Unfortunately, the real difficulty is determining the $Q_{kq}(i)$. In what follows we shall restrict our discussion to the dipole case, k = 1, and let $eQ_{1q} = p_q$ and express the results in Cartesian vectors.

At sites of low symmetry, an electric field can exist whose value is determined by the various point charges of the solid. The electric field due to the point charges of the solid at a site of low symmetry is given by

$$\vec{E}^{0}_{j} = -\sum_{i} \frac{q_i \vec{R}_{ij}}{R^{3}_{ij}} \quad , \tag{208}$$

and the field generated by the point dipoles is

$$\vec{E}^{d}_{j} = \sum_{i} \left[\frac{3\vec{R}_{ij}(\vec{R}_{ij}\cdot\vec{p}_{ij})}{R^{5}_{ij}} - \frac{\vec{p}_i}{R^{3}_{ij}} \right] \quad . \tag{209}$$

The dipole moment at site j is then given by

$$\vec{p}_j = \alpha\vec{E}_j = \alpha\left[\vec{E}^{0}_{j} + \vec{E}^{d}_{j}\right] \quad , \tag{210}$$

where α is the polarizability of the ion at site j. (If more than one species is considered, the polarizability of each type must be used.) The sum in equation (208) presents no problem and can be done quite simply. To perform the sum in equation (209), it is convenient to assume a fixed coordinate system in the unit cell and an associated

reference point (say position 1); then each dipole moment, $\vec{p}_j$, can be related to the dipole located at the reference moment, $\vec{p}_1$, by the symmetry operation of the crystal. Similarly, the field at each point, $\vec{E}_j$, can be related to $\vec{E}_1$. Having done this, we can write

$$\vec{E}_1^d = \underset{\sim}{G}(1)\cdot\vec{p}_1 \quad , \tag{211}$$

and from equation (210)

$$\vec{p}_1 = \alpha[\vec{E}_1^0 + \underset{\sim}{G}(1)\cdot\vec{p}_1] \quad . \tag{212}$$

The result given in equation (212) can then be solved for the dipole moment $\vec{p}_1$ to give

$$\vec{p}_1 = \alpha\underset{\sim}{B}(1)\cdot\vec{E}_1^0 \quad , \tag{213}$$

where

$$\underset{\sim}{B} = (1 - \alpha\underset{\sim}{G})^{-1} \quad .$$

The result obtained in equation (213) is rather interesting; if the polarizability, α, is near the reciprocal of one of the eigenvalues of the $\underset{\sim}{G}$ matrix, then the dipole moment becomes excessively large. This is suggestive of the type of catastrophe that occurs in the onset of a ferroelectric transition. Such a situation would, perhaps, be modified by the inclusion of the higher multipole moments in the calculation. It should be pointed out that the $\underset{\sim}{G}$ matrix defined in equations (209) and (212) is dependent only on the lattice constants and the symmetry of the crystal. The results here were expressed in terms of Cartesian coordinates but can equally well be done in spherical tensors. If higher moments were considered the spherical tensor form is much more convenient.

TABLE 18. SPACE GROUP 88 (FIRST SETTING): COORDINATES OF ALL IONS IN A UNIT CELL OF $YLiF_4$ AND DIPOLE MOMENTS OF EACH ION (p_x, p_y, and p_z of site 1 are chosen as u, v, and w respectively)

Site	Ion	x	y	z	p_x	p_y	p_z	Q_{kq}[a]
1	F	x	y	z	u	v	w	1
2	F	y	-x	-z	v	-u	-w	$(-1)^k(i)^q$
3	F	-x	-y	z	-u	-v	w	$(-1)^q$
4	F	-y	x	-z	-v	u	-w	$(-1)^k(-i)^q$
5	F	1/2 + x	1/2 + y	1/2 + z	u	v	w	1
6	F	1/2 + y	1/2 - x	1/2 - z	v	-u	-w	$(-1)^k(i)^q$
7	F	1/2 - x	1/2 - x	1/2 - z	-u	-v	w	$(-1)^q$
8	F	1/2 - y	1/2 + y	1/2 + z	-v	u	-w	$(-1)^k(-i)^q$
9	F	x	1/2 + y	1/4 - z	u	v	-w	$(-1)^{k+q}$
10	F	y	1/2 - x	1/4 + z	v	-u	w	$(-i)^q$
11	F	-x	1/2 - y	1/4 - z	-u	-v	-w	$(-1)^k$
12	F	-y	1/2 + x	1/4 + z	-v	u	w	$(i)^q$
13	F	1/2 + x	y	3/4 - z	u	v	-w	$(-1)^{k+q}$
14	F	1/2 + y	-x	3/4 + z	v	-u	w	$(-1)^q$
15	F	1/2 - x	-y	3/4 - z	-u	-v	-w	$(-1)^k$
16	F	1/2 - y	x	3/4 + z	-v	u	w	$(i)^q$
17	Li	0	0	0	-	-	-	-
18	Li	0	1/2	1/4	-	-	-	-
19	Li	1/2	1/2	1/2	-	-	-	-
20	Li	1/2	0	3/4	-	-	-	-
21	Y	0	0	1/2	-	-	-	-
22	Y	1/2	0	1/4	-	-	-	-
23	Y	1/2	1/2	0	-	-	-	-
24	Y	0	0	3/4	-	-	-	-

[a] *The last column relates those Q_{kq} to the reference point Q_{kq}. Thus the Q_{kq} for fluorine are all related to site 1.*

5.2 Self-Consistent Results for Scheelite Structure

The procedure given above is rather involved, so we shall go into the derivation of the $\underset{\sim}{G}$ tensor for the Scheelite structure ($CaWO_4$, $LiYF_4$, etc). The space group for Scheelite is 88 in the International Tables; the position of all the constituents is given in table 18. To be specific, $LiYF_4$ has been chosen, and the fluorine in site 1 at x, y, and z has been chosen as the reference point for the dipoles (u, v, w) and all other dipoles in the unit cell are related to u, v, and w. No dipoles can exist at the Y or Li sites since the lowest fields at these sites are quadrupole (k = 2).

To evaluate $\underset{\sim}{G}$ for the Scheelite structure, we shall choose the ion at site 1 in table 18 as j in equation (209). The $\vec{R}$ in equation (202), including the translational vectors (ℓ in x, m in y, n in z), is

$$\vec{R}_{i,1} = (\ell+x_i-x)a\hat{e}_x + (m+y_i-y)a\hat{e}_y + (n+z_i-z)c\hat{e}_x \quad , \tag{214}$$

where we shall, during this discussion, suppress the explicit dependence of $\vec{R}$ on ℓ, m, and n. We write equation (209) as

$$\vec{E}_1^d = \vec{F}_1^d + \vec{I}_1^d \quad , \tag{215}$$

where

$$\vec{F}_1^d = -\sum_i \frac{\vec{p}_i}{R_{i,1}^3} \tag{216}$$

and

$$\vec{I}_1^d = 3\sum_i \vec{R}_{i,1}\frac{\vec{R}_{i1}\cdot\vec{p}_i}{R_{i,1}^5} \quad , \tag{217}$$

where sums over ℓ, m, and n are implicit. Then using table 18, we write $\vec{F}_1^d$ explicitly as

$$F_x^d = -\frac{u}{R_{1,1}^3} - \frac{v}{R_{2,1}^3} + \frac{u}{R_{3,1}^3} + \frac{v}{R_{4,1}^3} - \frac{u}{R_{5,1}^3} - \frac{v}{R_{6,1}^3} + \frac{u}{R_{7,1}^3}$$

$$+ \frac{v}{R_{8,1}^3} - \frac{u}{R_{9,1}^3} - \frac{v}{R_{10,1}^3} + \frac{u}{R_{11,1}^3} + \frac{v}{R_{12,1}^3} - \frac{u}{R_{13,1}^3} - \frac{v}{R_{14,1}^3}$$

$$+ \frac{u}{R_{15,1}^3} + \frac{v}{R_{16,1}^3} \quad . \tag{218}$$

Then we can write

$$F_x^d = \sum_{i=1}^{8} \frac{(-1)^i}{R_{2i+1,1}^3} u + \sum_{i=1}^{8} \frac{(-1)^i}{R_{2i,1}^3} v + (0)w \quad . \tag{219}$$

If we let $\underset{\sim}{G} = \underset{\sim}{G}' + 3\underset{\sim}{G}''$ and restore the ℓ, m, n sum, we have

$$G'_{xx} = \sum_{\ell,m,n} \sum_{i=1}^{8} \frac{(-1)^i}{R^3_{2i+1,1}} \quad , \tag{220}$$

$$G'_{xy} = \sum_{\ell,m,n} \sum_{i=1}^{8} \frac{(-1)^i}{R^3_{2i,1}} \quad , \tag{221}$$

$$G'_{xz} = 0 \quad . \tag{222}$$

By similar methods we obtain

$$G'_{zz} = \sum_{\ell,m,n} \sum_{i=1}^{8} (-1)^i \left(\frac{1}{R^3_i} - \frac{1}{R^3_{i+8}} \right) \quad , \tag{223}$$

and the $\underset{\sim}{G}'$ tensor is symmetrical.

To evaluate the $\underset{\sim}{G}''$ term, the procedure is precisely the same as to evaluate the $\underset{\sim}{G}'$ term, except that we relate this to equation (217). It is convenient to express $\vec{R}_{i1} \cdot \vec{P}_i$ explicitly in tabular form as given in table 19 for easy reference when writing out each term of $\underset{\sim}{G}''$. We shall not write out the detailed expression as in equation (218), but this procedure gives

$$G''_{xx} = -\sum_{i=1}^{8} (-1)^i \left[x^2_{2i+1} - x_{2i} y_{2i} \right] \quad , \tag{224}$$

$$G''_{xy} = \sum_{i=1}^{8} (-1)^i \left[x^2_{2i} - x_{2i-1} y_{2i-1} \right] \quad , \tag{225}$$

$$G''_{xz} = -\sum_{i=1}^{8} (-1)^i \left[x_i z_i - x_{i+8} z_{i+8} \right] \quad , \tag{226}$$

$$G''_{yz} = -\sum_{i=1}^{8} (-1)^i \left[y_i z_i - y_{i+8} z_{i+8} \right] \quad , \tag{227}$$

$$G''_{zz} = -\sum_{i=1}^{8} (-1)^i [z_i^2 - z_{i+8}^2] \quad , \tag{228}$$

where

$$X_i Y_i = \frac{a^2 x(i) y(i)}{R_{i,1}^5} \quad ,$$

$$X_i^2 = \frac{a^2 x(i)^2}{R_{i,1}^5} \quad ,$$

$$Y_i^2 = \frac{a^2 y(i)^2}{R_{i,1}^5} \quad ,$$

$$X_i Z_i = \frac{acx(i) z(i)}{R_{i,1}^5} \quad ,$$

and all of the sums in equations (224) through (228) have the sum over ℓ, m, and n implied. The $\tilde{G}''$ is symmetric (this can be shown directly from evaluating, for example, G''_{xy} and G''_{yx} independently).

TABLE 19. VALUES OF $\vec{R} \cdot \vec{P}$ FOR DIFFERENT SIRES IN SCHEELITE[a]

Site	p_x	p_y	p_z	R • P
1	u	v	w	x(1)u + y(1)v + z(1)w
2	v	-u	-w	x(2)v - y(2)u - z(2)w
3	-u	-v	w	-x(3)u - y(3)v + z(3)w
4	-v	u	-w	-x(4)v + y(4)u - z(4)w
5	u	v	w	x(5)u + y(5)v + z(5)w
6	v	-u	-w	x(6)v - y(6)u - z(6)w
7	u	-v	w	-x(7)u - y(7)v + z(7)w
8	-v	u	-w	-x(8)v + y(8)u - z(8)w
9	u	v	-w	x(9)u + y(9)v - z(9)w
10	v	-u	w	x(10)v - y(10)u + z(10)w
11	-u	-v	-w	-x(11)u - y(11)v - z(11)w
12	-v	u	w	-x(12)v + y(12)u - z(12)w
13	u	v	-w	x(13)u + y(13)v - z(13)w
14	v	-u	w	x(14)v - y(14)u + z(14)w
15	-u	-v	-w	-x(15)u - y(15)v - z(15)w
16	-v	u	w	-x(16)v - y(16)u - z(16)w

[a] $x(i) = \ell + s_i - x_1$, $y(i) = m + y_i - y_1$, $z(i) = n + z_i - z_1$.

The equations for $\tilde{G}'$ and $\tilde{G}''$ were calculated for several lattices and the results are given in table 20. The crystal axial field components, A_{no}, were computed for $CaWO_4$ using $\alpha = 2.4$ Å^3 and oxygen charge of $-2e$, and using $\alpha = 0.24$ Å^3 and oxygen charge of $-e$. The results are shown in table 21 (Morrison, 1976).

After the above work had been done, the dipole terms in the A^d_{nm} were programmed for a computer for all the 230 space groups. In the program any number of inequivalent sites can have an associated dipole moment (we only considered one type of site above). Recently the members of P. Caro's group in France and G. F. De Sâ's group in Brazil (Faucher and Malta, 1981) have included the dipole and quadrupole moment in a self-consistent manner for $LaCl_3$ and have found that with the reported values of the dipole and quadrupole polarizabilities the resultant A^q_{nm} is much larger than A^o_{nm} or A^d_{nm}.

5.3 Self-Induced Effects

When a rare-earth ion is immersed in a solid it is possible for its electrons to experience a field due to the reaction of the medium back on the electrons. Both this type of field and the external fields due to the point charges of the medium can exist. This reaction is identical to the classical problem of a charged particle interacting with its induced image in a conducting plate or sphere. The interaction was recognized by Judd (1977), and it was he who suggested the polarization of the ligands as a possible source of a two-electron crystal-field interaction. In this section we shall consider the development of this interaction as derived earlier (Morrison, 1980), using the same technique used in the earlier work. In later sections this interaction will be developed in a more general way, deriving the multipolar interaction.

We consider an electron at $\vec{r}$ on a rare-earth ion and a ligand at $\vec{R}$ with polarizability α. The electric potential created by the electron is

$$\phi = \frac{-e}{|\vec{R}-\vec{r}|} \quad . \tag{229}$$

The electric field at the ligand is

$$\vec{E} = -\nabla_R \phi \quad ,$$

where ∇_R indicates that the derivative should be taken with respect to $\vec{R}$. Then,

$$\vec{E} = \frac{-e(\vec{R}-\vec{r})}{|\vec{R}-\vec{r}|^3} \quad . \tag{230}$$

TABLE 20. $\underset{\sim}{G}$ TENSOR AND X-RAY DATA FOR SEVERAL COMPOUNDS ($1/Å^3$)[a]

Comp.	a	c	x	y	z	G_{xx}	G_{xy}	G_{xz}	G_{yy}	G_{yz}	G_{zz}
$CaWO_4$	5.248	11.376	0.2413	0.1511	0.0861	-0.252608	-0.0731076	-0.0979719	0.197101	-0.040229	0.123419
$PbMoO_4$	5.4312	12.0165	0.2353	0.13660	0.08110	-0.224152	-0.0758124	-0.0976769	0.168517	-0.0426228	0.0768659
$YLiF_4$	5.1668	10.733	0.2820	0.1642	0.0815	-0.252131	-0.0826652	-0.125165	0.192571	-0.0446824	0.169842
YVO_4	7.120	6.289	0.1852	0	0.1749	-0.0734174	0	-0.241965	0.127677	0	-0.173764

[a]*The reference site 1, in all of the calculations, is the ligand at x, y, and z.*
[b]*This is not a Scheelite structure (YVO_4 is the zircon structure, space group 141, in the International Tables) but can be done in the Scheelite structure by translating the oxygen positions to the above (see Karayianis and Morrison, 1973).*

TABLE 21. AXIAL COMPONENTS OF CRYSTAL FIELD FOR TWO VALUES OF POLARIZABILITY OF OXYGEN AND OXYGEN CHARGE UNITS, $cm^{-1}/Å^n$

Component	$\alpha = 2.4(Å^3)$, $q_{Ox} = -2e$		$\alpha = 0.24(Å^3)$, $q_{Ox} = -e$	
	A^o_{n0}	A^d_{n0}	A^o_{n0}	A^d_{n0}
A_{20}	10115	-22954	2321.1	-692.58
A_{40}	-4315.4	14975	-1919.6	332.25
A_{60}	38.625	-897.94	7.2194	-10.206

The dipole moment induced on the ligand is given by

$$\vec{p} = \alpha \vec{E} \quad , \tag{231}$$

where α is the polarizability of the ligand.

Now if we consider a dipole at some arbitrary origin, the electric potential at point $\vec{R}_1$ *from* that origin is

$$\phi_1 = \frac{\vec{p} \cdot \vec{R}_1}{R_1^3} \quad . \tag{232}$$

To find this potential at the electron itself, we let $\vec{R}_1 = -(\vec{R}-\vec{r})$. Then equation (232) becomes

$$\phi_1 = \frac{-\vec{p} \cdot (\vec{R}-\vec{r})}{|\vec{R}-\vec{r}|^3} \quad . \tag{233}$$

The energy of the electron interacting with this potential is given by

$$\begin{aligned} U(\vec{r},\vec{R}) &= \frac{-e}{2} \phi_1(r) \\ &= \frac{e}{2} \frac{\vec{p} \cdot (\vec{R}-\vec{r})}{|\vec{R}-\vec{r}|^3} \quad , \end{aligned} \tag{234}$$

where the 1/2 is due to a self-interaction. We can write

$$\frac{\vec{R}-\vec{r}}{|\vec{R}-\vec{r}|^3} = -\nabla_R \frac{1}{|\vec{R}-\vec{r}|} \quad . \tag{235}$$

Then equation (234) becomes

$$U(\vec{r},\vec{R}) = \frac{-e}{2} \vec{p} \cdot \nabla_R \frac{1}{|\vec{R}-\vec{r}|} \quad , \tag{236}$$

and similarly

$$\vec{E} = e \nabla_R \frac{1}{|\vec{R}-\vec{r}|} \quad . \tag{237}$$

Using the result of equation (237) in equation (231) and substituting the result into equation (236), we have

$$U(\vec{r},\vec{R}) = \frac{-e^2}{2} \alpha \left(\nabla_R \frac{1}{|\vec{R}-\vec{r}|} \right) \cdot \left(\nabla_R \frac{1}{|\vec{R}-\vec{r}|} \right) \quad , \tag{238}$$

where ∇_R operates only on the function on its immediate right. To further reduce the result given in equation (238), we consider the operation

$$\nabla^2(\psi_1\psi_2) = \psi_1\nabla^2\psi_2 + \psi_2\nabla^2\psi_1 + 2(\nabla\psi_1)\cdot(\nabla\psi_2) \quad . \tag{239}$$

If ψ_1 and ψ_2 satisfy Laplace's equation (which they do), then

$$\nabla^2(\psi_1\psi_2) = 2(\nabla\psi_1)\cdot(\nabla\psi_2) \quad . \tag{240}$$

If we identify ψ_1 and ψ_2 with $1/|\vec{R} - \vec{r}|$ in equations (238) and (240), we can write $U(\vec{r},\vec{R})$ as

$$U(\vec{r},\vec{R}) = \frac{-\alpha e^2}{4}\,\nabla_R^2\,\frac{1}{|\vec{R}-\vec{r}|^2} \quad . \tag{241}$$

To proceed further we must expand the factors on the right side of equation (241). First we notice that

$$\begin{aligned} |\vec{R}-\vec{r}|^2 &= R^2 + r^2 - 2\vec{r}\cdot\vec{R} \\ &= 2Rr\left[\frac{R^2+r^2}{2Rr} - \hat{r}\cdot\hat{R}\right] \quad . \end{aligned} \tag{242}$$

If we let

$$t = \frac{R^2+r^2}{2rR} \quad , \tag{243}$$

then

$$\frac{1}{|\vec{R}-\vec{r}|^2} = \frac{1}{2rR}\left(\frac{1}{t-z}\right) \tag{244}$$

with $z = \hat{r}\cdot\hat{R}$.

The expansion

$$\frac{1}{t-z} = \sum_n (2n+1)Q_n(t)P_n(z) \tag{245}$$

is given by Rainville (1960); the leading term for large t is

$$Q_n(t) \simeq \frac{2^n(n!)^2}{t^{n+1}(2n+1)!} \quad . \tag{246}$$

From equation (243) we have

$$Q_n(t) \simeq \frac{2^{2n+1}(n!)^2}{(2n+1)!} \frac{r^{n+1}}{R^{n+1}} \tag{247}$$

for large R.

Substituting the result of equation (247) into equation (244) gives

$$\frac{1}{|R-r|^2} = \sum \frac{2^{2n}(n!)^2 r^n}{(2n)!R^{n+2}} P_n(z) \quad . \tag{248}$$

From the Legendre addition theorem, we have

$$\begin{aligned} P_n(z) &= P_n(\hat{r}\cdot\hat{R}) \\ &= \sum_{nm} C_{nm}(\hat{r})C^*_{nm}(\hat{R}) \end{aligned} \tag{249}$$

and

$$\frac{1}{|R-r|^2} = \sum_{n,m} \frac{2^{2n}(n!)^2}{(2n)!} \frac{r^n}{R^{n+2}} C_{nm}(\hat{r})C^*_{nm}(\hat{R}) \quad . \tag{250}$$

The remaining necessary operation is ∇^2_R, which can be written

$$\nabla^2_R = \frac{1}{R^2} \frac{d}{dR}\left(R^2 \frac{d}{dR}\right) - \frac{(\vec{L})^2}{R^2} \quad . \tag{251}$$

The only term in equation (250) that this operates on is

$$\frac{1}{R^{n+2}} C^*_{nm}(\hat{R}) \quad . \tag{252}$$

Using equations (251) and (252), we have

$$\nabla^2_R \left[r^{-n-2}C^*_{nm}(\hat{R})\right] = \left[\frac{(n+1)(n+2)}{R^{n+4}} - \frac{n(n+1)}{R^{n+4}}\right] C^*_{nm}(\hat{R}) \tag{253}$$

Finally,

$$\nabla^2_R\left[R^{-n-2}C^*_{nm}(\hat{R})\right] = \frac{2(n+1)}{R^{n+4}} C^*_{nm}(\hat{R}) \quad , \tag{254}$$

where we have used

$$(\vec{L})^2 C_{nm}(\hat{R}) = n(n+1)C_{nm}(\hat{R}) \quad , \tag{255}$$

a result we discussed in section 2.1. The result in equation (254) substituted into equation (250) gives

$$\nabla_R^2 \frac{1}{|R-r|^2} = \sum_{nm} \frac{2^{2n+1}(n!)(n+1)!}{(2n)!} \frac{r^n}{R^{n+4}} C_{nm}(\hat{r}) C^*_{nm}(\hat{R}) \quad . \tag{256}$$

The result given in equation (256) is substituted into equation (241). This result, when summed over all ligands at $\vec{R}_j$ with polarizability α_j, produces

$$U(r) = \frac{-e^2}{4} \sum_{\substack{nm \\ j}} \alpha_j \left[\frac{2^{2n+1} n!(n+1)!}{(2n)!} \frac{C^*_{nm}(\hat{R}_j)}{R_j^{n+4}} \right] r^n C_{nm}(\hat{r}) \quad . \tag{257}$$

If we write equation (257) as we have previously done with the point-charge model,

$$U(r) = \sum_{nm} \left(A^{SI}_{nm}\right)^* r^n C_{nm}(\hat{r}) \quad , \tag{258}$$

we have

$$A^{SI}_{nm} = \left(\frac{e^2}{4}\right) \frac{2^{2n+1} n!(n+1)!}{(2n)!} \sum_j \frac{\alpha_j C_{nm}(\hat{R}_j)}{R_j^{n+4}} \quad , \tag{259}$$

which are the self-induced crystal-field components due to induced dipoles only. Higher order multipole moments can be induced on the ligands, and these multipoles will contribute a correction. From previous experience, we should anticipate the total self-induced multipole fields to be of the form

$$A^{SI}_{nm} = \sum_{k=1}^{\infty} A^{SI}_{nm}(k) \tag{260}$$

with the result above being $A^{SI}_{nm}(1)$.

As in the point-charge model, if we express all lengths in Å and α_j in $Å^3$ then equation (259) becomes

$$A^{SI}_{nm}(1) = -\left(\frac{\alpha_o}{8\pi} \times 10^8\right) \frac{2^{2n+1} n!(n+1)!}{(2n)!} \sum_j \frac{\alpha_j C_{nm}(\hat{R}_j)}{R_j^{n+4}} \quad , \tag{261}$$

to express A^{SI}_{nm} in units of $cm^{-1}/Å^n$ ($\alpha_o/8\pi \times 10^8 = 29{,}035$).

6. MISCELLANEOUS CRYSTAL-FIELD EFFECTS

6.1 Judd's Interaction for Two Electrons

The interaction considered here is a development of a suggestion by Judd (1977) concerning a possible origin of two-electron crystal-field effects. Specifically, Judd suggested that such terms would arise if one of the electrons in the configuration $4f^N$ polarized a nearby ion, and the remaining N-1 electrons interacted with the induced multipolar moments. The investigation of this interaction was performed later (Morrison, 1980), assuming only a dipole polarizability. The interaction for two electrons that resulted is

$$V(1,2,R) = \sum_{\substack{a\alpha \\ b,k,q}} F(abk) r_1^a C_{a\alpha}(\hat{r}_1)\, r_2^b C_{b,q-\alpha}(\hat{r}_2) \times \langle a(\alpha)b(q-\alpha)|k(q)\rangle \frac{C^*_{kq}(\hat{R})}{R^{a+b+4}} \tag{262}$$

where

$$F(abk) = -\left(\alpha \frac{e^2}{2}\right)\langle a(0)b(0)|k(0)\rangle[(a+b+1)(a+b+2) - k(k+1)] \quad ,$$

and α is the dipole polarizability of the ion at R.

The development of the result given in equation (262) was similiar to that given in the derivation of the self-induced field in section 5.3. For the full multipolar result we shall use more general methods.

The electric potential of an electron at $\vec{r}$, as seen at a ligand at $\vec{R}$, is

$$\phi(\hat{R}_1) = \frac{-e}{|\vec{R}_1|} \quad , \tag{263}$$

where

$$\vec{R}_1 = \vec{R} - \vec{r}_1 \quad .$$

The multipolar inducing field E_{nm} at $\vec{R}_1$ can be defined by

$$\phi(\vec{R}_1+\vec{x}) = -\sum_{nm} E^*_{nm} x^n C_{nm}(\hat{x}) \quad . \tag{264}$$

By expanding equation (263), we obtain

$$\phi(\vec{R}_1+\vec{x}) = -e \sum_{nm} (-1)^n \frac{C^*_{nm}(\hat{R}_1) x^n}{R_1^{n+1}} C_{nm}(\hat{x}) \quad ; \tag{265}$$

then comparing equation (265) with equation (264) gives

$$E_{nm} = e(-1)^n C_{nm}(\hat{R}_1)/R_1^{n+1} \quad . \tag{266}$$

The multipole moment, Q_{nm}, is given by

$$Q_{nm} = \alpha_n E_{nm} \quad , \tag{267}$$

where the multipole polarizability is α_n.

The electric potential at an arbitrary point $\vec{R}_3$ from a multipole distribution is given by

$$\phi_Q(\vec{R}_3) = \sum \frac{Q^*_{nm} C_{nm}(\hat{R}_3)}{R_3^{n+1}} \quad , \tag{268}$$

and the energy of an electron at $\vec{r}_2$ interacting with the multipoles is

$$U = -e\phi_Q \quad (\vec{R}_3 = -\vec{R}_2) \tag{269}$$

with $\vec{R}_2 = \vec{R} - \vec{r}_2$. From equation (268), we obtain

$$U = -e \sum_{nm} \frac{Q^*_{nm}(-1)^n C_{nm}(\hat{R}_2)}{R_2^{n+1}} \quad . \tag{270}$$

Now from equations (267) and (266) we have

$$Q_{nm} = e\alpha_n(-1)^n \frac{C_{nm}(\hat{R}_1)}{R_1^{n+1}} \quad , \tag{271}$$

which, when substituted into equation (270), gives

$$U(\vec{r}_1\vec{r}_2,\vec{R}) = -e^2 \sum_{nm} \alpha_n \frac{C^*_{nm}(\hat{R}_1)}{R_1^{n+1}} \frac{C_{nm}(\hat{R}_2)}{R_2^{n+1}} \quad . \tag{272}$$

If we write

$$U(\vec{r}_1\vec{r}_2,\vec{R}) = \sum_n U^{(n)}(\vec{r}_1\vec{r}_2,\vec{R}) \quad , \tag{273}$$

we have

$$U^{(n)}(\vec{r}_1\vec{r}_2,\vec{R}) = -e^2\alpha_n \sum_m \frac{C^*_{nm}(\hat{R}_1)}{R_1^{n+1}} \frac{C_{nm}(\hat{R}_2)}{R_2^{n+1}} \quad . \tag{274}$$

If we were considering the self-interaction, at this point we would let $\vec{R}_2 = \vec{R}_1$ and take half the results. The sum on m would then collapse to unity and $U^{(n)}(r_1,r_1,R) = -e^2(\alpha_n/2)/R_1^{2n+2}$.

However, the two-electron interaction is more complicated. We use the two-center expansions to obtain

$$\frac{C^*_{nm}(\hat{R}_1)}{R_1^{n+1}} = \sum_{a\alpha} \binom{2a+2n}{2a}^{1/2} \langle a(\alpha)n(m)|a+n(\alpha+m)\rangle \frac{r_1^a C_{a\alpha}(\hat{r}_1)}{R^{a+n+1}} C^*_{a+n,\alpha+m}(\hat{R}) \quad , \tag{275}$$

where $\vec{R}_1 = \vec{R}-\vec{r}_1$, and

$$\frac{C_{nm}(\hat{R}_2)}{R_2^{n+1}} = \sum_{b\beta} \binom{2b+2n}{2b}^{1/2} \langle n(m)b(\beta)|b+n(\beta+m)\rangle \frac{r_2^b C^*_{b\beta}(\hat{r}_2)}{R^{b+n+1}} C_{b+n,\beta+m}(\hat{R}) \quad , \tag{276}$$

where

$$\vec{R}_2 = \vec{R}-\vec{r}_2 \ .$$

As indicated in equation (272), equations (275) and (276) are to be multiplied together. When these two equations are multiplied, the two spherical tensors in $\hat{R}$ can be recoupled as

$$C^*_{a+n,\alpha+m}(\hat{R})C_{b+n,\beta+m}(\hat{R}) = (-1)^{\alpha+m} \sum_k \langle b+n(0)a+n(0)|k(0)\rangle \times \langle b+n(\beta+m)a+n(-\alpha-m)|k(\beta-\alpha)\rangle C_{k,\beta-\alpha}(\hat{R}) \quad , \tag{277}$$

where we have used

$$C^*_{a+n,\alpha+m}(\hat{R}) = (-1)^{\alpha+m} C_{a+n,-\alpha-m}(\hat{R}) \quad . \tag{278}$$

It should be noted that the resultant projection in equation (277), $[C_{k,\beta-\alpha}(\hat{R})]$, is independent of m. Thus with a proper recoupling of the C-G in equations (275) and (276), the sum over m can be performed. Selecting the independent terms from the product of equations (275) and (276) and the result of equation (277), we have

$$S = \sum_m (-1)^{m+\alpha} \langle a(\alpha)n(m)|a+n(\alpha+m)\rangle\langle n(m)b(\beta)|b+n(\beta+m)\rangle \times \langle b+n(\beta+m)a+n(-\alpha-m)|k(\beta-\alpha)\rangle \quad , \tag{279}$$

which, when further reduced, gives

$$U^{(n)}(\vec{r}_1\vec{r}_2,\vec{R}) = -e^2\alpha_n \sum_{\substack{a\alpha\\ b\beta}} \sum_{k} \langle b+n(0)a+n(0)|k(0)\rangle\left[\binom{2a+2n}{2a}\binom{2b+2n}{2b}\right]^{1/2} \times r_1^a C_{a\alpha}(\hat{r}_1) r_2^b C^*_{b\beta} \frac{(\hat{R}_2)SC_{k,\beta-\alpha}(\hat{R})}{R^{a+b+2n+2}} \quad . \tag{280}$$

Thus the final desired result is obtained if we know S. In equation (279) we rearrange the C-G as follows:

$$\begin{aligned} \langle a(\alpha)n(m)|a+n(a+m)\rangle &= (-1)^{a-\alpha}\left(\frac{2a+2n+1}{2n+1}\right)^{1/2} \langle a(-\alpha)a+n(\alpha+m)|n(m)\rangle \quad , \\ \langle n(m)b(\beta)|b+n(\beta+m)\rangle &= (-1)^{n-m}\left(\frac{2b+2n+1}{2b+1}\right)^{1/2} \langle n(m)b+n(-\beta-m)|b(-\beta)\rangle \quad . \end{aligned} \tag{281}$$

We then recouple the two C-G on the right to give

$$\begin{aligned} &\langle a(-\alpha)a+n(\alpha+m)|n(m'\rangle\langle n(m)b+n(-\beta-m)|b(-\beta)\rangle \\ &= \sum_{f} \sqrt{(2f+1)(2n+1)}\, W(a,a+n,b,b+n;nf)\langle a+n(\alpha+m)b+n(-\beta-m)|f(\alpha-\beta)\rangle \\ &\quad \times \langle a(-\alpha)f(\alpha-\beta)|b(-\beta)\rangle \quad . \end{aligned} \tag{282}$$

The sum on m can now be performed (note that the phase, $(-1)^m$, in eq (281) cancels the $(-1)^m$ in eq (279)) if we change the phase in the first C-G on the right side of equation (282). This then fixes the sums on f at k. Thus

$$\begin{aligned} S = (-1)^{k-b+n}&\left[\frac{(2a+2n+1)(2b+2n+1)}{2b+1}\right]^{1/2} \sqrt{2k+1} \\ &\times W(a,a+n,b,b+n;nk)\langle a(-\alpha)k(\alpha-\beta)|b(-\beta)\rangle \quad . \end{aligned} \tag{283}$$

The C-G in equation (283) can be rearranged to give

$$S = (-1)^{\alpha}\left[(2a+2n+1)(2b+2n+1)\right]^{1/2} W(a,a+n,b,b+n;nk)\langle a(\alpha)b(\beta)|k(\alpha-\beta)\rangle \quad . \tag{284}$$

If we let

$$F_n(abk) = -(\alpha_n e^2)\langle a+n(0)b+n(0)|k(0)\rangle\sqrt{(2a+2n+1)(2b+2n+1)} \times W(a,a+n,b,b+n;nk)\left[\binom{2a+2n}{2a}\binom{2b+2n}{2b}\right]^{1/2} , \tag{285}$$

then, substituting into equation (280), we have

$$U^{(n)}(\vec{r}_1\vec{r}_2,\vec{R}) = \sum_{\substack{a,b\\k,q}} F_n(abk) r_1^a r_2^b \sum_\alpha \langle a(\alpha)b(q-\alpha)|k(q)\rangle C_{a\alpha}(\hat{r}_1) C_{b,q-\alpha}(\hat{r}_2) \times \frac{C^*_{kq}(\hat{R})}{R^{q+b+2n+2}} , \tag{286}$$

which is the final form of the two-electron multipolar interaction. To obtain the result given in equation (262), we would have to relate $\langle a+1(0)b+1(0)|k(0)\rangle$ to $\langle a(0)b(0)|k(0)\rangle$ and evaluate $W(a,a+1,b,b+1,1k)$, both of which can be found in Rose (1957: 47, 227). If this is done, then equation (286) will reduce to equation (262). In a solid the ligands at $\vec{R}$ are such that, when the sum is performed over the ligands, only certain k and q survive. Much of the above derivation has been given by Judd (1976) in a different context, and many of his elegant techniques could be used to simplify the resulting expressions. For example, using Judd's notation (1975), equation (286) becomes

$$U^{(n)}(\vec{r}_1\vec{r}_2,\vec{R}) = \sum_{\substack{ab\\k}} F_n(abk) r_1^a r_2^b [\underset{\sim}{C}_a(\hat{r}_1)\underset{\sim}{C}_b(\hat{r}_2)]_k \cdot \underset{\sim}{C}_k(\hat{R})/R^{a+b+2n+2} , \tag{287}$$

where

$$[\underset{\sim}{C}_a(\hat{r}_1)\underset{\sim}{C}_b(\hat{r}_2)]_{kq} = \sum_\alpha \langle a(\alpha)b(q-\alpha)|k(q)\rangle C_{a\alpha}(\hat{r}_1) C_{b,q-\alpha}(\hat{r}_2) .$$

The tensor in orbital space, given in equation (286),

$$T_{kq}(a,b) = \sum_\alpha \langle a(\alpha)b(q-\alpha)|k(q)\rangle C_{a\alpha}(\hat{r}_1) C_{b,q-\alpha}(\hat{r}_2) , \tag{288}$$

should be considered carefully. For a fixed value of k the number of terms in the sum over a and b is restricted by $a + b \leq k$; for equivalent electrons a and b are restricted to even integers; and for $0 \leq (a,b)$

≤ 6, the total number of terms is not excessive. But since a and b can reach the maximum value of 6 for the configuration $4f^n$, the value of k in the k sum (similiar to the lattice sum) must go up to 12, that is, $k \leq 12$.

If as in previous work (Morrison, 1980) the sum over all the electrons is performed in equation (286) along with the sum over the ligands, the results are

$$H^{(n)}(\vec{R}) = 1/2 \sum_{\substack{ij \\ R}} U^{(n)}(\vec{r}_i, \vec{r}_j, \vec{R}) \quad , \tag{289}$$

where the factor 1/2 accounts for the self-interaction terms that are present when an electron interacts with its own induced multipole, as well as for the interactions that occur twice when $i \neq j$. This interaction contains a large number of corrections to the free-ion parameters, a few of which shall be discussed in the following.

6.2 Slater Integral Shifts

The Slater integrals for the free-ion interactions are given by the Coulomb interaction as

$$H_1 = \sum_{i>j} \frac{e^2}{|\vec{r}_i - \vec{r}_j|} \quad , \tag{290}$$

which for equivalent electrons can be written

$$= \sum_{k,q} F^{(k)} C^*_{kq}(\hat{r}_j) C_{kq}(\hat{r}_i) \quad , \tag{291}$$

where

$$F^{(k)} = e^2 \int_0^\infty \int_0^\infty \frac{r_<^k}{r_>^{k+1}} \left[R_{n\ell}(r_1) R_{n\ell}(r_2)\right]^2 dr_1 dr_2 \quad .$$

Since the interaction represented by equation (291) is spherically symmetric in the space of all the electrons, corrections to the $F^{(k)}$ can only arise from terms in an interaction that are spherically symmetric in the space of the electrons. Thus, in equation (286) if we let $k = 0$, we have such an interaction, and the following results are achieved:

$$F_n(ab0) = -\alpha_n e^2 \langle a+n(0)a+n(0)|0(0)\rangle \sqrt{(2a+2n+1)(2b+2n+1)}$$
$$\times W(a,a+n,a,a+n;n0)\left[\binom{2a+2n}{2a}\binom{2b+2n}{2b}\right]^{1/2} \qquad (292)$$
$$= -\alpha_n e^2 (-1)^{a+n}\binom{2a+2n}{2a}/\sqrt{2a+2n+1} \quad ,$$

where we have used

$$\langle a(\alpha)b(-\alpha)|0(0)\rangle = (-1)^{a-\alpha}/\sqrt{2b+1}\ \delta_{ab} \qquad (293)$$

and

$$W(a,a+n,a,a+n;n0) = (-1)^n/[(2a+1)(2a+2n+1)]^{1/2} \quad .$$

Then equation (286) becomes

$$U^{(n)}(\vec{r}_1,\vec{r}_2,\vec{R}) = -\alpha_n e^2 \sum_a \binom{2a+2n}{2a} \sum_\alpha r_1^a r_2^a \frac{C^*_{a\alpha}(\hat{r}_1)C_{a\alpha}(\hat{r}_2)}{R^{2a+2n+2}} \quad , \qquad (294)$$

which is the same form as equation (291). Thus,

$$\Delta F_n^{(k)} = -\sum_i \alpha_n(i) e^2 \sum_a \binom{2a+2n}{2a} \frac{[\langle r^a\rangle]^2}{R_i^{2a+2n+2}} \qquad (295)$$

for the Slater integral shifts due to the electron multipolar interaction with the ligands of multipolar polarizabilities α_n.

6.3 Shifts of Energy Gap $4f^N$-$4f^{N-1}n\ell$

The shifts in the energy gaps between the $4f^N$-$4f^{N-1}n\ell$ discussed here are dependent on one-electron operators, and it is best to begin the discussion by returning to equation (274) and proceeding from there. As mentioned following equation (274), the self-interaction is obtained by letting $\vec{R}_2 = \vec{R}_1$ in equation (274), obtaining

$$U^{(n)}(\vec{r},\vec{R}) = -\frac{e^2\alpha_n}{2}\frac{1}{R_1^{2n+2}} \quad , \qquad (296)$$

where $\vec{R}_1 = \vec{R} - \vec{r}$. The quantity R_1^{2n+2} in equation (296) can be expanded as in equation (242):

$$R_1^{2n+2} = [R^2 + r^2 - 2\vec{R}\cdot\vec{r}]^{n+1} \qquad (297)$$

or

$$R_1^{2n+2} = (2Rr)^{n+1}[t-z]^{n+1} \quad , \tag{298}$$

where

$$t = \left(R^2 + r^2\right)/2rR \tag{299}$$

and

$$z = \hat{r}\cdot\hat{R} \quad . \tag{300}$$

Then we have

$$U^{(n)}(\vec{r},\vec{R}) = -\frac{e^2\alpha_n}{2}\frac{1}{(2Rr)^{n+1}}\frac{1}{|t-z|^{n+1}} \quad ; \tag{301}$$

the expansion

$$\frac{1}{t-z} = \sum_k (2k+1)Q_k(t)P_k(z) \tag{302}$$

is given in Rainville (1960: 182). Also we can write

$$\frac{1}{(t-z)^{n+1}} = \frac{(-1)^n}{n!}\frac{d^n}{dt^n}\frac{1}{t-z} \quad . \tag{303}$$

For our purposes here we want only the k = 0 term of equation (302) ($P_0(z) = 1$). From equation (301) we know

$$U^{(n)}(r,R) = \frac{-e^2\alpha_n}{2}\frac{1}{(2rR)^{n+1}}\frac{(-1)^n}{n!}Q_0^{(n)}(t) \quad . \tag{304}$$

By using equation (303) in equation (302) with k = 0, we get

$$Q_0(t) \approx t^{-1} + t^{-3} + \ldots \tag{305}$$

and

$$Q_0^{(n)}(t) \approx (-1)^n n!t^{-n-1} + (-1)^n\frac{(n+2)!}{6}t^{-n-3} + \ldots \tag{306}$$

Using equation (306) in equation (304), we have

$$U^{(n)}(r,R) = \frac{-e^2\alpha_n}{2}\frac{1}{(2rR)^{n+1}}\left[\frac{1}{t^{n+1}} + \frac{(n+1)(n+2)}{6t^{n+3}}\right] \quad . \tag{307}$$

For large R > r, equation (299) gives

$$t \simeq \frac{R}{2r} \quad .$$

Thus equation (307) becomes

$$U^{(n)}(r,R) = \frac{-e^2\alpha_n}{2}\left[\frac{1}{R^{2n+2}} + \frac{(n+1)(n+2)}{3}\,\frac{r^2}{R^{2n+4}}\right] \quad . \tag{308}$$

The result given in equation (308) is a generalization of the result (Morrison, 1980) for a ligand with dipole polarizability (n = 1 in equation (308)). Thus we have, for n = 1,

$$U^{(1)}(r,R) = \frac{-e^2\alpha}{2}\,\frac{1}{R^4} + \frac{2r^2}{R^6} \quad , \tag{309}$$

where we have written $\alpha_1 = \alpha$. In the remainder of this section we shall discuss only the dipole part of the interaction as given in equation (309).

If we let W_{4f} represent the lowest energy of the $4f^N$ configuration and let $W_{n'\ell'}$ represent the corresponding energy of the $4f^{n-1}n'\ell'$ configuration, we may write $W_{4f} = W^0_{4f} + \Delta_{4f}$ and $W^0_{n'\ell'} = W^0_{n'\ell'} + \Delta_{n'\ell'}$, where W^0_{4f} and $W^0_{n'\ell'}$ are the corresponding quantities in the free ion and Δ_{4f} and $\Delta_{n'\ell'}$ are the shifts represented by equation (309). Thus, we can write

$$\Delta_{f\ell'} = \Delta^0_{f\ell'} - \frac{\alpha e^2}{R^6}\left(\langle r^2\rangle_{f\ell'} - \langle r^2\rangle_{4f}\right) \quad , \tag{310}$$

where $\langle r^2\rangle_{f\ell'} = \langle 4f^{N-1}n'\ell'|r^2|4f^{N-1}n'\ell'\rangle$ and $\langle r^2\rangle_{4f} = \langle 4f^N|r^2|4f^N\rangle$. The result in equation (310) is for a single ligand at R, and if we let there be Z_i ligands at R_i with polarizability α_i, we have

$$\Delta_{f\ell'} = \Delta^0_{f\ell'} - \sigma_2 \sum \frac{\alpha_i Z_i e^2}{R_i^6} \quad , \tag{311}$$

where $\sigma_2 = \langle r^2 \rangle_{f\ell'} - \langle r^2 \rangle_{4f}$. Since, in general, $\langle r^2 \rangle_{f\ell'}$ is greater than $\langle r^2 \rangle_{4f}$, we have the result, observed experimentally, that the free ion interconfigurational energy gap is reduced when the ion is embedded in a solid. This result is intuitively obvious, since the presence of the polarizable ligand tends to counteract the central potential of the rare-earth ion.

Recently, Yang and DeLuca (1976) have measured the energy difference of the lowest $4f^N$ and $4f^{N-1}5d$ configurations for Nd^{3+}, Er^{3+}, and Tm^{3+} in the host materials LaF_3, YF_3, LuF_3, and $LiYF_4$ (table 22). The distances of the nearest neighbor ligands are given in table 23 for the compounds reported by Yang and DeLuca. We computed the values of $S = \sum_i \alpha_i Z_i e^2 / R_i^6$ from the results of table 23. With all quantities measured in angstrom units, $S = C_0 \sum (\alpha_i Z_i / R_i^6)$, where $C_0 = 116{,}140$ and the units of S are $cm^{-1}/(Å)^3$. The polarizability of flourine is assumed to be 1.0 $Å^3$. Experimental values of σ_2 were computed from the results of table 22 and the appropriate value of S. If it is assumed that the values of σ_2 are dependent on the ion only, these σ_2 should be relatively host independent. With this assumption, the average value for σ_2 given in table 24 can be used to calculate the energy shifts of any host, if the x-ray positions and the polarizability of the ligands are known.

TABLE 22. EXPERIMENTAL ENERGY (IN UNITS OF 10^3 cm^{-1}) OF LOWEST ENERGY LEVEL OF $4f^{N-1}5d$ FOR FREE ION, Δ_{fd}^0 AND Δ_{fd}

Ion	Free ion[a]	LaF_3[b]	YF_3[b]	LuF_3[b]	$LiYF_4$[b]
Nd	70.1	60.0	58.4	57.1	54.6
Er	75.4	64.7	64.3	63.8	62.5
Tm	74.3	64.4	63.4	63.0	61.5

[a] *Sugar and Reader, 1973, Chem. Phys. 59, 2083.*
[b] *Yang and Deluca, 1976, Appl Phys. Lett. 29, 499.*

TABLE 23. LIGAND DISTANCE, R (Å), AND MULTIPLICITY, Z, FOR COMPOUNDS LISTED IN TABLE 22[a]

Compound	Ligand distances (multiplicity)					
$LiYF_4$	2.245 (×4)	2.293 (×4)	-	-	-	-
LaF_3	2.246 (×2)	2.416 (×2)	2.443 (×1)	2.49 (×2)	2.64 (×2)	-
YF_3	2.253 (×1)	2.253 (×1)	2.266 (×2)	2.299 (×2)	2.323 (×2)	2.595 (×1)
LuF_3	2.191 (×1)	2.243 (×2)	2.257 (×2)	2.257 (×1)	2.277 (×2)	2.618 (×1)

[a] *X-ray data used in these calculations are from C. Keller and H. Smutz, 1965, J. Inorg. Nucl. Chem. 27, 900, for $LiYF_4$; A. Zalkin, D. H. Templeton, and T. E. Hopkins, 1966, Inorg. Chem. 5, 1466, for LaF_3; and A. Zelkin and D. H. Templeton, 1953, J. Am. Chem. Soc. 75, 2453, for YF_3 and LuF_3.*

TABLE 24. SUM S ($cm^{-1}/Å^2$) OF EQUATION (313) FOR VALUES IN TABLE 23, $\Delta^0_{fd} - \Delta_{fd}$ FROM TABLE 22, AND σ_2 COMPUTED FROM EQUATION (311)

Compound	S	Nd[a]		Er[a]		Tm[a]	
		$\Delta^0_{fd}-\Delta_{fd}$	σ_2	$\Delta^0_{fd}-\Delta_{fd}$	σ_2	$\Delta^0_{fd}-\Delta_{fd}$	σ_2
$LiYF_4$	6815	15500	2.274	12900	1.893	12800	1.878
LaF_3	5184	10100	1.948	10700	2.064	9900	1.910
YF_3	6898	11700	1.696	11100	1.609	10900	1.580
LuF_3	7516	13000	1.730	11600	1.543	11300	1.503
Av σ_2	-	-	1.912	-	1.777	-	1.718

[a] *Yang and DeLuca, 1976, Appl. Phys. Lett. 29, 499.*

The results obtained for the three ions studied here agree qualitatively with what would be expected from the usual lanthanide contraction (Reisfeld and Jorgensen, 1977), that is, $\sigma_2(Nd^{3+}) > \sigma_2(Er^{3+}) > \sigma_2(Tm^{3+})$. A more extensive comparison of equation (310) with the experimental data in oxide and chloride host materials is necessary before any quantitative claims can be made. Nevertheless, the results indicate that equation (310) can be a useful rule of thumb indicating the host dependence of the energy spacings between the various configurations of rare-earth ions.

The results here can be used to predict a host-dependent spin-orbit parameter by using equation (309) in the usual spin-orbit Hamiltonian for a central potential:

$$\Delta\zeta = \frac{h^2 e^2}{m^2 c^2} \sum_i \frac{Z_i \alpha_i}{R_i^6} \quad . \tag{312}$$

Similarly, the result given can be used to give host-dependent Slater parameters as

$$\Delta F^{(k)} = -\sum_i \frac{\alpha_i Z_i e^2}{R_i^{2k+4}} \left[\langle r^k \rangle_f\right]^2 \quad , \tag{313}$$

where the various quantities are the same as in equation (311). The result given in equation (313) has been noted (Copeland et al, 1978) for a general two-electron interaction and is intimately related to a previous result where the ligands are replaced by an isotropic solid. In view of the difficulty of choosing the parameters used in the result given in Morrison et al (1967), it would appear that equation (313) is a preferable form.

LITERATURE CITED

Bethe, H. A., 1929, Ann. Phys. (Leipzig) 3, 133.

Bishton, S. S., and D. J. Newman, 1970, J. Phys. C 3, 1753.

Carnall, W. T., H. Crosswhite, and H. M. Crosswhite, 1978, Argonne National Laboratory, ANL-78-XX-95.

Condon, E. V., and G. H. Shortly, 1959, The Theory of Atomic Spectra (Cambridge; Cambridge, England).

Copeland, C. M., G. Balasubramanian, and D. J. Newman, 1978, J. Phys. C 11, 2029.

Cowan, R. D., and D. C. Griffin, 1976, J. Opt. Soc. Am. 66, 1010.

Dieke, G. H., and H. M. Crosswhite, 1963, Appl. Opt. 2, 675.

Erdős, P., and J. H. Kang, 1972, Phys. Rev. B6, 3383.

Faucher, M., and O. Malta, 1981, private communication, to be published.

Fraga, S., K. M. S. Saxena, and J. Karwowski, 1976, Physical Science Data 5, Handbook of Atomic Data (Elsevier, New York).

Freeman, A. J., and R. E. Watson, 1962, Phys. Rev. 127, 2058.

Hutchings, M. T., and D. K. Ray, 1963, Proc. Phys. Soc. 81, 663.

International Tables for X-Ray Crystallography, 1952, Vol. I, page 178.

Johnson, L. F., G. D. Boyd, K. Nassau, and R. Soden, 1962, Phys. Rev. 126, 1046.

Judd, B. R., 1962, Phys. Rev. 127, 750.

Judd, B. R., 1963, Operator Techniques in Atomic Spectroscopy (McGraw-Hill; New York). Chapters 1, 2, 3, and 4 contain a very good discussion of the topics given in sect. 3 in almost identical notation.

Judd, B. R., 1976, Math. Proc. Camb. Phil. Soc. 80, 535.

Judd, B. R., 1977, Phys. Rev. Lett. 39, 242.

Karayianis, N., 1970, J. Chem. Phys. 53, 2460.

Karayianis, N., and C. A. Morrison, 1973, Rare-Earth Ion-Host Lattice Interactions. 1. Point Charge Lattice Sum in Scheelites, Harry Diamond Laboratories, HDL-TR-1648.

Koster, G. F., J. O. Dimmock, R. G. Wheeler, and H. Statz, 1963, Properties of the Thirty-Two Point Groups (MIT, Cambridge, MA).

Leavitt, R. P., C. A. Morrison, and D. E. Wortman, 1974, J. Chem. Phys. 61, 1250.

Low, W., 1958a, Phys. Rev. 109, 247.

Low, W., 1958b, Phys. Rev. 109, 256.

Mason, S. F., R. D. Peacock, and B. Stewart, 1975, Mol. Phys. 30, 1829.

Morrison, C. A., N. Karayianis, and D. E. Wortman, 1977, Rare-Earth Ion-Host Lattice Interactions. 4. Predicting Spectra and Intensities of Lanthanides in Crystals, Harry Diamond Laboratories, HDL-TR-1816.

Morrison, C. A., and R. P. Leavitt, 1981, Vol. 5 of Handbook of the Physics and Chemistry of Rare Earths, edited by K. A. Gschneidner and L. Eyring (North-Holland, Amsterdam).

Morrison, C. A., D. R. Mason, and C. Kikuchi, 1967, Phys. Lett. 24A, 607.

Morrison, C. A., 1976, Solid State Comm. 18, 153.

Morrison, C. A., 1980, J. Chem. Phys. 72, 1002.

Newman, D. J., 1973, J. Phys. Chem. Solids 34, 541.

Nielson, C. W., and G. F. Koster, 1964, Spectroscopic Coefficients for ρ^n, d^n and f^n Configurations (MIT, Cambridge, MA).

Ofelt, G. S., 1962, J. Chem. Phys. 37, 511.

Rainville, E. D., 1960, Special Functions (Macmillan, New York), 182.

Reisfeld, R., and C. K. Jorgensen, 1977, Lasers and Excited States of Rare Earths (Springer-Verlag, Berlin).

Rose, M. E., 1957, Elementary Theory of Angular Momentum (Wiley, New York).

Rotenberg, M., R. Bevins, N. Metropolis, and J. K. Wooten, Jr., 1969, The 3-j and 6-j Symbols (Technology, Cambridge, MA).

Schiff, L. I., 1968, Quantum Mechanics, 3rd ed. (McGraw-Hill, New York).

Sengupta, D., and J. O. Artman, 1970, Phys. Rev. B1, 2986.

Sternheimer, R. M., 1951, Phys. Rev. 84, 244.

Sternheimer, R. M., 1966, Phys. Rev. 146, 140.

Sternheimer, R. M., M. Blume, and R. F. Peierls, 1968, Phys. Rev. 173, 376.

Sugar, J., and J. J. Reader, 1973, Chem. Phys. 59, 2083.

Wortman, D. E., R. P. Leavitt, and C. A. Morrison, 1975a, Analysis of the Ground Configuration of Trivalent Thulium in Single-Crystal Yttrium Vanadate, Harry Diamond Laboratories, HDL-TR-1653.

Wortman, D. E., R. P. Leavitt, and C. A. Morrison, 1973b, J. Phys. Chem. Solids 35, 591.

Wybourne, B. G., 1965, Spectroscopic Properties of Rare Earths (Wiley, New York), 72.

Yang, K. H., and J. A. DeLuca, 1976, Appl. Phys. Lett. 29, 499.

ANNOTATED BIBLIOGRAPHY

Reports Directly Applicable to Development of Crystal-Field Theory at Harry Diamond Laboratories

1. N. Karayianis and C. A. Morrison, Rare Earth Ion-Host Lattice Interactions. 1. Point Charge Lattice Sum in Scheelites, Harry Diamond Laboratories, HDL-TR-1648 (October 1973).

2. N. Karayianis and C. A. Morrison, Rare Earth Ion-Host Crystal Interactions. 2. Local Distortion and Other Effects in Reconciling Lattice Sums and Phenomenological B_{km}, Harry Diamond Laboratories, HDL-TR-1682 (January 1975).

3. R. P. Leavitt, C. A. Morrison, and D. E. Wortman, Rare Earth Ion-Host Crystal Interactions. 3. Three-Parameter Theory of Crystal Fields, Harry Diamond Laboratories, HDL-TR-1673 (June 1975).

4. C. A. Morrison, N. Karayianis, and D. E. Wortman, Rare Earth Ion-Host Lattice Interactions. 4. Predicting Spectra and Intensities of Lanthanides in Crystals, Harry Diamond Laboratories, HDL-TR-1816 (June 1977).

5. D. E. Wortman, C. A. Morrison, and N. Karayianis, Rare Earth Ion-Host Lattice Interactions. 5. Lanthanides in $CaWO_4$, Harry Diamond Laboratories, HDL-TR-1794 (June 1977).

6. D. E. Wortman, N. Karayianis, and C. A. Morrison, Rare Earth Ion-Host Lattice Interactions. 6. Lanthanides in $LiYF_4$, Harry Diamond Laboratories, HDL-TR-1770 (August 1976).

7. N. Karayianis, D. E. Wortman, and C. A. Morrison, Rare Earth Ion-Host Lattice Interactions. 7. Lanthanides in YVO_4, Harry Diamond Laboratories, HDL-TR-1775 (August 1976).

8. N. Karayianis, C. A. Morrison, and D. E. Wortman, Rare Earth Ion-Host Lattice Interactions. 8. Lanthanides in YPO_4, Harry Diamond Laboratories, HDL-TR-1776 (August 1976).

9. D. E. Wortman, N. Karayianis, and C. A. Morrison, Rare Earth Ion-Host Lattice Interactions. 9. Lanthanides in $YASO_4$, Harry Diamond Laboratories, HDL-TR-1772 (August 1976).

10. C. A. Morrison, N. Karayianis, and D. E. Wortman, Rare Earth Ion-Host Lattice Interactions. 10. Lanthanides in $Y_2SiBe_2O_7$, Harry Diamond Laboratories, HDL-TR-1766 (August 1976).

11. D. E. Wortman, C. A. Morrison, and N. Karayianis, Rare Earth Ion-Host Lattice Interactions. 11. Lanthanides in $Y_3Al_5O_{12}$, Harry Diamond Laboratories, HDL-TR-1773 (August 1976).

12. N. Karayianis, D. E. Wortman, and C. A. Morrison, Rare Earth Ion-Host Lattice Interactions. 12. Lanthanides in $Y_3Ga_5O_{12}$, Harry Diamond Laboratories, HDL-TR-1793 (July 1977).

13. C. A. Morrison, N. Karayianis, and D. E. Wortman, Rare Earth Ion-Host Lattice Interactions. 13. Lanthanides in $YAlO_3$, Harry Diamond Laboratories, HDL-TR-1788 (February 1977).

14. C. A. Morrison, D. E. Wortman, and N. Karayianis, Rare Earth Ion-Host Lattice Interactions. 14. Lanthanide Pentaphosphates, Harry Diamond Laboratories, HDL-TR-1779 (February 1977).

15. C. A. Morrison, N. Karayianis, and D. E. Wortman, Theoretical Free-Ion Energies, Derivatives, and Reduced Matrix Elements. I. Pr^{3+}, Tm^{3+}, Nd^{3+}, and Er^{3+}, Harry Diamond Laboratories, HDL-TR-1814 (July 1977).

16. C. A. Morrison and N. Karayianis, Operator-Equivalents, Harry Diamond Laboratories, HDL-TR-1132 (June 1963).

17. N. Karayianis and C. A. Morrison, Operator-Equivalents for Ground States of Equivalent Electrons, Harry Diamond Laboratories, HDL-TR-1133 (June 1963).

18. R. R. Stephens and D. E. Wortman, Comparison of the Ground Term, Energy Levels, and Crystal Field Parameters of Terbium in Scheelite Crystals, Harry Diamond Laboratories, HDL-TR-1367 (November 1967).

19. D. E. Wortman, Absorption and Fluorescence Spectra and Crystal Field Parameters of Tb^{3+} in $CaWO_4$, Harry Diamond Laboratories, HDL-TR-1377 (February 1968).

20. D. E. Wortman and D. Sanders, Absorption and Fluorescence Spectra of Ho^{3+} in $CaWO_4$, Harry Diamond Laboratories, HDL-TR-1480 (March 1970).

21. D. E. Wortman, Optical Spectrum of Triply Ionized Erbium in Calcium Tungstate, Harry Diamond Laboratories, HDL-TR-1510 (June 1970).

22. D. E. Wortman and D. Sanders, Optical Spectrum of Trivalent Dysprosium in Calcium Tungstate, Harry Diamond Laboratories, HDL-TR-1540 (April 1971).

23. D. E. Wortman, Triply Ionized Neodymium in Lithium Yttrium Fluoride, Harry Diamond Laboratories, HDL-TR-1554 (June 1971).

24. C. A. Morrison and D. E. Wortman, Free Ion Energy Levels of Triply Ionized Thulium Including the Spin-Spin, Orbit-Orbit and Spin-Other-Orbit Interactions, Harry Diamond Laboratories, HDL-TR-1563 (November 1971).

25. D. E. Wortman, R. P. Leavitt, and C. A. Morrison, Analysis of the Ground Configuration of Trivalent Thulium in Single-Crystal Yttrium Vanadate, Harry Diamond Laboratories, HDL-TR-1653 (December 1973).

26. C. A. Morrison and D. E. Wortman, Studies Relative to Possible Laser Pumped by Nuclear Beta Rays. II. Power and Shielding Calculations for Radioactive $LiTmF_4$, Harry Diamond Laboratories, HDL-TR-1647 (January 1974).

27. N. Karayianis, A Reinterpretation of the $^3H_6$ and $^3H_5$ Multiplets of Tm^{3+}: YVO_4, Harry Diamond Laboratories, HDL-TR-1666 (April 1974).

28. D. E. Wortman, C. A. Morrison, and R. P. Leavitt, Analysis of the Ground Configuration of Tm^{3+} in $CaWO_4$, Harry Diamond Laboratories, HDL-TR-1663 (December 1974).

29. N. Karayianis, The Significance of Crystal Field Parameters for the ^4I Term of Nd^{3+} in $CaWO_4$, Harry Diamond Laboratories, HDL-TR-1674 (December 1974).

30. D. E. Wortman, N. Karayianis, and C. A. Morrison, Analysis of the Ground Term Energy Levels for Triply Ionized Neodymium in Yttrium Orthovanadate, Harry Diamond Laboratories, HDL-TR-1685 (December 1974).

31. D. E. Wortman, C. A. Morrison, and R. P. Leavitt, Optical Spectra and Analysis of Pr^{3+} in $CaWO_4$, Harry Diamond Laboratories, HDL-TR-1726 (November 1975).

32. C. A. Morrison, N. Karayianis, and D. E. Wortman, A Possible Use of the Surface States of Transition and Rare-Earth Metal Ions in

the Theory of Catalysis, Harry Diamond Laboratories, HDL-TR-1752 (April 1976).

33. D. E. Wortman, C. A. Morrison, and N. Karayianis, Absorption and Fluorescence Spectra of Rare-Earth Ions in Single-Crystal $LiYbF_4$, $LiTmF_4$, and $LiYF_4$, Harry Diamond Laboratories, HDL-TR-1791 (March 1977).

34. R. P. Leavitt and C. A. Morrison, Energy Shift of Alkali Earths in the Vicinity of Metal Surfaces, Harry Diamond Laboratories, HDL-TR-1802 (June 1977).

35. C. A. Morrison, N. Karayianis, and D. E. Wortman, Feasibility Study of Rare Earth Semiconductor Lasers of the Type Y_2HFS_5, Harry Diamond Laboratories, HDL-TR-1836 (December 1977).

36. R. P. Leavitt and C. A. Morrison, Higher Order Terms in the Magnetic Interaction of an Ion in a Solid, Harry Diamond Laboratories, HDL-TR-1852 (May 1978).

37. D. E. Wortman, C. A. Morrison, and R. P. Leavitt, Energy Levels and Line Intensities of Pr^{3+} in $LiYF_4$, Harry Diamond Laboratories, HDL-TR-1875 (February 1979).

38. C. A. Morrison, D. E. Wortman, R. P. Leavitt, and H. P. Jenssen, Assessment of $Pr^{3+}:KY_3F_1O$ as a Blue-Green Laser, Harry Diamond Laboratories, HDL-TR-1897 (February 1980).

39. C. A. Morrison and R. P. Leavitt, Line Broadening and Shifts of Rare-Earth Ion Energy Levels in Solids, Harry Diamond Laboratories, HDL-TM-80-30 (November 1980).

Articles Related to Development of Crystal-Field Theory at Harry Diamond Laboratories

1. N. Karayianis and C. A. Morrison, Physical Basis for Hund's Rule, Am. J. Phys. 32, 216 (March 1964).

2. N. Karayianis, Physical Basis for Hund's Rule, II, Am. J. Phys. 33, 201 (March 1965).

3. N. Karayianis and C. A. Morrison, Projected Angular Momentum States, J. Math. Phys. 6, 876 (June 1965).

4. C. A. Morrison, D. R. Mason, and C. Kikuchi, Modified Slater Integrals for an Ion in a Solid, Phys. Lett. 24A, 607 (1967).

5. D. E. Wortman, Analysis of the Ground Term of Tb^{3+} in $CaWO_4$, Phys. Rev. 175, 488 (1968).

6. D. E. Wortman, Absorption and Fluorescence Spectra and Crystal Field Parameters of Tb^{3+} in $CaWO_4$, Bull. Am. Phys. Soc. 13, 686 (1968).

7. N. Karayianis, Effective Spin-Orbit Hamiltonian, J. Chem. Phys. 53, 2460 (15 September 1970).

8. N. Karayianis and R. T. Farrar, Spin-Orbit and Crystal Field Parameters for the Ground Term of Nd^{3+} in $CaWO_4$, J. Chem. Phys. 53, 3436 (November 1970).

9. E. A. Brown, J. Nemarich, N. Karayianis, and C. A. Morrison, Evidence for Yb^{3+} 4f Radial Wavefunction Expansion in Scheelites, Phys. Lett. 33A, 375 (November 1970).

10. D. E. Wortman and D. Sanders, Ground Term Energy Levels of Triply Ionized Holmium in Calcium Tungstate, J. Chem. Phys. 53, 1247 (1970).

11. D. E. Wortman, Ground Term Energy Levels and Possible Effect on Laser Action for Er^{3+} in $CaWO_4$, J. Opt. Soc. Am. 60, 1143 (1970).

12. N. Karayianis, Theoretical Energy Levels and G Values for the ^4I Terms of Nd^{3+} and Er^{3+} in $LiYF_4$, J. Phys. Chem. Solids 32, 2385 (1971).

13. D. E. Wortman, Optical Spectrum of Triply Ionized Erbium in Calcium Tungstate, J. Chem. Phys. 54, 314 (1971).

14. D. E. Wortman, Ground Term of Nd^{3+} in $LiYF_4$, Bull. Am. Phys. Soc. 16, 594 (1971).

15. D. E. Wortman and D. Sanders, Optical Spectrum of Trivalent Dysprosium in Calcium Tungstate, J. Chem. Phys. 55, 3212 (1971).

16. D. E. Wortman, Ground Term Energy States for Nd^{3+} in $LiYF_4$, J. Phys. Chem. Solids 33, 311 (1972).

17. D. E. Wortman, R. P. Leavitt, and C. A. Morrison, Analysis of the Ground Configuration of Tm^{3+} in YVO_4, J. Phys. Chem. Solids 35, 591 (1974).

18. R. P. Leavitt, C. A. Morrison, and D. E. Wortman, Description of the Crystal Field for Tb^{3+} in $LiYF_4$, Phys. Rev. B11, 92 (1 January 1975).

19. H. P. Jenssen, A. Linz, R. P. Leavitt, C. A. Morrison, and D. E. Wortman, Analysis of the Optical Spectrum of Tm^{3+} in $LiYF_4$, Phys. Rev. B11, 92 (1 January 1975).

20. N. Karayianis, C. A. Morrison, and D. E. Wortman, Analysis of the Ground Term Energy Levels for Triply Ionized Neodymium in Yttrium Orthovanadate, J. Chem. Phys. 62, 412 (May 1975).

21. D. E. Wortman, C. A. Morrison, and R. P. Leavitt, Analysis of the Ground Configuration of Tm^{3+} in $CaWO_4$, Phys. Rev. B12, 4780 (1 December 1975).

22. C. A. Morrison, D. E. Wortman, and N. Karayianis, Crystal-Field Parameters for Triply-Ionized Lanthanides in Yttrium Aluminum Garnet, J. Phys. C-Solid State Phys. 9, L191 (1976).

23. N. Karayianis, D. E. Wortman, and H. P. Jenssen, Analysis of the Optical Spectrum of Ho^{3+} in $LiYF_4$, J. Phys. Chem. Sol. 37, 675 (June 1976).

24. C. A. Morrison, Dipolar Contributions to the Crystal Fields in Ionic Solids, Solid State Commun. 18, 153-154 (1976).

25. C. A. Morrison, R. P. Leavitt, D. E. Wortman, and N. Karayianis, Induced Dipole Contributions to the Potential in the Surface Region of an Ionic Solid, Surface Science 62, 397 (1977).

26. L. Esterowitz, F. J. Bartoli, R. E. Allen, D. E. Wortman, C. A. Morrison, and R. P. Leavitt, Energy Levels and Line Intensities of Pr^{3+} in $LiYF_4$, Phys. Rev. B19, 6442 (15 June 1979).

27. C. A. Morrison and R. P. Leavitt, Crystal Field Analysis of Triply Ionized Rare Earth Ions in Lanthanum Trifluoride, J. Chem. Phys. 71, 2366 (15 September 1979).

28. C. A. Morrison, Host Dependence of the Rare-Earth Ion Energy Separation $4f^N - 4f^{N-1}n\ell$, J. Chem. Phys. 72, 1001 (15 January 1980).

29. R. P. Leavitt and C. A. Morrison, Crystal Field Analysis of Triply Ionized Rare Earth Ions in Lanthanum Trifluoride. II. Intensity Calculations, J. Chem. Phys. 73, 749 (15 July 1980).

30. C. A. Morrison, R. P. Leavitt, and D. E. Wortman, Crystal Field Analysis of Triply Ionized Lanthanides in $Cs_2NaLnCl_6$, J. Chem. Phys. 73, 2580 (15 September 1980).

31. C. A. Morrison and R. P. Leavitt, Crystal-Field Analysis of Nd^{3+} and Er^{3+} in $Bi_4Ge_3O_{12}$, J. Chem. Phys. 74, 25 (1 January 1981).

32. J. B. Gruber, R. P. Leavitt, and C. A. Morrison, Absorption Spectrum and Energy Levels of $Tm^{3+}:LaCl_3$, J. Chem. Phys. 74, 2705 (1 March 1981).

33. K. K. Deb, R. G. Buser, C. A. Morrison, and R. P. Leavitt, Energy Levels and Intensities of Triply Ionized Rare-Earth Ions in Cubic Lanthanum Oxyfluoride: An Efficient $^4F_{3/2} - {}^4I_{9/2}$ LaOF:Nd Laser, J. Opt. Soc. Am. 71, 1463 (1981).

34. R. P. Leavitt and C. A. Morrison, Higher Order Terms in the Magnetic Interaction of an Ion with a Solid, Phys. Rev. B25, 1965 (1982).

35. N. C. Chang, J. B. Gruber, R. P. Leavitt, and C. A. Morrison, Optical Spectra, Energy Levels, and Crystal-Field Analysis of Tripositive Rare Earth Ions in Y_2O_3. I. Kramers Ions in C_2 Sites, J. Chem. Phys. 76, 3877 (1982).

36. C. A. Morrison and R. P. Leavitt, Spectroscopic Properties of Triply Ionized Lanthanides in Transparent Host Materials, in Volume 5, Handbook on Physics and Chemistry of Rare Earths, ed. by K. A. Gschneidner, Jr., and LeRoy Eyring, North Holland, New York (to appear 1983).

37. R. P. Leavitt, J. B. Gruber, N. C. Chang, and C. A. Morrison, Optical Spectra, Energy Levels, and Crystal-Field Analysis of Tripositive Rare-Earth Ions in Y_2O_3. II. Non-Kramers Ions in C_2 Sites, J. Chem. Phys. 76, 4775 (1982).

APPENDIX A.--RELATIONS THAT ARE USEFUL IN ANALYSIS OF RARE-EARTH ION SPECTRA

APPENDIX A

CONTENTS

		Page
A-1.	CLEBSCH-GORDAN COEFFICIENTS	101
	A-1.1 Relation to 3-j Symbol	101
	A-1.2 Symmetry	101
	A-1.3 Orthogonality	101
	A-1.4 Special Values	101
A-2.	WIGNER-ECHART THEOREM	102
	A-2.1 Tensor T_{kq} (in L space) Only	102
	A-2.2 Mixed Tensor $T^{\kappa k}_{\lambda q}$	102
	A-2.3 Matrix Elements of Crystal Field	102
	A-2.4 Matrix Elements of Spin-Orbit Interaction	102
A-3.	COMMUTATION RELATIONS	103
	A-3.1 Angular Momentum Operators	103
	A-3.2 Spherical Tensors	103
A-4.	RACAH COEFFICIENTS AND 9j SYMBOLS	104
	A-4.1 Working Definition	104
	A-4.2 Orthogonality	104
	A-4.3 Relation to 6-j Symbol	104
	A-4.4 9j or X Symbol	104
A-5.	SPHERICAL BASIS VECTORS	104
	A-5.1 Unit Vectors	104
	A-5.2 Examples	105
	A-5.3 Generalizations	105
A-6.	EXPANSIONS	105
	A-6.1 Addition Theorem	105
	A-6.2 Single-Center Expansion	106
	A-6.3 Two-Center Expansions	106
	A-6.4 Miscellaneous Expansions	106

The following equations include the most commonly used relationships needed for arriving at the results given in the main body of the report.

A-1. CLEBSCH-GORDAN COEFFICIENTS

A-1.1 Relation to 3-j Symbol

$$\langle a(\alpha)b(\beta)|c(\gamma)\rangle = \sqrt{2c+1}\,(-1)^{-a+b-\gamma}\begin{pmatrix} a & b & c \\ \alpha & \beta & -\gamma \end{pmatrix} \tag{A-1}$$

A-1.2 Symmetry

$$\langle a(\alpha)b(\beta)|c(\gamma)\rangle = (-1)^{a+b-c}\langle a(-\alpha)b(-\beta)|c(-\gamma)\rangle \tag{A-2}$$

$$= (-1)^{a+b-c}\langle b(\beta)a(\alpha)|c(\gamma)\rangle \tag{A-3}$$

$$= (-1)^{a-\alpha}\sqrt{\frac{2c+1}{2b+1}}\,\langle a(\alpha)c(-\gamma)|b(-\beta)\rangle \tag{A-4}$$

(In eq (A-1), (A-2), (A-3), and (A-4), $\alpha + \beta = \gamma$.)

A-1.3 Orthogonality

$$\delta_{cc'} = \sum_{\alpha} \langle a(\alpha)b(\gamma-\alpha)|c(\gamma)\rangle\langle a(\alpha)b(\gamma-\alpha)|c'(\gamma)\rangle \tag{A-5}$$

$$\delta_{\alpha\alpha'}\delta_{\gamma\gamma'} = \sum_{c} \langle a(\alpha)b(\gamma-\alpha)|c(\gamma)\rangle\langle a(\alpha')b(\gamma'-\alpha')|c(\gamma')\rangle \tag{A-6}$$

A-1.4 Special Values

$$\langle a(0)b(0)|c(0)\rangle = (-1)^{s/2}\left(\frac{2c+1}{s+1}\right)^{1/2}\frac{T(s)}{T(s_1)T(s_2)T(s_3)} \tag{A-7}$$

where

$$s_1 = -a+b+c,\ s_2 = a-b+c,\ s_3 = a+b-c,\ s = a+b+c$$

and

$$T(s) = \frac{\left(\frac{s}{2}\right)!}{\sqrt{s!}}$$

$$\langle a(\alpha)b(\beta)|a+b(\alpha+\beta)\rangle = \left[\frac{\binom{2a}{a+\alpha}\binom{2b}{b+\beta}}{\binom{2a+2b}{a+b+\alpha+\beta}}\right]^{1/2} \tag{A-8}$$

$$\binom{a}{b} = \frac{a!}{b!(a-b)!}\ .$$

APPENDIX A

$$\langle \ell(0)k+2(0)|\ell(0)\rangle = -\left(\frac{k+1}{k+2}\right)\left[\frac{(2\ell+k+2)(2\ell-k)}{(2\ell-k-1)(2\ell+k+3)}\right]^{1/2}\langle \ell(0)k(0)|\ell(0)\rangle \qquad \text{(A-9)}$$

A-2. WIGNER-ECHART THEOREM

A-2.1 Tensor T_{kq} (in L Space) Only

$$\langle L'M'|T_{kq}|LM\rangle = \langle L(M)k(q)|L'(M')\rangle\langle L'\|T_k\|L\rangle \qquad \text{(A-10)}$$

A-2.2 Mixed Tensor $T^{\kappa k}_{\lambda q}$

κ in S space projection λ

k in L space projection q

$$\langle L'M_L'S'M_S'|T^{\kappa k}_{\lambda q}|LM_LSM_S\rangle = \langle L(M_L)k(q)|L'(M_L')\rangle\langle S(M_S)\kappa(\lambda)|S'(M_S')\rangle \times \langle L'S'\|T^{\kappa k}\|LS\rangle \qquad \text{(A-11)}$$

A-2.3 Matrix Elements of Crystal Field

$$\langle J'M'L'S'|H_3|JMLS\rangle = \sum_{kq} B^*_{kq}\langle J(M)k(q)|J'(M')\rangle\langle J'L'S\|U^{(k)}\|JLS\rangle\sqrt{2\ell+1}\langle \ell\|C_k\|\ell\rangle \qquad \text{(A-12)}$$

$$\langle J'L'S\|U^{(k)}\|JLS\rangle = \sqrt{2J+1}W(kLJ'S;L'J)(L'S\|U^k\|LS) \qquad \text{(A-13)}$$

(The matrix elements $(L'S\|U^k\|LS)$ are tabulated in Neilson and Koster, 1964.)

A-2.4 Matrix Elements of Spin-Orbit Interaction

$$\langle J'M'L'S'|H_2|JMLS\rangle = -\zeta[\ell(\ell+1)(2\ell+1)]^{1/2}\,\delta_{JJ'}\delta_{MM'} \times W(1SL'J;S'L) \times (L'S'\|V^{11}\|LS) \qquad \text{(A-14)}$$

(The matrix elements $(L'S'\|V^{11}\|LS)$ are tabulated in Neilson and Koster, 1964.)

A-3. COMMUTATION RELATIONS

A-3.1 Angular Momentum Operators

$$[\ell_\mu(i),\ell_\nu(j)] = \sqrt{2}\,\langle 1(\nu)1(\mu)|1(\mu+\nu)\rangle \ell_{\mu+\nu}(i)\delta_{ij} \tag{A-15}$$

$$[s_\mu(i),s_\nu(j)] = \sqrt{2}\,\langle 1(\nu)1(\mu)|1(\mu+\nu)\rangle s_{\mu+\nu}(i)\delta_{ij} \tag{A-16}$$

$$\vec{L} = \sum_i \vec{\ell}(i),\ \vec{S} = \sum_i \vec{s}(i),\ \vec{J} = \vec{L}+\vec{S} \tag{A-17}$$

$$[\ell_\mu(j),J_\nu] = [\ell_\mu(j),L_\nu] = [\ell_\mu(j),\ell_\nu(j)] \tag{A-18}$$

$$[s_\mu(j),J_\nu] = [s_\mu(j),S_\nu] = [s_\mu(j),s_\nu(j)] \tag{A-19}$$

A-3.2 Spherical Tensors

$$C_{kq}(i) = C_{kq}(\hat{r}_i) = \sqrt{\frac{4\pi}{2k+1}}\,Y_{kq}(\hat{r}_i) \tag{A-20}$$

$$[J_\mu,C_{kq}(i)] = \sqrt{k(k+1)}\,\langle k(q)1(\mu)|k(q+\mu)\rangle C_{k,q+\mu}(i)$$

$$[\nabla_\mu,f(r)C_{kq}] = \sum_{k'} \langle 1(\mu)k(q)|k'(q+\mu)\rangle\langle 1(0)k(0)|k'(0)\rangle C_{k',q+\mu} \times \left[\frac{\partial f}{\partial r} + \frac{\sqrt{6}}{r} f(r)\left[k(k+1)(2k+1)\right]^{1/2} W(k1k'1;k1)\right] \tag{A-21}$$

$$[\nabla_\mu,r^k C_{kq}] = -[k(2k+1)]^{1/2}\,\langle k(q)1(\mu)|k-1(q+\mu)\rangle r^{k-1}C_{k-1,q+\mu} \tag{A-22}$$

$$[\nabla_\mu,r^{-k-1}C_{kq}] = -\left[(k+1)(2k+1)\right]^{1/2}\,\langle k(q)1(\mu)|k+1(q+\mu)\rangle r^{-k-2}C_{k+1,q+\mu} \tag{A-23}$$

In equations (A-21) through (A-23), $C_{kq} = C_{kq}(\hat{r})$.

APPENDIX A

A-4. RACAH COEFFICIENTS AND 9-j SYMBOLS

A-4.1 Working Definition

$$\langle a(\alpha)b(\beta)|e(\alpha+\beta)\rangle\langle e(\alpha+\beta)d(\delta)|c(\alpha+\beta+\delta)\rangle$$
$$= \sum_f \sqrt{(2e+1)(2f+1)}\, W(abcd;ef)\langle b(\beta)d(\delta)|f(\beta+\delta)\rangle\langle a(\alpha)f(\beta+\delta)|c(\alpha+\beta+\delta)\rangle \tag{A-24}$$

$$W(abcd;0f) = \frac{(-1)^{f-b-d}\delta_{ab}\delta_{cd}}{\sqrt{(2b+1)(2d+1)}} \tag{A-25}$$

A-4.2 Orthogonality

$$\sum_e (2e+1)(2f+1)W(abcd;ef)W(abcd;eg) = \delta_{fg} \tag{A-26}$$

A-4.3 Relation to 6-j Symbol

$$W(abcd;ef) = (-1)^{a+b+c+d}\begin{Bmatrix} a & b & e \\ d & c & f \end{Bmatrix} \tag{A-27}$$

A-4.4 9-j or X Symbol

$$X(abc,def,ghi) = \sum_k (2k+1)W(aidh;kg)W(bfhd;ke)W(aibf;kc) \tag{A-28}$$

$$X(abc,def,gh0) = \frac{\delta_{cf}\delta_{gh}(-1)^{c+g-a-e}W(abde;cg)}{\sqrt{(2c+1)(2g+1)}} \tag{A-29}$$

A-5. SPHERICAL BASIS VECTORS

A-5.1 Unit Vectors

$$\hat{e}_{\pm 1} = \mp(\hat{e}_x \pm i\hat{e}_y)/\sqrt{2} \tag{A-30}$$

$$e_o = \hat{e}_z \tag{A-31}$$

$$\hat{e}^*_\mu = (-1)^\mu \hat{e}_{-\mu} \tag{A-32}$$

$$\hat{e}^*_\mu \cdot \hat{e}_\nu = \delta_{\mu\nu} \tag{A-33}$$

$$\hat{e}_\mu \times \hat{e}_\nu = -i\sqrt{2}\,\langle 1(\nu)1(\mu)|1(\mu+\nu)\rangle \hat{e}_{\mu+\nu} \tag{A-34}$$

A-5.2 Examples

$$\vec{\ell} = \sum_{\mu} \hat{e}_{\mu}^{*} \ell_{\mu} \tag{A-35}$$

$$\vec{s} = \sum_{\nu} \hat{e}_{\nu}^{*} s_{\nu} \tag{A-36}$$

$$\vec{\ell} \cdot \vec{s} = \sum_{\mu} \ell_{\mu}^{*} s_{\mu} = \sum_{\mu} (-1)^{\mu} \ell_{-\mu} s_{\mu} \tag{A-37}$$

$$\hat{r} = \sum_{\mu} \hat{e}_{\mu}^{*} C_{1\mu}(\hat{r}) \tag{A-38}$$

A-5.3 Generalizations

Let $A_{a\alpha}$, $B_{b\beta}$, etc, be spherical tensors and define

$$\underset{\sim}{A}_a \cdot \underset{\sim}{B}_a = \sum_{\alpha} (-1)^{\alpha} A_{a\alpha} B_{a,-\alpha} = \underset{\sim}{B}_a \cdot \underset{\sim}{A}_a \ .$$

($\underset{\sim}{A}$ and $\underset{\sim}{B}$ commute.)

$$\{\underset{\sim}{A}_a \ \underset{\sim}{B}_b\}_{cr} = \sum \langle a(\alpha) b(\gamma-\alpha) | C(\gamma) \rangle \ A_{a\alpha} B_{b,\gamma-\alpha} \ .$$

Then

$$\underset{\sim}{A}_a \cdot \underset{\sim}{B}_a = (-1)^a \sqrt{2a+1} \ \{\underset{\sim}{A}_a \cdot \underset{\sim}{B}_a\}_0$$

$$\begin{aligned} \{\underset{\sim}{A}_a \underset{\sim}{B}_b\}_c \cdot \underset{\sim}{C}_c &= (-1)^{a+b-c} \{\underset{\sim}{B}_b \underset{\sim}{A}_a\}_c \cdot \underset{\sim}{C}_c \\ &= (-1)^a \sqrt{\frac{2c+1}{2b+1}} \ \{\underset{\sim}{A}_a \underset{\sim}{C}_c\}_b \cdot \underset{\sim}{B}_b \\ &= (-1)^a \sqrt{\frac{2c+1}{2a+1}} \ \{\underset{\sim}{C}_c \underset{\sim}{B}_b\} \cdot \underset{\sim}{A}_a \ . \end{aligned}$$

A-6. EXPANSIONS

A-6.1 Addition Theorem

$$P_k(\hat{r} \cdot \hat{R}) = \sum_{q} C_{kq}(\hat{r}) C_{kq}^{*}(\hat{R}) \tag{A-39}$$

(P_k is a Legendre polynomial.)

$$C_{a\alpha}(\hat{r}) C_{b\beta}(\hat{r}) = \sum_{k} \langle a(0) b(0) | k(0) \rangle \langle a(\alpha) b(\beta) | k(\alpha+\beta) \rangle C_{k,\alpha+\beta}(\hat{r}) \tag{A-40}$$

APPENDIX A

$$T_{KQ}(r_1,r_2) = \sum_{\alpha} \langle a(\alpha)b(Q-\alpha)|K(Q)\rangle C_{a,\alpha}(\hat{r}_1)C_{b,Q-\alpha}(\hat{r}_2)$$
$$= [\hat{C}_a(r_1)\hat{C}_b(r_2)]_{KQ} \qquad \text{(A-41)}$$

A-6.2 Single-Center Expansion

$$\frac{1}{|\vec{R}-\vec{r}|} = \sum_{kq} \frac{r^k C_{kq}(\hat{r})C^*_{kq}(\hat{R})}{R^{k+1}} \qquad \text{(A-42)}$$

$$= \sum_{k} \frac{r^k}{R^{k+1}} C_k(\hat{r})\cdot C_k(\hat{R}) \qquad \text{(A-43)}$$

A-6.3 Two-Center Expansions

$$\frac{1}{|\vec{R}-\vec{x}-\vec{y}|} = \sum_{ab}\binom{2a+2b}{2a}^{1/2} [C_a(\hat{x})C_b(\hat{y})]_{a+b}\cdot C_{a+b}(\hat{R}) \frac{x^a y^b}{R^{a+b+1}} \qquad \text{(A-44)}$$

$$\frac{1}{|\vec{R}-\vec{x}-\vec{y}|} = \sum_{kq} \frac{y^k}{|\vec{R}-\vec{x}|^{k+1}} C_{kq}(\hat{y})C^*_{kq}(\widehat{R-x}) \qquad \text{(A-45)}$$

$$\frac{C_{kq}(R-x)}{|\vec{R}-\vec{x}|^{k+1}} \qquad \text{(A-46)}$$
$$= \sum_{a\alpha}\binom{2a+2k}{2a}^{1/2} \langle a(\alpha)k(q)|a+k(\alpha+q)\rangle C^*_{a\alpha}(\hat{x})C_{a+k,\alpha+q}(\hat{R}) \frac{x^a}{R^{a+k+1}}$$

A-6.4 Miscellaneous Expansions

$$\frac{e^{-\lambda|\vec{R}-\vec{r}|}}{\lambda|\vec{R}-\vec{r}|} = \frac{2}{\pi} \sum_{a\alpha} (2a+1)i_a(\lambda r)k_a(\lambda R)C_{a\alpha}(\hat{r})C^*_{a\alpha}(\hat{R}) \qquad \text{(A-47)}$$

($i_n(z) = \sqrt{\pi/2z}\, I_{n+1/2}(z)$, $k_n(z) = \sqrt{\pi/2z}\, K_{n+1/2}(z)$; I and K are Bessel functions.)

$$\frac{e^{i\lambda|\vec{R}-\vec{r}|}}{\lambda|\vec{R}-\vec{r}|} = \sum_{a\alpha} (2a+1)j_a(\lambda r)[y_a(\lambda R) + ij_a(\lambda R)]C_{a\alpha}(\hat{r})C^*_{a\alpha}(\hat{R}) \qquad \text{(A-48)}$$

(j_a and y_a are spherical Bessel functions.)

APPENDIX B.--ELECTROSTATICS

APPENDIX B

CONTENTS

		Page
B-1.	INTRODUCTION	109
B-2.	EXAMPLES	109
	B-2.1 Point Charge at Origin	109
	B-2.2 Point Charge at $\vec{R}$	110
B-3.	ATOMS AND MOLECULES	112
B-4.	POSSIBLE APPLICATION TO CATALYSIS	114
B-5.	ELECTROSTATIC POTENTIAL DUE TO MULTIPOLAR DISTRIBUTION	114

B-1. INTRODUCTION

The dominant quantity in electrostatics is the electric potential. Once having found the potential, we can obtain all other essentials by suitable operation on the potential. In particular, if the potential, $\phi(r)$, is given, then the electric field is obtained by taking the gradient of $\phi(r)$, that is,

$$\vec{E} = -\nabla\phi(r) \quad . \tag{B-1}$$

In equation (B-1), it is assumed that ϕ is a function of the general field coordinates $\vec{r}$; however, since ϕ may also involve other coordinates in a complicated manner, care must be taken to separate the field point from other coordinates so that the gradient in equation (B-1) is with respect to $\vec{r}$. We shall always here interpret the gradient operator in equation (B-1) to be taken with respect to the field point $\vec{r}$.

B-2. EXAMPLES

A few examples will suffice to clearly illustrate the above points.

B-2.1 Point Charge at Origin

If there is point charge q at the origin of our coordinate system, then the potential at the field point $\vec{r}$ is given by

$$\phi = \frac{q}{|\vec{r}|} \quad ,$$

$$r = \left(x^2 + y^2 + z^2\right)^{1/2} \quad . \tag{B-2}$$

The electric field for this simple system is given by -grad ϕ, and is

$$E = \frac{q\vec{r}}{|\vec{r}|^3} \quad , \tag{B-3}$$

since

$$\nabla \frac{1}{|\vec{r}|} = -\frac{\vec{r}}{r^3} \quad . \tag{B-4}$$

The relation given in equation (B-4) can be worked out in detail by taking each vector component of ∇ as

$$\nabla \frac{1}{|\vec{r}|} = \hat{e}_x \frac{\partial}{\partial x} \frac{1}{|\vec{r}|} + \hat{e}_y \frac{\partial}{\partial y} \frac{1}{|\vec{r}|} + \hat{e}_z \frac{\partial}{\partial z} \frac{1}{|\vec{r}|}$$

where $|\vec{r}|$ is given by equation (B-2).

APPENDIX B

The potential of a dipole at the origin can be obtained by a slight extension of equation (B-2). If we assume the dipole is made up of two oppositely charged particles, q and -q, located symmetrically about the origin at $\vec{\epsilon}/2$ and $-\vec{\epsilon}/2$, respectively, the resulting potential using equation (B-2) is

$$\phi^d = \frac{q}{|\vec{r}-\vec{\epsilon}/2|} - \frac{q}{|\vec{r}+\vec{\epsilon}/2|} \quad . \tag{B-6}$$

By noting that

$$|\vec{r}+\vec{\epsilon}/2| = \left[(\vec{r}+\vec{\epsilon}/2)\cdot(\vec{r}+\vec{\epsilon}/2)\right]^{1/2} \simeq \left(r+\vec{\epsilon}\cdot\vec{r}\right)^{1/2}$$

and

$$\left(r^2+\vec{\epsilon}\cdot\vec{r}\right)^{1/2} \simeq 1/r\left(1 - \frac{\vec{\epsilon}\cdot\vec{r}}{2r^2}\right)$$

and substituting these results into equation (B-6), we get

$$\phi^d \simeq q\,\frac{\vec{\epsilon}\cdot\vec{r}}{r^3} \quad . \tag{B-7}$$

It is customary to let $\vec{\epsilon} \to 0$ and $q \to \infty$ in such a way that $q\vec{\epsilon}$ remains finite and is the point dipole moment $\vec{p}$. Then equation (B-7) gives

$$\phi^d = \frac{\vec{p}\cdot\vec{r}}{r^3} \quad , \tag{B-8}$$

which can be and is taken as the potential at the field point $\vec{r}$ due to a dipole of moment $\vec{p}$ at the origin. The potential given in equation (B-8) can be written in a more compact and frequently more useful form using equation (B-4) or

$$\phi^d = -\vec{p}\cdot\nabla\,\frac{1}{|\vec{r}|} \quad . \tag{B-9}$$

B-2.2 Point Charge at $\vec{R}$

We consider a point charge q now located at a point $\vec{R}$ from the origin; we wish to evaluate the potential at the field point $\vec{r}$. Then

$$\phi \simeq \frac{1}{|\vec{R}-\vec{r}|} \quad , \tag{B-10}$$

APPENDIX B

B-3. ATOMS AND MOLECULES

We now wish to find the energy of interaction of two charges in the presence of a remote polarizable ion. The coordinate system is such that the charges q_1 at $\vec{r}_1$ and q_2 at $\vec{r}_2$ have a common origin. The polarizable ion of charge Q is located at $\vec{R}$ such that $R >> r_1$ or r_2. The electrostatic potential at $\vec{r}$ due to the charge q_1, given by equation (B-2), is

$$\phi(\vec{r}_1,\vec{r}) = \frac{q_1}{|\vec{r}_1-\vec{r}|} \quad . \tag{B-16}$$

We use two arguments in the potential to signify the source point, $\vec{r}_1$, and the field point, $\vec{r}$. If there were no charges or sources other than q_1 and q_2, the energy of interaction would be

$$\begin{aligned} U(\vec{r}_1\vec{r}_2) &= q_2\phi(\vec{r}_1,\vec{r})\Big|_{\vec{r}=\vec{r}_2} \\ &= \frac{q_1q_2}{|\vec{r}_1-\vec{r}_2|} \quad , \end{aligned} \tag{B-17}$$

a familiar result. Thus we can write the energy of a point charge, q_i, in a field whose sources are independent of q_i as

$$U(\vec{r}_i) = q_i\phi(\vec{r})\Big|_{\vec{r}=\vec{r}_i} \quad . \tag{B-18}$$

With these results the energy of the system due to the point charges only is

$$U_o = \frac{q_1q_2}{|\vec{r}_1-\vec{r}_2|} + \frac{q_1Q}{|\vec{R}-\vec{r}_1|} + \frac{q_2Q}{|\vec{R}-\vec{r}_2|} \quad . \tag{B-19}$$

The energy given in equation (B-19) does not include the energy due to the polarization of the ion at $\vec{R}$. To evaluate the polarization energy we must first find the dipole moment induced in the ion. From equation (B-12) (with $\vec{R} = \vec{r}_1$) we have for the potential at $\vec{r}$ due to q_1:

$$\phi(\vec{r}_1,\vec{r}) = \frac{q_1}{|\vec{r}-\vec{r}_1|} \quad , \tag{B-20}$$

and from equation (B-13):

$$E(\vec{r}) = q_1 \frac{\vec{r}-\vec{r}_1}{|\vec{r}-\vec{r}_1|^3} \quad . \tag{B-21}$$

The dipole moment at $\vec{R}$ is given by

$$\vec{p} = \alpha E(\vec{r})\Big|_{\vec{r}=\vec{R}}$$

$$= \alpha q_1 \frac{\vec{R}-\vec{r}_1}{|\vec{R}-\vec{r}_1|^3} \tag{B-22}$$

where α is the polarizability of the ion at R.

The potential at $\vec{r}$ due to this dipole at $\vec{R}$ is given by equation (B-14):

$$\phi^d(\vec{r}) = -\vec{p} \cdot \frac{\vec{R}-\vec{r}}{|\vec{R}-\vec{r}|^3} \tag{B-23}$$

and the energy of interaction with the charge q_2 is

$$U^d(\vec{r}_1\vec{r}_2) = q_2\phi(\vec{r})\Big|_{\vec{r}=\vec{r}_2} \tag{B-24}$$

from equation (B-17). Substituting equations (B-23) and (B-22) into equation (B-24), we have

$$U^d(\vec{r}_1\vec{r}_2) = -\alpha q_1 q_2 \frac{(\vec{R}-\vec{r}_1)\cdot(\vec{R}-\vec{r}_2)}{|\vec{R}-\vec{r}_1|^3|\vec{R}-\vec{r}_2|^3} \quad , \tag{B-25}$$

which is symmetric in the two charges and positions. Thus, we could have obtained the identical result if we had used charge q_2 and its field to find the induced dipole and evaluated the potential due to this dipole at $\vec{r}_1$. It is possible to extend these results to more complicated systems, but if this is seriously intended the more elegant techniques given by Judd[1] should be used. The result given in equation (B-25) was used to develop a two-electron crystal-field interaction[2] following a suggestion of Judd.

---

[1] *B. R. Judd, Math. Proc. Camb. Phil. Soc., 80 535 (1976).*
[2] *C. A. Morrison, J. Chem. Phys. 72, 1001 (1980).*

B-4. POSSIBLE APPLICATION TO CATALYSIS

Perhaps a more important application of equation (B-25) is the application of this result to the theory of homogeneous catalysis. In homogeneous catalysis an inert gas ($Q = 0$ in eq (B-19)) is introduced into a mixture of gases represented by q_1 and q_2. We assume here that q_1 and q_2 represent the charges on atoms 1 and 2 and the inert gas is to speed up a desired compound formed by some combination of q_1 and q_2. The interaction energy given by equations (B-25) and (B-17) is

$$U(\vec{r}_1\vec{r}_2) = \frac{q_1q_2}{|\vec{r}_1-\vec{r}_2|} - \alpha q_1q_2 \frac{(\vec{R}-\vec{r}_1)\cdot(\vec{R}-\vec{r}_2)}{|\vec{R}-\vec{r}_1|^3|\vec{R}-\vec{r}_2|^3} \quad . \tag{B-26}$$

We see that if q_1 and q_2 are of the same sign, the interaction with the catalyst at $\vec{R}$ is such as to reduce the repulsion. To apply equation (B-26) to the present case we can take $\vec{r}_2 = -\vec{r}_1$ with no loss in generality, and equation (B-26) becomes

$$U(\vec{r},\vec{R}) = \frac{q_1q_2}{|r|} - \alpha q_1q_2 \frac{(\vec{R}-\vec{r}/2)\cdot(\vec{R}+\vec{r}/2)}{|\vec{R}-\vec{r}/2|^3|\vec{R}+\vec{r}/2|^3} \quad , \tag{B-27}$$

with $\vec{r} = \vec{r}_1 - \vec{r}_2 = 2\vec{r}_1$, where $\vec{r}$ is the distance between atoms 1 and 2.

Thus if the two atoms have the same sign, the repulsive forces are reduced; this reduction may be sufficient to allow the two atoms to get close enough to permit electron exchange, which may be necessary to speed up a desired compound formed by some combination of q_1 and q_2.

B-5. ELECTROSTATIC POTENTIAL DUE TO MULTIPOLAR DISTRIBUTION

In much of our work we shall need the expression for the electrostatic potential due to a distribution of multipolar moments. A straightforward derivation of the desired results can be obtained by an application of the simple laws of electrostatics given above. If we have a charge distribution, $\rho(\vec{x})$, at the origin of a coordinate system, then the electric potential at $\vec{R}$ from the origin is

$$d\phi(\vec{r}) = \frac{\rho(\vec{x})d\tau_x}{|\vec{r}-\vec{x}|} \quad , \tag{B-28}$$

where $d\tau_x$ is the volume element at $\vec{x}$ from the origin. The denominator in equation (B-28) can be expanded in Legendre polynomials as

$$\frac{1}{|\vec{r}-\vec{x}|} = \sum_{n=0}^{\infty} \frac{x^n}{r^n} P_n(\cos\theta_{xr}) \qquad \text{(B-29)}$$

where θ_{xr} is the angle between $\vec{x}$ and $\vec{r}$ and we have assumed $|\vec{r}| >> |\vec{x}|$. By Legendre's addition theorem,

$$P_n(\cos\theta_{xr}) = \sum_{m=-n}^{n} C_{nm}(\hat{r})C^*_{nm}(\hat{r}) \quad , \qquad \text{(B-30)}$$

where $\hat{x}$ and $\hat{r}$ are unit vectors along $\vec{x}$ and $\vec{r}$, respectively, and $\vec{x}\cdot\vec{r} = \cos(\theta_{rx})$. If we substitute equation (B-30) into equation (B-29), we have

$$\frac{1}{|\vec{r}-\vec{x}|} = \sum_{nm} \frac{x^n}{r^{n+1}} C_{nm}(\hat{x})C^*_{nm}(\hat{r}) \quad . \qquad \text{(B-31)}$$

In equation (B-31) we have dropped the limits on the sum, a technique we shall use throughout unless the sums are restricted, in which case the limits shall be explicitly given. If the result given in equation (B-31) is substituted into equation (B-28) we have

$$\phi(\vec{r}) = \int d\tau_x \rho(\vec{x}) \sum_{n,m} \frac{x^n}{r^{n+1}} C_{nm}(\hat{x})C^*_{nm}(\hat{r}) \quad . \qquad \text{(B-32)}$$

Integrating the results in equation (B-32) produces

$$\phi(\vec{r}) = \sum_{n,m} \frac{Q_{nm}}{r^{n+1}} C^*_{nm}(\hat{r}) \quad , \qquad \text{(B-33)}$$

where we have defined the multipolar moment as

$$Q_{nm} = \int \rho(\vec{x}) x^n C_{nm}(\hat{x})\, d\tau_x \quad . \qquad \text{(B-34)}$$

The definition of the nth multipolar moment given in equation (B-34) agrees with the customary definition for n = 1 (dipole moment) but differs from a number of others for n = 2. Frequently Q_{2m} is defined by

$$Q_{2m} = \int \rho(\vec{x})[\, 2x^2 C_{2m}(\hat{x})]\, d\tau_x \quad ; \qquad \text{(B-35)}$$

we shall use only the definition given in equation (B-34).

APPENDIX B

Since the electric potential is real, equation (B-33) can be written

$$\phi(\vec{r}) = \sum_{nm} \frac{Q^*_{nm} C_{nm}(\hat{r})}{r^{n+1}} \quad . \tag{B-36}$$

We shall use the form given by equation (B-33) or equation (B-36) depending on which is the more convenient in a particular problem.

If the charge distribution $\rho(\vec{x})$ is located at $\vec{r}$ from the origin, the potential is given by

$$\phi(\vec{r}) = \int \frac{\rho(\vec{x})\, d\tau_x}{|\vec{r}+\vec{x}|} \quad , \tag{B-37}$$

$$\phi(\vec{r}) = \sum_{nm} \frac{(-1)^n Q^*_{nm} C_{nm}(\hat{r})}{r^{n+1}} \quad , \tag{B-38}$$

a result which could have been obtained from equation (B-36) by letting $\vec{r} \to -\vec{r}$ and noting that $C_{nm}(-\hat{r}) = (-1)^n C_{nm}(\hat{r})$. It should be noted that the replacement $\vec{r} \to -\vec{r}$ in equation (B-28) converts the denominator there into the denominator in equation (B-37).

We then have from equation (B-36) the electric potential at $\vec{r}$ due to a charge distribution at the origin, and from equation (B-38), we have the electric potential at the origin due to a charge distribution at $\vec{r}$.

A second and independent definition of Q_{nm} is given by

$$Q_{nm} = \alpha_n E_{nm} \quad , \tag{B-39}$$

where α_n is the nth-pole polarizability and E_{nm} is the nth multipole-inducing field. For n = 1 (dipole) we have

$$Q_{1m} = \alpha_1 E_{1m} \quad , \tag{B-40}$$

which is the spherical representation of the relative

$$\vec{p} = \alpha \vec{E} \quad , \tag{B-41}$$

where $\alpha = \alpha_1$ is the ordinary polarizability and $\vec{E}$ the ordinary electric field. If we write the vector relations in equation (B-41) in spherical form, we have

$$\vec{E} = \sum_m \hat{e}^*_m E_{1m} \tag{B-42}$$

and

$$\vec{p} = \sum_m \hat{e}^*_m p_{1m}$$

(usually E_{1m} and p_{1m} are written E_m and p_m). Then, from equations (B-42) and (B-41), we have

$$p_{1m} = \alpha E_{1m} \quad . \tag{B-43}$$

The inducing multipolar field at a point can be obtained by a suitable generalization of the electric potential at $\vec{x}$ in a uniform field $\vec{E}$, that is,

$$\phi = -\vec{x}\cdot\vec{E} \quad ,$$

which when written in spherical form is

$$\phi = -\sum_m E^*_{1m} x C_{1m}(\hat{x}) \quad . \tag{B-44}$$

Thus we write the multipolar inducing field at $\vec{R}$ as

$$\phi(\vec{R}+\vec{x}) = -\sum_{nm} E^*_{nm}(\hat{R}) x^n C_{nm}(\hat{x}) \quad , \tag{B-45}$$

which agrees with equation (B-44) for n = 1. As an example of the use of equation (B-45), we consider a point charge q_0 at $\vec{R}$ whose potential is

$$\phi(\vec{R}) = \frac{q_0}{|R|} \quad . \tag{B-46}$$

We wish to find the multipolar expansion at the origin, thus:

$$\phi(\vec{R}+\vec{x}) = \frac{q_0}{|\vec{R}-\vec{x}|} \quad ,$$

$$\phi(\vec{r}+\vec{x}) = q_0 \sum_{nm} \frac{C^*_{nm}(\hat{R})}{R^{n+1}} x^n C_{nm}(\hat{x}) \quad . \tag{B-47}$$

The multipolar inducing field at the origin is given by comparing the coefficients of $x^n C_{nm}(x)$ in equations (B-47) and (B-45), that is,

$$E_{nm} = -q_0 \frac{C_{nm}(\hat{R})}{R^{n+1}} \quad . \tag{B-48}$$

APPENDIX B

Similarly, if we have the charge q_0 at the origin and wish the multipolar inducing field at $\vec{R}$, the multipolar inducing field is

$$E_{nm} = -q_0(-1)^n \frac{C_{nm}(\hat{R})}{R^{n+1}} \quad . \tag{B-49}$$

If we have an ion at the origin whose nth-pole multipolarizability is α_n, the induced moment Q_{nm} is given by

$$Q_{nm} = \alpha_n E_{nm} \quad , \tag{B-50}$$

and from equation (B-48) we have

$$Q_{nm} = -\alpha_n q_0 \frac{C_{nm}(\hat{R})}{R^{n+1}} \quad . \tag{B-51}$$

The potential at the point $\vec{r}$ of this induced dipole at the origin is given by equation (B-36) to obtain

$$\phi(r) = \sum_{nm} - \alpha_n q_0 \frac{C^*_{nm}(\hat{R})}{R^{n+1}} \frac{C_{nm}(\hat{r})}{r^{n+1}} \quad , \tag{B-52}$$

where, to repeat, $\vec{R}$ is the position of the charge q_0 and $\vec{r}$ is the field point.

The following problem illustrates all of the above. Assume a point charge q_0 at $\vec{r}$ and a dielectric sphere of radius a at the origin with dielectric constant ε. The potential in the two regions is

$$\phi_i(r) = \sum a^*_{nm} r^n C_{nm}(\hat{r}) \quad , \quad r < a \quad ,$$

and

$$\phi_o(r) = \frac{q_0}{|\vec{R}-\vec{r}|} + \sum \frac{b^*_{nm} C_{nm}(\hat{r})}{r^{n+1}} \quad , \quad r < a \quad .$$

By equating the potential at r = a and the derivatives

$$\varepsilon \frac{\partial \phi_i}{\partial r}\bigg|_{r=a} = \frac{\partial \phi_o}{\partial r}\bigg|_{r=a}$$

(normal components of D are continuous), a_{nm} and b_{nm} can be determined. From equation (B-52) we have

$$b_{nm} = -\frac{\alpha_n q_0 C_{nm}(\hat{R})}{R^{n+1}} \quad ,$$

if we take

$$\alpha_n = [n(\varepsilon - 1)a^{2n+1}]/(\varepsilon n + n + 1) \quad .$$

Notice that this α_n agrees with the α_n given by Judd[1] (Judd's K is our ε).

If we assume that α_1 and a are known, then we can eliminate ε from α_n to obtain

$$\alpha_n = \frac{3n\alpha_1 a^{2n+1}}{(n-1)\alpha_1 + (2n+1)a^3} \quad ,$$

which could be used to estimate the α_n for $n > 1$ for an ion whose α_1 is known and a might be taken as the ionic radius. Comparing equation (B-52) with the expression for ϕ_o we have

$$b_{nm} = -\alpha_n q_0 C_{nm}(\hat{R})/R^{n+1} \quad .$$

[1] *B. R. Judd, Math. Proc. Camb. Phil. Soc., 80 535 (1976).*

DISTRIBUTION

ADMINISTRATOR
DEFENSE TECHNICAL INFORMATION CENTER
ATTN DTIC-DDA (12 COPIES)
CAMERON STATION, BUILDING 5
ALEXANDRIA, VA 22314

COMMANDER
US ARMY ARMAMENT RES & DEV COMMAND
ATTN DRDAR-TSS, STINFO DIV
DOVER, NJ 07801

COMMANDER
US ARMY MISSILE & MUNITIONS CENTER
& SCHOOL
ATTN ATSK-CTD-F
ATTN DRDMI-TB, REDSTONE SCI INFO CENTER
REDSTONE, ARSENAL, AL 35809

US ARMY MATERIEL SYSTEMS ANALYSIS
ACTIVITY
ATTN DRXSY-MP
ABERDEEN PROVING GROUND, MD 21005

DIRECTOR
US ARMY BALLISTIC RESEARCH LABORATORY
ATTN DRDAR-TSB-S (STINFO)
ABERDEEN PROVING GROUND, MD 21005

DIRECTOR
US ARMY ELECTRONICS WARFARE LABORATORY
ATTN J. CHARLTON
ATTN DELET-DD
FT MONMOUTH, NJ 07703

HQ USAF/SAMI
WASHINGTON, DC 20330

TELEDYNE BROWN ENGINEERING
CUMMINGS RESEARCH PARK
ATTN DR. MELVIN L. PRICE,
MS-44
HUNTSVILLE, AL 35807

ENGINEERING SOCIETIES LIBRARY
ATTN ACQUISITIONS DEPT
345 EAST 4TH STREET
NEW YORK, NY 10017

COMMANDER
US ARMY TEST & EVALUATION COMMAND
ATTN DR. D. H. SLINEY
ATTN TECH LIBRARY
ABERDEEN PROVING GROUND, MD 21005

COMMANDER
ATTN DRSEL-WL-MS, ROBERT NELSON
WHITE SANDS MISSILE RANGE, NM 88002

DIRECTOR
NAVAL RESEARCH LABORATORY
ATTN CODE 2620, TECH LIBRARY BR
ATTN CODE 5554,
DR. S. BARTOLI
ATTN DR. L. ESTEROWITZ
ATTN CODE 5554, R. E. ALLEN
WASHINGTON, DC 20375

DEPARTMENT OF COMMERCE
NATIONAL BUREAU OF STANDARDS
ATTN LIBRARY
ATTN H. S. PARKER
WASHINGTON, DC 20230

DIRECTOR
LAWRENCE RADIATION LABORATORY
ATTN DR. MARVIN J. WEBER
ATTN DR. HELMUT A. KOEHLER
LIVERMORE, CA 94550

CARNEGIE MELLON UNIVERSITY
SCHENLEY PARK
ATTN PHYSICS & EE, DR. J. O. ARTMAN
PITTSBURGH, PA 15213

UNIVERSITY OF MICHIGAN
COLLEGE OF ENGINEERING NORTH CAMPUS
DEPARTMENT OF NUCLEAR ENGINEERING
ATTN DR. CHIHIRO KIKUCHI
ANN ARBOR, MI 48104

COMMANDER
USA RSCH & STD GP (EUR)
ATTN CHIEF, PHYSICS & MATH BRANCH
FPO NEW YORK 09510

DIRECTOR
DEFENSE ADVANCED RESEARCH PROJECTS
AGENCY
1400 WILSON BLVD
ARLINGTON, VA 22209

DIRECTOR
DEFENSE NUCLEAR AGENCY
ATTN TECH LIBRARY
WASHINGTON, DC 20305

DIRECTOR OF DEFENSE RES & ENGINEERING
ATTN TECHNICAL LIBRARY, 3C128
WASHINGTON, DC 20301

OFFICE, CHIEF OF RESEARCH, DEVELOPMENT, &
ACQUISITION
DEPARTMENT OF THE ARMY
ATTN DAMA-ARZ-A, CHIEF SCIENTIST
DR. M. E. LASSER
ATTN DAMA-ARZ-B, DR. I. R. HERSHNER
WASHINGTON, DC 20310

COMMANDER
US ARMY RESEARCH OFFICE (DURHAM)
PO BOX 12211
ATTN DR. ROBERT J. LONTZ
ATTN DR. CHARLES BOGOSIAN
RESEARCH TRIANGLE PARK, NC 27709

COMMANDER
US ARMY MATERIALS & MECHANICS RESEARCH CENTER
ATTN DRXMR-TL, TECH LIBRARY BR
WATERTOWN, MA 02172

COMMANDER
NATICK LABORATORIES
ATTN DRXRES-RTL, TECH LIBRARY
NATICK, MA 01762

COMMANDING OFFICER
USA FOREIGN SCIENCE & TECHNOLOGY CENTER
FEDERAL OFFICE BUILDING
ATTN DRXST-BS, BASIC SCIENCE DIV
CHARLOTTESVILLE, VA 22901

DIRECTOR
NIGHT VISION & ELECTRO-OPTICS LABORATORY
ATTN TECHNICAL LIBRARY
ATTN R. BUSER
ATTN DR. K. K. DEB
ATTN MR. J. PAUL
FT BELVOIR, VA 22060

COMMANDER
ATMOSPHERIC SCIENCES LABORATORY
ATTN TECHNICAL LIBRARY
WHITE SANDS MISSILE RANGE, NM 88002

DIRECTOR
ADVISORY GROUP ON ELECTRON DEVICES
ATTN SECTRY, WORKING GROUP D
201 VARICK STREET
NEW YORK, NY 10013

OFFICE OF NAVAL RESEARCH
ATTN DR. V. O. NICOLAI
ARLINGTON, VA 22217

DEPARTMENT OF MECHANICAL, INDUSTRIAL, & AEROSPACE ENGINEERING
PO BOX 909
ATTN DR. S. TEMKIN
PISCATAWAY, NJ 08854

MASSACHUSETTS INSTITUTE OF TECHNOLOGY
CRYSTAL PHYSICS LABORATORY
ATTN DR. H. P. JENSSEN
ATTN DR. A. LINZ
CAMBRIDGE, MA 02139

NATIONAL OCEANIC & ATMOSPHERIC ADM
ENVIRONMENTAL RESEARCH LABS
ATTN LIBRARY, R-51, TECH RPTS
BOULDER, CO 80302

SETON HALL UNIVERSITY
CHEMISTRY DEPARTMENT
ATTN DR. H. BRITTAIN
SOUTH ORANGE, NJ 07099

OAK RIDGE NATIONAL LABORATORY
ATTN DR. R. G. HAIRE
OAK RIDGE, TN 37830

ARGONNE NATIONAL LABORATORY
9700 SOUTH CASS AVENUE
ATTN DR. W. T. CARNALL
ATTN DR. H. M. CROSSWHITE
ARGONNE, IL 60439

AMES LABORATORY DOE
IOWA STATE UNIVERSITY
ATTN DR. K. A. GSCHNEIDNER, JR.
AMES, IA 50011

ARIZONA STATE UNIVERSITY
DEPT. OF CHEMISTRY
ATTN DR. L. EYRING
TEMPE, AZ 85281

PORTLAND STATE UNIVERSITY
ATTN DR. J. B. GRUBER
PORTLAND, OREGON 92707

PENNSYLVANIA STATE UNIVERSITY
MATERIALS RESEARCH LABORATORY
ATTN DR. W. B. WHITE
ATTN DR. B. K. CHANDRASEKHAR
UNIVERSITY PARK, PA 16802

UNIVERSITY OF VIRGINIA
DEPT OF CHEMISTRY
ATTN DR. F. S. RICHARDSON
CHARLOTTESVILLE, VA 22901

AEROSPACE CORPORATION
PO BOX 92957
ATTN DR. M. BIRNBAUM
ATTN DR. N. C. CHANG
LOS ANGELES, CA 90009

JOHNS HOPKINS UNIVERSITY
DEPT. OF PHYSICS
ATTN PROF. B. R. JUDD
BALTIMORE, MD 21218

KALAMAZOO COLLEGE
DEPT. OF PHYSICS
ATTN PROF. K. RAJNAK
KALAMAZOO, MI 49007

US ARMY ELECTRONICS RESEARCH
& DEVELOPMENT COMMAND
ATTN TECHNICAL DIRECTOR, DRDEL-CT

HARRY DIAMOND LABORATORIES
ATTN CO/TD/TSO/DIVISION DIRECTORS
ATTN RECORD COPY, 81200
ATTN HDL LIBRARY, 81100 (2 COPIES)
ATTN HDL LIBRARY, 81100 (WOODBRIDGE)
ATTN TECHNICAL REPORTS BRANCH, 81300
ATTN LEGAL OFFICE, 97000
ATTN CHAIRMAN, EDITORIAL COMMITTEE
ATTN MORRISON, R. E., 13500 (GIDEP)
ATTN LANHAM, C., 00213
ATTN WILLIS, B., 47400
ATTN KARAYIANIS, N., 13200
ATTN KULPA, S., 13300
ATTN LEAVITT, R., 13200
ATTN NEMARICH, J., 13300
ATTN WORTMAN, D., 13200
ATTN SATTLER, J., 13200
ATTN WEBER, B., 13300
ATTN SIMONIS, G., 13200
ATTN WORCHESKY, T., 13200
ATTN TOBIN, M., 13200
ATTN DROPKIN, H., 13200
ATTN CHIEF, 00210
ATTN CHIEF, 13000
ATTN CHIEF, 15000
ATTN CROWNE, F., 13200
ATTN MORRISON, C., 13200 (10 COPIES)